

Copyright
by
J. Tyler Manning
2016

**Mechanisms of Attenuation
Of the Live Attenuated Junin virus Strain Candid #1**

by

J. Tyler Manning, B.S.

Dissertation

Presented to the Faculty of the Graduate School of

The University of Texas Medical Branch

in Partial Fulfillment

of the Requirements

for the Degree of

Doctor of Philosophy

The University of Texas Medical Branch

August 2016

Mechanisms of Attenuation Of the Live Attenuated Junin virus Strain Candid #1

Publication No. _____

J. Tyler Manning, B.S.

The University of Texas Medical Branch, 2016

Supervisor: Slobodan Paessler

Millions of individuals are at risk of arenavirus infection worldwide, with untreated infections often resulting in potentially lethal disease. Junin virus (JUNV), the causative agent of Argentine hemorrhagic fever (AHF), is currently the only pathogenic arenavirus for which a vaccine is currently in use. The Candidate #1 (Candid #1) vaccine strain, which was obtained from the 44th mouse brain passage of the parental XJ strain, has significantly reduced the incidence of disease in endemic areas. However, the mechanisms of attenuation and protection remain largely unknown. We have previously identified the glycoprotein (GP) gene as the primary attenuating gene of Candid #1 in our Hartley guinea pig model of AHF. Here, I provide a detailed mechanism through which the Candid #1 GP negatively effects the highly regulated life cycle of the virus within infected cells. Candid #1 loses an N-linked glycosylation motif prior to the 44th mouse brain passage of the XJ strain, which coincides with a significant decrease in fully processed and cleaved glycoprotein complexes (GPCs) and a significant increase in full-length GP. JUNV GPs in which this N-linked glycosylation motif are absent fail to reach the cell surface and aggregate within the endoplasmic reticulum (ER). Evidence of ER-associated autophagy is present with aggregation of the full-length GP, and upregulation of both ER stress-associated markers and LC3-II. Mutations present in the matrix protein (Z) contribute to the attenuation of Candid #1 to a smaller degree. An amino acid substitution within the RING domain of the Candid #1 Z protein results in the protein budding from the cell independently, and there is a significant decrease in interaction between GP and Z in a plasmid expression system. Together, these results demonstrate that the Candid #1 has a significantly altered life cycle compared to that of a wild-type arenavirus, including the overexpression of viral proteins, accumulation of GPC in the ER, and independent budding of the Z protein.

TABLE OF CONTENTS

List of Figures	viii
Chapter 1: Introduction to JUNV and AHF	10
Phylogeny, Geographic Distribution, and Epidemiology	10
Phylogeny of Arenaviruses and JUNV	10
Geographical Distribution of JUNV and Epidemiology of AHF	12
Clinical Presentation and Pathogenesis of AHF	14
Signs, symptoms, and progression of AHF	14
Pathogenesis of AHF	16
Immune Response to JUNV	17
Innate Immune Response	18
Adaptive Immune Response	19
Prevention and Treatment of AHF.....	20
Inactivated, Subunit, and Vector-based Vaccines.....	20
Live Attenuated Vaccines	22
Therapeutics	25
Animal Models of AHF	26
Natural Host	26
Mice	27
Guinea Pigs	28
Nonhuman Primates.....	29
Virion Architecture, Genome Organization, and Life Cycle of JUNV	30
Virion Architecture and Genome Organization	30
Life Cycle of JUNV	31
Virus Protein-Protein Interactions	34
Z Protein Structure and Self-Interaction	34
Z-LP Interaction.....	35
Z-NP Interaction	36
Z-GPC Interaction.....	37
Glycoprotein Processing and Endoplasmic Reticulum Stress	38
Protein Processing and Glycosylation Pathways	38

GPC Processing within the ER and Trafficking to the Cell Surface	40
GPC Folding in the Endoplasmic Reticulum.....	40
Maturation and Cleavage of Arenavirus GPC	42
ER Stress and the Unfolded Protein Response	43
Manipulation of the Arenavirus Genome	45
Segment Reassortment.....	45
Minigenome Systems.....	45
Recombinant Arenaviruses	46
Project Aims	47
Chapter 2: Materials and Methods.....	49
Cells, Viruses, and Biosafety.....	49
Rescue of Recombinant JUNV Clones.....	49
Growth Kinetics and Titration	50
Generation of Expression Plasmids for GPC.....	50
Minigenome Assay for Rom and Can.....	51
Western Blotting	52
Virus Genome Sequencing and Quantitative PCR	53
Confocal Microscopy.....	53
Flow Cytometry	54
Chapter 3: Differential Processing and Trafficking of the GPCs of Rom and Can Strains	55
Introduction.....	55
Results.....	57
Preliminary Data: The glycoprotein of the JUNV Can strain is less efficiently cleaved into G1 and G2 than the glycoprotein of the Rom strain.....	57
The T168A substitution in G1 is the primary contributor to the decrease in cleaved GPC	59
Absence of glycosylation at N166 results in the ER retention of GPC ...	61
The T168A substitution in G1 limits the amount of GPC present on the cell surface	64
The T168A substitution causes lysosomal degradation of GPC.....	66

Growth kinetics and plaque morphology of recombinant JUNVs expressing GPCs with or without the T168A substitution are similar in cell culture	69
Viruses expressing the T168A substitution in G1 induce ER stress during infection	70
Discussion	72
Chapter 4: Effects of the N-terminal and RING Domain Substitutions in Can Z on Protein-Protein Interactions	78
Introduction.....	78
Results.....	80
Preliminary data: rRom expressing the Can Z protein exhibits a decrease in infectious particle production	80
The RING domain substitution in Z is responsible for the decrease in infectious particle production	81
The V64G substitution in Z decreases interaction with the LP	84
The V18A substitution is required to maintain Z interaction with Can GPC	86
Discussion	89
Chapter 5: The Can Polymerase Exhibits a Decreased Sensitivity to Z-mediated Inhibition.....	92
Introduction.....	92
Results.....	94
Preliminary Data: rRom that expresses CanLP more actively synthesizes RNA than the wild-type virus.....	94
The Rom polymerase synthesizes RNA at a more rapid rate than the Can polymerase	95
The Can LP is less sensitive to inhibition by either Rom or Can Z.....	97
Discussion	100
Bibliography	106
Vita	131

List of Figures

Figure 1.1: Phylogenetic analysis New and Old World arenaviruses using complete NP amino acid sequences.	12
Figure 1.2: Chronological expansion of AHF endemic area.	15
Figure 1.3: Generating the Candidate #1 vaccine from the XJ clinical isolate ...	25
Figure 1.4: Decrease in AHF incidence upon introduction of the Candidate #1 vaccine into endemic areas.	26
Figure 1.5: The arenavirus life cycle	32
Figure 3.1: GPC Processing phenotypes in HEK293 cells	60
Figure 3.2: Effect of T168A substitution on the cleavage of GPC	62
Figure 3.3: The effect of the N166 glycan on the efficiency of GPC trafficking	64
Figure 3.4: Amino acid differences between Rom and XJ13 affect trafficking of the protein through the Golgi	65
Figure 3.5: Surface expression of GPC compared to total cellular GPC	67
Figure 3.6: The T168A substitution causes lysosomal degradation of GPC	69
Figure 3.7: Growth kinetics and plaque phenotype of rRom viruses expressing various GPC proteins	71
Figure 3.8: Viral protein expression profiles in Vero cells.	73

Figure 3.9: Differential intracellular processing of Rom and Can GPC	78
Figure 4.1: Can Z reduces infectious particle production in rRom	83
Figure 4.2: The V64G substitution decreases the titer and reduces plaque size	84
Figure 4.3: The V64G substitution decreases the infectious particle production of rRom	85
Figure 4.4: The V64G substitution reduces the affinity of Z for LP	87
Figure 4.5: The Can GPC-Z interaction is enhanced with both the Z-V18A and GPC-R484G substitutions	89
Figure 5.1: rRom viruses expressing the Can LP synthesize more RNA than viruses expressing Rom LP.	96
Figure 5.2: The Rom LP is more active than the Can LP in a minigenome system.	98
Figure 5.3: Rom LP is more sensitive to inhibition by Z than Can LP.	100
Figure 5.4: Can LP is less sensitive to Z inhibition regardless of the NP or RNA template.	101
Figure 5.5: Can life cycle.	105

Chapter 1: Introduction to JUNV and AHF

PHYLOGENY, GEOGRAPHIC DISTRIBUTION, AND EPIDEMIOLOGY

Phylogeny of Arenaviruses and JUNV

The family *arenaviridae* is a family of segmented negative sense RNA (nsRNA) viruses consisting of a single genus, *Arenavirus*. The members of the *arenaviridae* family are most closely related phylogenetically to the members of the *bunyaviridae* and the *orthomyxoviridae*. The three families share a similar intracellular virus life cycle despite utilizing different cellular compartments for assembly and budding. There are currently 22 viral species within the arenavirus family that are recognized by the International Committee for Taxonomy of Viruses (ICTV) (Salvato et al., 2012). Prior to 2014, the *arenaviridae* was a single virus family, but has since been divided into two separate genera. The mammarenaviruses represent all arenaviruses that infect mammalian hosts, whereas the heptarenaviruses represent those infecting snakes (Buchmeier et al., 2014). The members of the mammarenavirus genus are divided into the Old World (OW) arenaviruses and the New World (NW) arenaviruses based on phylogenetic relationships between members (Bowen et al., 1997), geographical distribution, and serological cross-reactivity (Wulff et al., 1978). The OW arenaviruses can be isolated in Europe, Africa, and Asia and comprise the Lassa-Lymphocytic choriomeningitis serocomplex. This serocomplex includes Lymphocytic choriomeningitis virus (LCMV), Lassa virus (LASV), Mobala virus (MOBV), Mopeia virus (MOPV), and Ippy virus (IPPV). The viruses are confined to their respective geographic regions with the exception of LCMV, which can be isolated worldwide due to the range of its natural host, *Mus musculus*. Three recently discovered

OW arenavirus species, Morogoro virus (Gunther, unpublished data), Kodoko virus (Lecompte et al., 2007) and Dandenong virus (Palacios et al., 2008), have not yet been recognized by the ICTV in the most recent committee report. The NW arenaviruses can be isolated in North and South America and comprise the Tacaribe serocomplex, which is further divided into four clades termed clades A, B, C, and A/Rec. Clade A contains Pirital virus (PIRV), Allpahuayo virus (ALLV), Pichinde virus (PICV), Parana virus (PARV), and Flexal virus (FLEV). Clade B includes Machupo virus (MACV), Junin virus (JUNV), Tacaribe virus (TCRV), Sabia virus (SABV), Guanarito virus (GTOV), Amapari virus (AMAV), Cupixi virus (CPXV). Clade C contains Oliveros virus (OLVV) and Latino virus (LATV). While members of clades A, B, and C can be found in South America, clade A/Rec viruses are located in North America and contain the species Whitewater

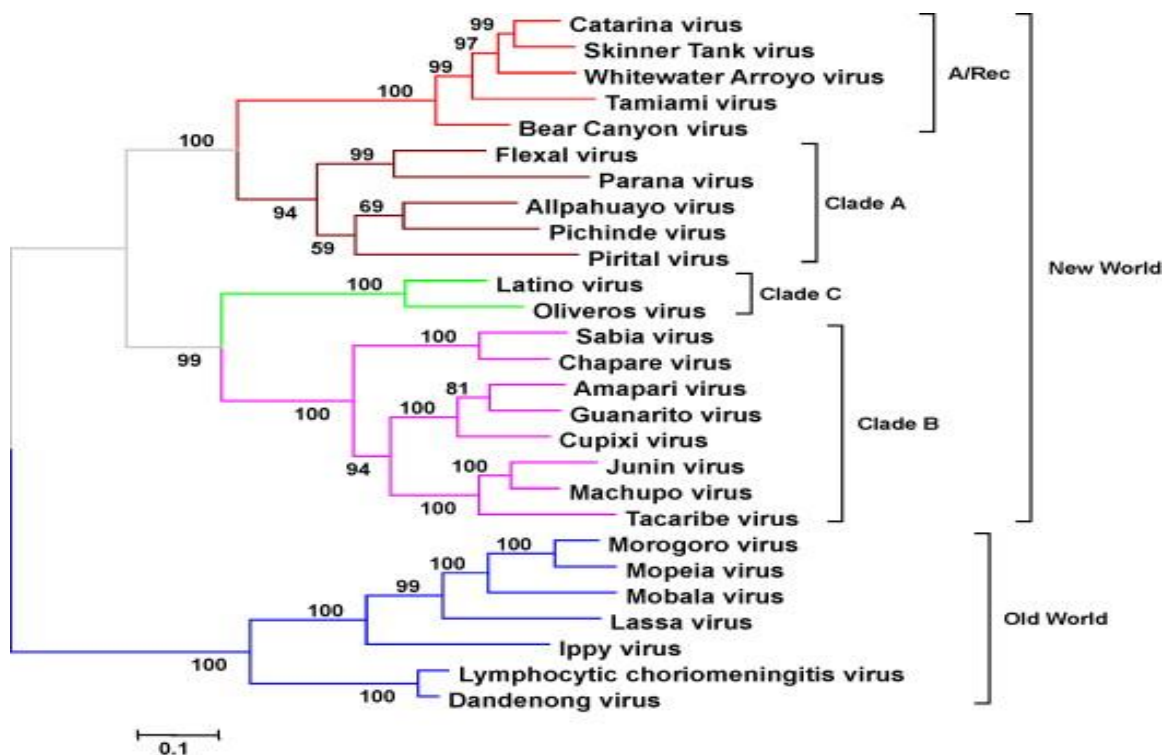


Figure 1.1. Phylogenetic analysis New and Old World arenaviruses. Phylogenetic tree representing both the OW and NW arenaviruses. Clades within the NW arenaviruses are separated by color, with Junin virus lying within Clade B with several other pathogenic arenaviruses (Sabia, Chapare, Guanarito, and Machupo). The figure was reproduced with permission from (Emonet et al., 2009).

Arroyo virus (WWAV), Tamiami virus (TAMV), and Bear Canyon virus (BCNV) (Charrel et al., 2003). The origin of the A/Rec clade is suggested to be a recombination event between members of clades A and B (Archer and Rico-Hesse, 2002; Charrel et al., 2001; Charrel et al., 2002; Fulhorst et al., 2001). However, this observation has recently been credited to be a result of the analytical method used for phylogenetic analysis and does not represent evidence of a true recombination event (Milazzo et al., 2008). Recently discovered NW arenavirus species that have not been recognized by the ICTV include Pinhal virus (Emonet, unpublished data), Catarina virus (Cajimat et al., 2007), Skinner Tank virus (Cajimat et al., 2008), and Chapare virus (Delgado et al., 2008).

Geographical Distribution of JUNV and Epidemiology of AHF

The distribution of each virus species is limited to the geographic distribution of its associated natural rodent host, and each arenavirus species is closely associated with either a single rodent species or a few very closely related rodent species (Charrel et al., 2003). African arenaviruses circulate within regions between rodents of the family *Muridae*, genus *Praomys*, *Mastomys*, or *Arvicanthis*. American arenaviruses circulate among rodents of the family *Cricetidae*, genus *Calomys*, *Oryzomys*, *Neotoma*, *Sigmodon*, *Nephelomys*, *Zygodontomys*, *Oecomys*, *Neacomys*, or *Akodon* (Zapata and Salvato, 2013). The only arenavirus to achieve worldwide distribution is LCMV, which can be attributed to the worldwide distribution of its natural host, *Mus musculus* (Salazar-Bravo et al., 2002).

Arenaviruses typically produce persistent infections within their rodent hosts with chronic viremia, and shed infectious particles through urine, feces, and saliva (Justines and Johnson, 1968; Peralta et al., 1979; Skinner et al., 1977). The infectious particles can infect other rodents or even humans through direct contact with abraded skin or mucosal surfaces. Although infections in rodents are generally considered to be asymptomatic, arenavirus infection can cause changes in weight, extensive viral dissemination, and reduction in size

and fertility. These changes are dependent on viral load as well as both virus and host genetics (Borremans et al., 2011; Vitullo et al., 1987; Vitullo and Merani, 1988). While transmission of the OW arenavirus LASV appears to transmit vertically in *Mastomys natalensis* (Zapata and Salvato, 2013), the NW arenavirus JUNV appears to undergo more frequent horizontal transmission, although vertical transmission can still occur. The natural host of JUNV, *Calomys musculus*, shows a pattern of transmission among males with evidence of scarring, implying that transmission is occurring during aggressive encounters (Mills et al., 1994; Sabattini and Maiztegui, 1970; Vitullo and Merani, 1990).

Argentine hemorrhagic fever (AHF), the clinical disease caused by JUNV infection, emerged in 1958 within the Buenos Aires region of Argentina. The emergence of the disease coincided with the large-scale deforestation of the region to create farmland. *Calomys musculus* mice began to inhabit the cornfields and surrounding areas near Buenos Aires as a result of the deforestation, and the species population reaches its peak density during the harvest season between March and June. These events led to an

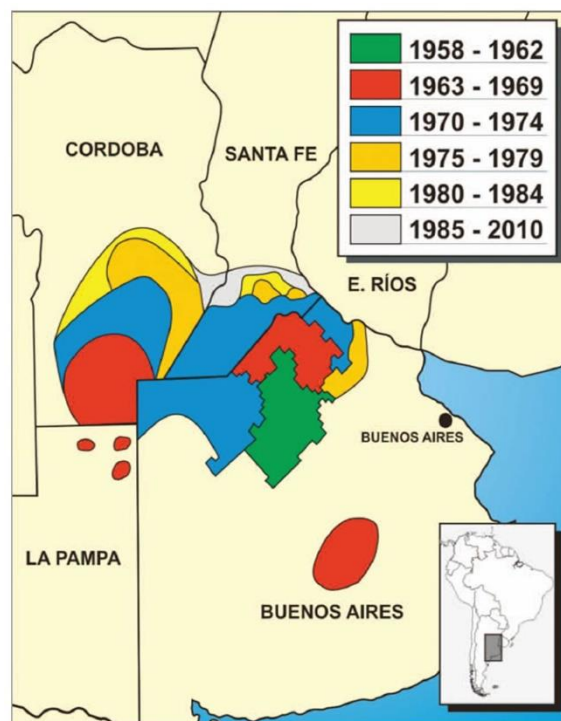


Figure 1.2. Chronological expansion of AHF endemic area. Reproduced with permission from (Ambrosio et al., 2011).

increased interaction frequency between farmers and *C. musculus*. Exposure to JUNV is proposed to occur through either direct contact with infected rodents, contact with rodent excreta, or inhalation of aerosolized infectious particles created by the harvesting machinery (Maiztegui, 1975; Peters, 2006). While person-to-person transmission is rare, exposure to body fluids of direct patient contact can lead to occasional nosocomial secondary infections (Grant et al., 2012). The original endemic region consisted of a 16,000 km² area of humid grasslands in the northern Buenos Aires province, leaving around 270,000 individuals at risk of exposure. However, the endemic region continued to spread over the next few decades to include another 134,000 km² of land across three separate provinces north of Buenos Aires (Santa Fe, La Pampa, and Cordoba) (Fig. 1.2), leaving over three million individuals at risk of exposure to JUNV (Maiztegui et al., 1986). The current endemic area leaves around five million individuals at risk of exposure. Prior to the introduction of a vaccine to protect against AHF, the number of annual cases ranged from a few hundred to more than three thousand (Enria et al., 2008). A live-attenuated vaccine, Candidate #1 (Can) was generated by the United States Army Medical Research Institute of Infectious Diseases (USAMRIID) and is currently administered to the at-risk population in Argentina. The vaccine has reduced the number of annual clinical AHF cases to 30-50 (Ambrosio et al., 2011).

CLINICAL PRESENTATION AND PATHOGENESIS OF AHF

Signs, symptoms, and progression of AHF

The incubation period for JUNV in human infections can range from one to two weeks, and infections have an 80 percent morbidity rate with an associated 15-20 percent

mortality. AHF consists of three phases: prodromal, neurological-hemorrhagic, and convalescent (Enria et al., 2004).

The prodromal phase begins upon the onset of flu-like symptoms, which includes chills, headache, myalgia of the lower back, malaise, anorexia, and a moderate hyperthermia. This phase lasts approximately one week and additional symptoms may appear during this time, including nausea or vomiting, epigastric pain, photophobia, retro-orbital pain, dizziness, or mild diarrhea. During this time, clinical signs manifest themselves. Flushing of the face, neck, and upper chest are common, and cutaneous petechiae can be found along the upper chest, axillary regions, and arms. Patients also commonly present with periorbital edema and conjunctival congestion, and the gums may appear congested and bleed spontaneously. An enanthem of the soft palate is noted in the majority of patients. The cervical lymph nodes are typically swollen. There are usually no pulmonary abnormalities, splenomegaly, or hepatomegaly. As the patient nears the end of this phase they may become irritable and lethargic, and a fine tremor in the hand and tongue can appear (Enria et al., 2008). Clinical findings during the first week of symptoms include leukopenia and thrombocytopenia, with white blood cell counts and platelet counts falling to 1,000-2,000 and 50,00-100,000/ μ L, respectively. Aspartate transaminase, creatine phosphokinase, and lactate dehydrogenase are all slightly elevated, and proteinuria is observed (Enria et al., 2008).

About 20 to 30 percent of patients transition into the neurologic-hemorrhagic phase, which begins between 8 and 12 days after the onset of symptoms. Severe hemorrhagic manifestations appear, including melena, hematemesis, hemoptysis, hematomas, hematuria, and epistaxis. Neurological symptoms onset with confusion, ataxia, and irritability. The symptoms progress to delirium, convulsions, and coma. Secondary bacterial infections can occur, resulting in further complications (Enria et al., 2008).

Survivors experience convalescence that lasts between 1 and 3 months, displaying irritability, asthenia, memory changes, and hair loss. Approximately one tenth of the

patients who receive immune plasma will develop a late neurological syndrome (LNS). After a period free of symptoms, the LNS presents with hyperthermia, cerebellar ataxia, and cranial nerve palsy (Enria et al., 2004; Enria et al., 2008). This LNS has not been reported among patients who recovered without receiving specific treatment (Enria et al., 1985; Maiztegui et al., 1979). Only a single case has presented in a patient who received intravenous ribavirin (Enria et al., 1987).

Pathogenesis of AHF

Inhalation of aerosolized infectious particles is believed to be the most common route of infection, and JUNV virus replication is proposed to occur at the initial site of infection, usually the lungs. JUNV presumably escapes the lungs through the uptake of the virus by macrophages and migration of the infected macrophages to the draining lymph nodes (Gonzalez et al., 1980; Gonzalez et al., 1982). The virus spreads to additional parenchymal tissues through the vascular system and affects a number of organs, including the vascular system, myocardium, adrenal system, lymphoid organs, kidneys, and the central nervous system (Buchmeier et al., 2013).

Macrophages are important cellular targets during arenavirus infection, and evidence of macrophage infection in clinical cases has been demonstrated through immunofluorescent staining of viral antigens and electron microscopy of budding virions. Destruction of the lymph nodes and splenic white pulp has also been observed in lethal cases of AHF, suggesting the tropism of JUNV for lymphatic tissue (Gonzalez et al., 1980). It is possible that the tropism of JUNV for macrophages plays a key role in the evasion of the host immune response. One study has shown that human macrophages infected with a virulent strain of JUNV fail to produce detectable interferon (IFN) (Groseth et al., 2011), whereas a separate study shows that murine macrophages infected with an attenuated strain of JUNV activate the IFN response through detection of the JUNV GP by

toll-like receptor 2 (TLR2) (Cuevas et al., 2011). Virulent strains of the OW and NW arenaviruses Pichinde and Lassa both establish productive infections in macrophages, yet the infected macrophages fail to activate and produce pro-inflammatory cytokines (Baize et al., 2004; Fennewald et al., 2002; Lukashevich et al., 1999). Survival of Lassa fever (LF) has been shown to correlate with elevated pro-inflammatory cytokine levels in the patients' plasma, whereas low levels of these cytokines in the plasma correlates with a poor prognosis (Mahanty et al., 2001).

The hemorrhagic manifestations of AHF have been attributed to the thrombocytopenia, reduction in serum complement activity, low levels of blood coagulation activity, and decreased platelet aggregation (de Bracco et al., 1978; Heller et al., 1995; Weissenbacher et al., 1987). There is evidence for an inhibitor of platelet aggregation during JUNV infection (Weissenbacher et al., 1987), but the specific inhibitor remains elusive. Interestingly, infection of endothelial cells with a virulent JUNV strain produced no detectable cytopathic effects *in vitro* (Gomez et al., 2003), which is consistent with the absence of vascular destruction *in vivo* (Weissenbacher et al., 1987). Additionally, infection of endothelial cell cultures with JUNV resulted in a decrease in expression and secretion of coagulation factors including von Willebrand factor (VWF), which contrasts with clinical data that describes an increase in VWF in patient serum (Molinas et al., 1989). This data suggests that there is another source of VWF secretion in AHF patients. However, endothelial cell cultures infected with a virulent strain of JUNV induced the production of nitric oxide and prostaglandin PGI₂, which increase vascular permeability (Gomez et al., 2003). Decreases in factor VIII and IX, elevated factor V, and an increase in activated partial thromboplastin time have also been associated with AHF (Enria et al., 2008; Heller et al., 1995).

IMMUNE RESPONSE TO JUNV

Innate Immune Response

Severity of the acute disease has shown to have a positive correlation with high endogenous levels of IFN- α (Levis et al., 1985), and elevated levels of IFN- α result in a poor prognosis. Elevated IFN- α during the acute disease is typically accompanied by the presence of hyperthermia, chills, and backache. Additionally, abnormal platelet function and low platelet counts are commonly reported in correlation with elevated IFN- α (Lerer et al., 1991; Levis et al., 1984; Levis et al., 1985). Elevated levels of IFN- α have been observed during the acute illness of JUNV infection in both guinea pigs and rhesus macaques, further validating the clinical data (Dejean et al., 1987; Dejean et al., 1988; Kenyon et al., 1992).

While high levels of IFN- α are correlative in severe disease and poor prognosis, the degree to which the cytokine is causative of the severity of the acute disease signs and symptoms remains unclear. The infection of CD34+ hematopoietic progenitor cells with JUNV did not affect their survival or the ability of the cells to form megakaryocytes. However, the infection did trigger a robust production of cytokines. The induction of cytokine production was triggered by IFN- α , which acted via the paracrine route and resulted in impaired platelet formation and release from the megakaryocytes (Pozner et al., 2010). These *in vitro* findings suggest a role for IFN- α in the development of thrombocytopenia during the acute disease, raising the possibility that elevated IFN- α is a key contributor to the coagulopathy observed in severe cases of AHF.

The cytokines IL-6, IL-8, IL-10, and TNF- α are typically elevated in patients exhibiting a wide range of disease severities, indicating the involvement of both the pro- and anti-inflammatory pathways in the disease (Marta et al., 1999). *In vitro* infection of human peripheral blood mononuclear cells (PBMCs) with the virulent Romero (Rom) strain of JUNV did not upregulate their production of IL-6, IL-10, IL-12, type I IFN, or

TNF- α , so it is unlikely that the source of the cytokines is of mononuclear origin. Interestingly, infection of PBMCs with the non-pathogenic NW arenavirus TCRV results in an increased production of IL-6, IL-10, and TNF- α (Groseth et al., 2011). Another possible source of type I IFN during JUNV infection could be parenchymal cells. Human lung epithelial carcinoma cells (A549) produce type I IFN and IFN-stimulated genes (ISGs) upon infection by either the virulent Rom strain of JUNV and the attenuated Can strain. Phosphorylation of the signal transducer and activator of transcription (STAT) 1 also occurs during infection with either Rom or Can, and RIG-I serves as the primary means of detection upon infection with either strain (Huang et al., 2012). While the expression of type I IFN is high in clinical cases, it is interesting that JUNV appear to be resistant to the type I IFN response. In a murine cell line, pre-treatment of the cells with type I IFN completely abolished replication of both Rom and Can. However, treatment of A549 cells with type I IFN only reduced replication of Rom and Can by approximately 3-log and 2-log, respectively. The sensitivity of JUNV to type I IFN in murine cells may contribute to the resistance to disease in mice, and the resistance to type I IFN in human cells may play a role in the pathogenesis of AHF in clinical cases (Huang et al., 2014).

Adaptive Immune Response

During the acute phase of AHF there is typically a depletion of both T and B lymphocytes, and the ratio of CD4 to CD8 T cells is reduced. The cell counts usually return to the normal range during convalescence (Vallejos et al., 1989). Polymorphonuclear cells (PMNCs) can mediate antibody-dependent cell cytotoxicity (ADCC) with a similar efficiency to peripheral blood mononuclear cells (PBMCs) during acute and early convalescent AHF, suggesting a role for ADCC in clearing JUNV-infected cells (Ambrosio et al., 1992). Consequently, necrosis of lymphoid tissue in the spleen has been observed in JUNV-infected guinea pigs (Kenyon et al., 1985; Weissenbacher et al., 1975b).

While the T cell response to JUNV has not been well characterized, LCMV has been utilized extensively to study the adaptive immune response during arenavirus infections. There is a strong proliferation of CD8⁺ T cells during the first week of LCMV infection in mice, which peaks at 8 days post-infection (Buchmeier et al., 1980; Butz and Bevan, 1998). The expanded subset of CD8⁺ T cells consists of cells that react to specific epitopes derived from viral glycoprotein complex (GPC) and nucleoprotein (NP), and the T cells exhibit a potent cytotoxic activity against LCMV-infected cells (Blattman et al., 2000; Murali-Krishna et al., 1998). Infection of mice with the Can strain of JUNV shows a similar kinetic of CD8⁺ T cell activation that peaks 7 days post-infection (Cuevas and Ross, 2014).

The antibody response to JUNV infection plays a significant role in both clearing the infection and providing immunity. Attenuated strains of JUNV are lethal in immunosuppressed animals, and virulent strains of JUNV are lethal in immunocompetent animals due to the absence of an effective antibody response that results in ADCC (Kenyon et al., 1985). However, guinea pigs immunized with either the GPC of JUNV or infected with attenuated JUNV strains generate high levels of neutralizing antibodies against the GPC, and the guinea pigs are protected against challenge by a virulent JUNV strain (Avila et al., 1979; Seregin et al., 2010; Weissenbacher et al., 1975a). Additionally, treatment of AHF using immune plasma is effective during the early stages of illness in both marmosets and human clinical cases (Avila et al., 1987; Enria et al., 2008).

PREVENTION AND TREATMENT OF AHF

Inactivated, Subunit, and Vector-based Vaccines

A number of replication-incompetent and vector-based vaccine candidates have been tested for efficacy in animal models of AHF. Initially, the sub-viral components were tested for their immunogenicity by treating purified virus particles with a nonionic detergent to disrupt the viral envelope. The fraction containing the glycoprotein was the only fraction that was capable of providing complete protection against a subsequent challenge with a virulent JUNV by stimulating the production of neutralizing antibodies (Cresta et al., 1980).

Formalin-inactivated JUNV strain XJ Clone 3 (XJCl3) has been evaluated for its efficacy in guinea pigs as a vaccine, and the killed virus stimulated the production of neutralizing antibodies. However, despite the high antibody titers, protection against a virulent JUNV strain was not achieved (Videla et al., 1989). While there are several effective formalin-inactivated vaccines that are effective and currently in use, there are other examples of ineffective formalin-inactivated vaccines. The formalin-fixed respiratory syncytial virus (RSV) did not pass clinical trials due to the exacerbation of disease despite the production of antibodies. The inactivated virus was unable to stimulate signaling pathways involving specific pattern recognition receptors (PRRs) that are necessary to activate a CD8⁺ T cell response. Additionally, toll-like receptor (TLR) stimulation is necessary in mice to yield high-avidity antibodies, which could explain the low-avidity antibodies produced in response to the inactivated RSV vaccine (Delgado et al., 2009; Varga, 2009). Children who were previously vaccinated with a formalin-inactivated measles virus have also presented with atypical measles infections (Fulginiti et al., 1967). Thus, inactivated JUNV particles may fail to produce high-avidity antibodies due to the absence of PRR recognition of virus antigens upon vaccination. An alphavirus-based replicon system expressing the envelope glycoprotein (GPC) of the Can strain of JUNV resulted in a partial protection against the virulent Rom strain, and a second booster vaccination provided complete protection (Seregin et al., 2010). This supports the hypothesis that the activation of PRR-based signaling achieved through replication-

competent vaccines helps to stimulate the production of mature, high-avidity antibodies that are capable of providing protection.

Live Attenuated Vaccines

Antibodies developed against two closely related viruses can sometimes cross-protect against both viruses. Thus, the non-pathogenic NW arenavirus TCRV was tested as a potential vaccine to protect against AHF. Guinea pigs are able to completely clear TCRV within 30 days post-infection, and they generate a robust immune response that includes the development of antibodies that are cross-reactive to JUNV. The antibodies persist for two years, and only a single dose of TCRV is required to provide full protection against challenge by a virulent JUNV strain at 18 months post-vaccination (Weissenbacher et al., 1976; Weissenbacher et al., 1975a). Marmosets are also able to clear TCRV infection efficiently, and no viremia is present at 3 weeks post-inoculation. The marmosets do not show any abnormal blood cell counts, and maintain normal hematocrit and hemoglobin. There are neutralizing anti-TCRV antibodies present 3 weeks post-infection, and subsequent challenge with the virulent JUNV XJ strain at two months post-TCRV-infection yields no detectable disease symptoms and no detectable viremia. The marmosets also developed neutralizing anti-JUNV antibodies (Weissenbacher et al., 1982).

The XJ strain was isolated in 1958 from a human clinical case (Parodi et al., 1958), and has been used to develop multiple live-attenuated virus strains. The XJ strain was plaqued in immortalized rabbit kidney (MA-111) cells to create the XJ Clone 3 (XJC13) strain, which was determined to be attenuated in both mice and guinea pigs. The XJC13 strain also stimulated the production of high titers of neutralizing antibodies and eliciting long-term immunity (Avila et al., 1979; Candurra et al., 1989). The positive results in pre-clinical studies allowed the vaccine candidate to advance to clinical studies using a seed vaccine that was created in suckling mouse brains, and the vaccine strain was administered

to 636 volunteers over a two year period. Their health and immunological status were both monitored for nine years post-vaccination, and most vaccinees developed a subclinical illness. However, all clinical and laboratory values and parameters were within normal ranges for all of the volunteers. Only 165 of the original 636 individuals were tested nine years post-vaccination, and 90 percent of those individuals had maintained detectable levels of neutralizing antibodies. Despite the positive results, the clinical trials were suspended since the virus was prepared in suckling mouse brains and cloned in heteroploid cell lines (Ambrosio et al., 2011; Ruggiero et al., 1981).

XJ0, another attenuated strain derived from the XJ parental strain, was reported to provide complete protection from a virulent JUNV strain in guinea pigs. The studies were terminated upon discovering persistence of the strain in the lymphohemopoietic organs of guinea pigs (Ambrosio et al., 2011; de Guerrero et al., 1985).

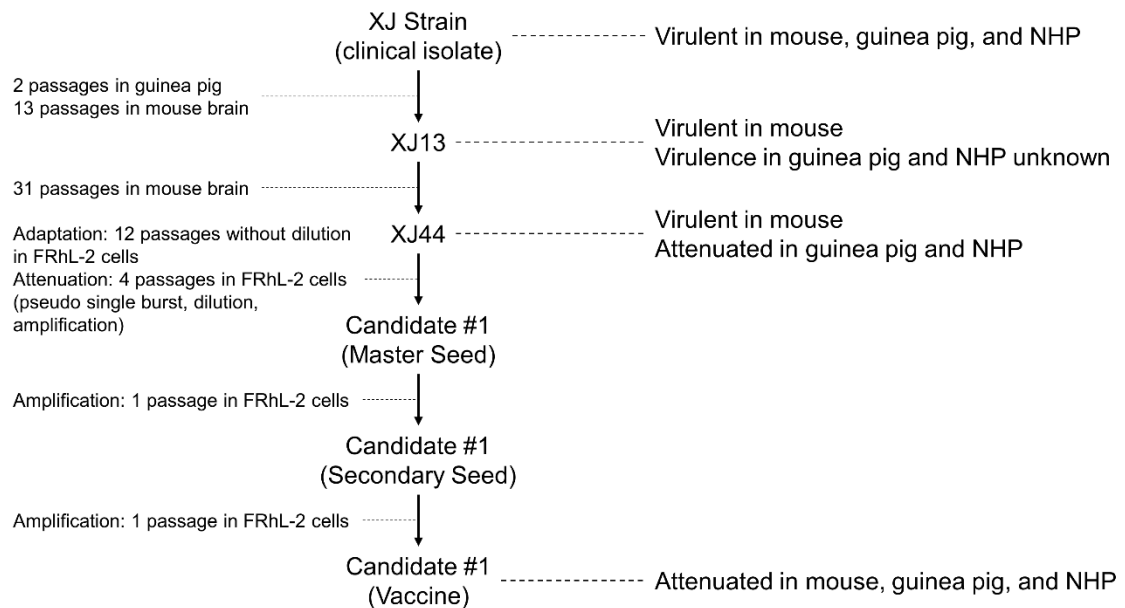


Fig. 1.3. Generating the Candidate #1 vaccine from the XJ clinical isolate.

The live attenuated vaccine currently approved for use in endemic areas is the Can strain, and was developed in a joint effort between the Argentine Ministry of Health and

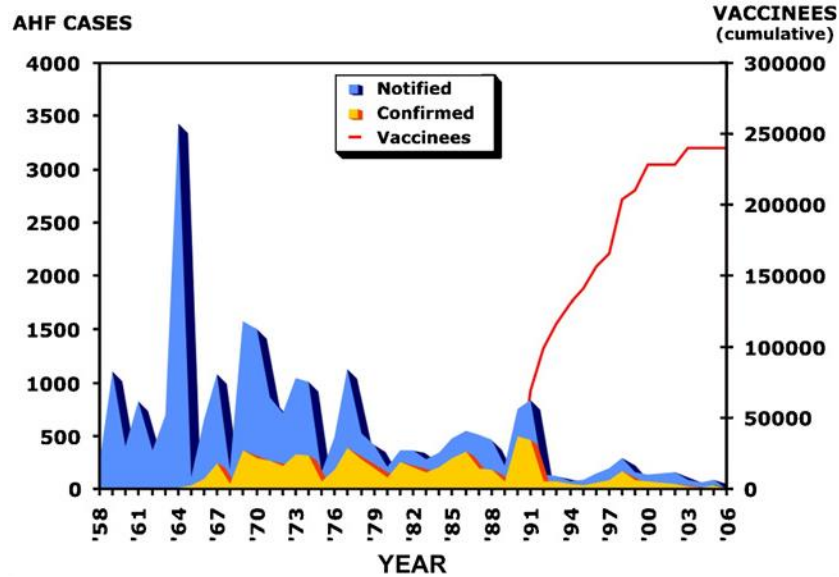


Figure 1.4. Decrease in AHF incidence upon introduction of the Candidate #1 vaccine into endemic areas. Reproduced with permission from (Enria et al., 2008).

Social Action and USAMRIID under funding from the United Nations Development Program and Pan American Health Organization (Ambrosio et al., 2011). The XJ strain served as the parental strain, and the virus was passed 2 times in guinea pigs followed by 44 times in newborn mouse brains. The homogenate from the 44th mouse brain passage was subjected to adaptation and further clonal selection in a diploid fetal rhesus monkey (FRhL-2) cell line for a total of 16 passages. The primary and secondary seed stocks were each amplified a single time in FRhL-2 cells to yield the Can vaccine stock (Fig. 1.3) (Ambrosio et al., 2011; Goni et al., 2010). The Can vaccine underwent extensive testing for both safety and immunogenicity in mice, guinea pigs, and rhesus monkeys (McKee et al., 1992; Medeot et al., 1990) and was determined to be both safe and efficacious in its ability to generate a protective response. The Can vaccine was subjected to clinical trials that included over 6,500 volunteers within the endemic region of Argentina, and it proved to be highly immunogenic and protective against AHF. Additionally, there was an absence of any adverse side effects in the study (Maiztegui et al., 1998). Use of the vaccine within endemic areas over the last few decades has significantly reduced the incidence of disease (Fig. 1.4).

Therapeutics

The use of immune plasma from seropositive donors is the standard treatment for AHF in endemic regions. The mortality rate among clinical cases is reduced from 15-30% to 1-2% when the treatment is received within the 8 days of symptoms (Maiztegui, 1975). However, 8-10% of the patients treated with immune plasma develop a late neurological syndrome (LNS) that does not occur after acute infections that are cleared naturally (Maiztegui, 1975). Symptoms of the LNS include ataxia, fever, cerebral nerve palsies, tremors, and gait lateralization (Maiztegui et al., 1979). The window in which treatment is effective correlates with the absence of the virus in the central nervous system (CNS). Once the virus gains access to the CNS, the efficacy of immune therapy is drastically reduced in guinea pigs (Zeitlin et al., 2016).

IgG purified from immune plasma has also been evaluated as a potential treatment. Fractions containing IgG_{1,2,3,4} or just the F(ab')₂ region of IgG were administered to JUNV-infected guinea pigs. While the fraction containing IgG_{1,2,3,4} was completely protective against lethal disease at a dose of 6,000 TU/kg, the F(ab')₂ region alone provided no protection after two doses of 15,000 TU/kg. While neutralizing antibodies are important in clearing the virus, the neutralization of JUNV particles is not sufficient to protect against lethal disease, as demonstrated by the lack of protection provided by the F(ab')₂ regions alone. It is possible that ADCC is necessary to control the infection through the elimination of infected cells (Kenyon et al., 1990). The ability to produce chimeric monoclonal antibodies (mAbs) in transgenic *Nicotiana benthamiana* plants allows for a greater availability of treatment, and anti-JUNV mAbs produced in *N. benthamiana* have provided complete protection against lethal disease when administered within the first 6 days post-infection (Zeitlin et al., 2016).

The only small molecule drug that is currently approved for JUNV infection is Ribavirin, a nucleoside analog. Ribavirin is clinically proven to be an effective broad-range antiviral drug (Parker, 2005). In rhesus macaques, lethal LASV-associated disease was only prevented whenever the drug was administered prior to 6 days post-infection. Otherwise, treatment only resulted in a delayed time to death (Jahrling et al., 1980). Ribavirin yielded similar results in JUNV-infected guinea pigs. The drug only served to increase the mean survival time of the guinea pigs, but ultimately did not alter the disease outcome regardless of the route of inoculation (Kenyon et al., 1986). However, multiple doses over an extended period of time has been demonstrated to significantly increase the mean survival of JUNV-infected guinea pigs (Salazar et al., 2012). In the clinical setting, ribavirin has proven successful whenever treatment begins shortly after exposure to JUNV (Weissenbacher et al., 1987).

ANIMAL MODELS OF AHF

Natural Host

Evidence suggests that *Calomys musculinus* may maintain a lifelong persistent infection. In a laboratory setting, newborn *C. musculinus* pups did not develop neurological symptoms after intranasal inoculation of JUNV. However, the infection was lethal in 70% of the pups. Infectious particles were detected in the blood, urine, and oral swab in survivors throughout the 480 day study. By the end point of the study, all survivors exhibited dissemination of the virus to the spleen, kidneys, brain, and salivary glands. There was also a significant reduction in fertility (Lampuri et al., 1982; Vitullo et al., 1987; Vitullo and Merani, 1988). A separate study demonstrated that adult *C. musculinus* did not

develop any symptomatic disease upon intranasal inoculation of the Cba An 9446 strain of JUNV. After 150 days, only 50% of the rodents maintained a persistent infection. The remaining half seroconverted but no infectious particles were detectable. During gestation, the virus did not transmit to any fetuses, but 50% of the weaned pups that were nursed by viremic mothers became infected (Vitullo and Merani, 1990). The findings in the laboratory setting support the suggested mechanisms of both horizontal and vertical transmission in nature.

Mice

Infection of laboratory mice produces a lethal disease that includes the typical symptoms of viral encephalitis, including tremors, spontaneous convulsions, walking lateralization, and eventual paralysis of the hind legs. Similar disease progression occurred despite the JUNV strain or mouse strain used in the study. However, the severity of disease is dependent on age. Mice between 1 and 10 days of age are most susceptible to the infection, whereas older mice experienced a significantly more mild disease with changes in the presentation of symptoms (Boxaca et al., 1973). The virus reaches a similar titer in the brain at around day 5 regardless of the age of the mouse at the time of inoculation. However, mice beyond 30 days old at the time of inoculation are able to clear the virus from the brain by day 10. Treatment of the young mice with an IFN inducer significantly increased their survival time (Boxaca et al., 1973; Weissenbacher et al., 1975b). While JUNV actively infects neurons and astrocytes in the mouse brain (Lascano and Berria, 1974), the damage appears to be immune-mediated. Thymectomized mice are completely protected from lethal JUNV-mediated disease, and instead develop a persistent infection which can be detected for up to 7 weeks in the brain with no signs of inflammation throughout the infection. The protective effect can be counteracted by providing the mice with spleen cells of immune adult mice (Weissenbacher et al., 1969).

While immunocompetent adult mice do not exhibit severe disease signs and symptoms, C3H/HeJ mice lacking a functional TLR-4 develop a lethal disease when infected intracranially with the XJ strain. No neutralizing antibody response is detectable in this disease model, and the mice experience a delayed hypersensitivity reaction. However, the mice are not susceptible to the XJ strain by any other route of infection (Campetella et al., 1988).

Recently, mice lacking a functional IFN- $\alpha/\beta\gamma$ receptor were evaluated as an animal model of JUNV infection. The Rom strain caused a uniformly lethal disease among the mice when injected intraperitoneally. While IFN- $\alpha/\beta\gamma$ receptor knockout mice develop a disseminated infection, the pathology is somewhat different from what is observed in humans. The mice display a multifocal myocarditis, increase in white pulp in the spleen, hepatocellular necrosis, and patches of mononuclear cells in the cortices of the kidneys. The brains of infected mice pronounced leptomeningitis and perivascular cuffing of neutrophils. While humans have been reported to develop myocarditis, only about one quarter of patients developed meningoencephalitis (Elsner et al., 1973). The lesions in the kidneys of IFN- $\alpha/\beta\gamma$ receptor knockout mice are different from those observed in human cases, which are typically hemorrhagic lesions (Cossio et al., 1975).

Upon discovering that JUNV utilizes transferrin receptor 1 (TfR1) to enter target cells, it was hypothesized that the lack of this receptor in mice played a role in the decreased virulence in mouse models of disease (Radoshitzky et al., 2007). However, it was later discovered that JUNV could infect murine cells via a TfR1-independent mechanism and induce innate immune response pathways in the cells (Cuevas et al., 2011). Thus, the entry mechanism is likely different for JUNV in human cells and murine cells.

Guinea Pigs

While mice treated with immunosuppressive drugs exhibit a decreased mortality when challenged with virulent JUNV strains, immunosuppression of guinea pigs causes a lethal disease resembling AHF. This result provides evidence that a competent immune system is necessary to clear the infection in guinea pigs (Kenyon et al., 1985).

JUNV-induced disease in guinea pigs has shown some variability between JUNV strains in terms of mortality, time to death, and distribution among organs. While a number of strains cause a visceral illness with a high viremia, and replication occurring primarily in the spleen, lymph nodes, and bone marrow. These organs all displayed necrosis in the severe cases, and the guinea pigs succumbed to illness around 13-15 days post-infection. Another group of strains caused a neurological illness with a transient level of replication, lymphocyte depletion within the spleen and lymph nodes, and no viremia or replication in the bone marrow. Virus can be found in the brain with a broad range of poliomyelitis between guinea pigs. Leg paralysis is common before death, appearing between days 28-34 post-infection. Only one virus strain caused illness that exhibited characteristics from each pattern of illness. However, none of the strains were capable of replicating the signs, symptoms, and pathology observed in their respective human cases (Kenyon et al., 1988).

The Rom strain of JUNV is virulent in both inbred Strain 13 and outbred Hartley guinea pigs, causing a disease that closely resembles clinical cases of AHF in terms of pathology and clinical values. Hartley guinea pigs develop a lethal viremic infection with both thrombocytopenia and leukopenia, as well as elevated aspartate aminotransferase in the serum. Infected Hartley guinea pigs succumb to infection between 13 and 17 days post-infection. The only observable dissimilarity is the absence of petechiae on the skin of infected guinea pigs (Yun et al., 2008). These findings validate Hartley guinea pigs as a relevant animal model for the study of JUNV pathogenesis and vaccine development.

Nonhuman Primates

Marmosets are susceptible to JUNV and develop a severe disease that resembles clinical AHF, exhibiting both hemorrhagic and neurologic manifestations prior to succumbing to disease by 3 weeks post-infection (Weissenbacher et al., 1979). There is also evidence that treatment of marmosets with immune plasma results in the development of a LNS that resembles human LNS (Weissenbacher et al., 1986). Infection of marmosets with TCRV triggered an immune response that was capable of cross-protecting the marmosets against JUNV for between 2 and 16 month depending on the route of TCRV inoculation (Samoilovich et al., 1988; Samoilovich et al., 1984; Weissenbacher et al., 1982). Additionally, the live attenuated Can strain has been evaluated for safety and immunogenicity in rhesus macaques, demonstrating complete protection against virulent JUNV strains (McKee et al., 1992, 1993).

VIRION ARCHITECTURE, GENOME ORGANIZATION, AND LIFE CYCLE OF JUNV

Virion Architecture and Genome Organization

Arenavirus particles are pleomorphic in structure, and can range in size from 40 to 300 nm, but are typically 110-130 nm in size (Murphy and Whitfield, 1975). The virions consist of a nucleocapsid that is surrounded by a bi-lipid membrane envelope which is densely packed with glycoproteins. The virions are granular in appearance in electron micrographs due to the propensity of the budding machinery to incorporate ribosomes into infectious particles, and their appearance in micrographs contributed to the name of the virus family (*arenosus*, or sandy). Although this phenomenon is ubiquitous among all arenavirus species, it has yet to be determined whether the incorporation of ribosomes into the virions is advantageous for the life cycle (Buchmeier et al., 2013).

The arenavirus genome is comprised of two ambisense, single-stranded RNA segments. Each segment encodes two genes in an opposite orientation to one another. The large (L) segment is approximately 7 kb in length and encodes the matrix (Z) protein and the RNA-dependent RNA polymerase (LP). The Z protein is responsible for budding through interaction with itself and the cellular endosomal sorting complexes required for transport (ESCRT) machinery, recruitment of the ribonucleoprotein (RNP) complex, and interaction with the GPC on the cell surface. The Z protein additionally downregulates the activity of the viral replication complex through inhibition of the polymerase, and can also manipulate the cellular immune response to the infection (Fehling et al., 2012). The small (S) segment is approximately 3.4 kb in length and encodes both the nucleoprotein (NP) and the glycoprotein complex (GPC). The GPC undergoes both co- and post-translational processing within the endoplasmic reticulum (ER) and Golgi apparatus, where it is heavily glycosylated and eventually cleaved into a stable signal peptide (SSP) and two separate glycoproteins (G1 and G2). The G1-G2 cleavage is carried out by the Subtilisin Kexin Isozyme-1 (SKI-1)/Site-1 Protease (S1P). The mature complexes are included into budding virions on the cell surface and are responsible for host cell attachment and entry of the virions into target cells (Burri et al., 2012a; Burri et al., 2012b). The NP is an essential co-factor in the replication of the virus genome, and the protein has been shown to block the ability of the cellular antiviral machinery to recognize the viral RNA (Buchmeier et al., 2013).

Life Cycle of JUNV

Upon binding to its cellular receptor TfR1, JUNV undergoes clathrin-mediated endocytosis (Martinez et al., 2007). Once inside the endosome, the low pH allows the endosomal-viral membrane fusion triggered by the GPC (Klewitz et al., 2007). Viral replication is initiated upon the release of the RNP complex into the host cell.

Initial rounds of replication consist of the synthesis of anti-genomic copies of the L and S segments and mRNA that encodes both the NP and LP. Synthesis of viral RNA is initiated by a 19 nucleotide promoter region at the 3'-end of the genomic and anti-genomic segments. This sequence is recognized by the LP and is highly conserved among all arenavirus species (Kranzusch et al., 2010). Due to the high degree of complementarity between the 5' and 3' ends of the segments, a panhandle structure is hypothesized to form (Salvato and Shimomaye, 1989). Termination can occur in one of two ways. In order to generate mRNA, primary transcription is terminated within the intergenic region (IGR) of either segment, which forms a secondary hairpin structure. This structure has also been suggested to stabilize the 3' end of the mRNA since polyadenylation does not occur

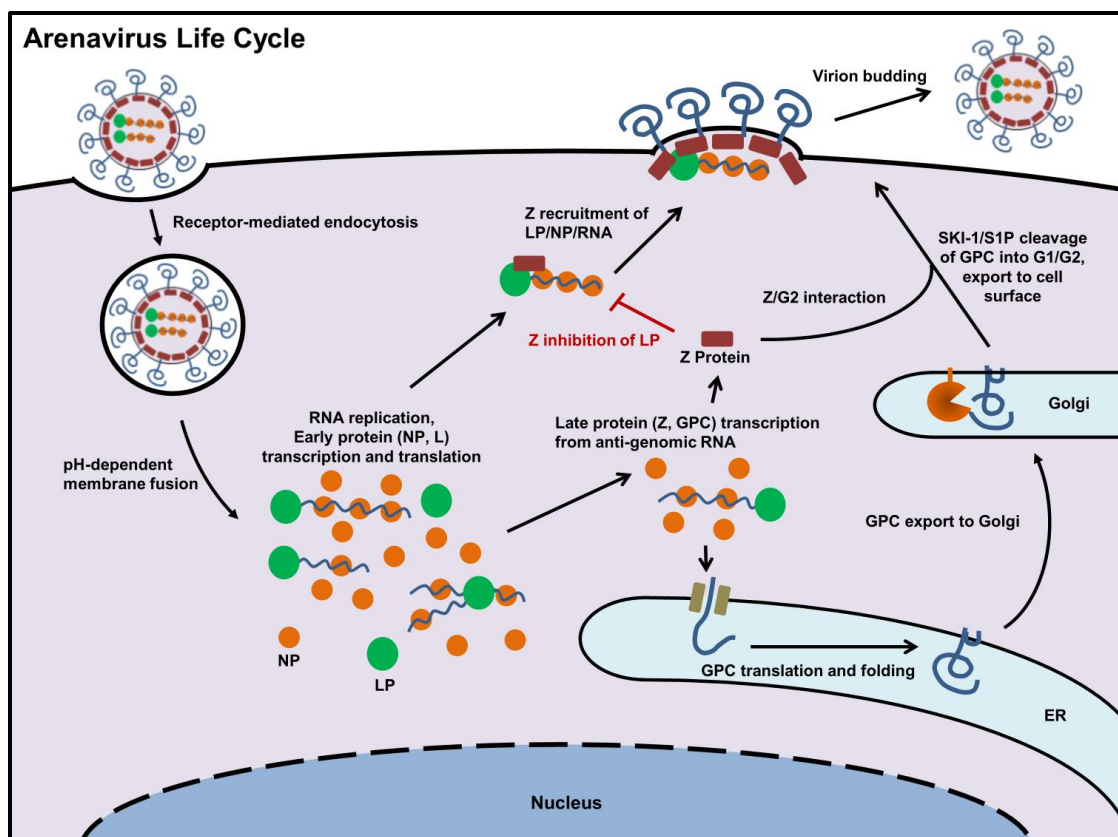


Figure 1.5: The Arenavirus Life Cycle. After entry, replication of the genome and transcription of the genes coding for the trans-acting replication factors (polymerase (LP), and nucleoprotein (NP)) occur. The transcription and expression of the genes coding for the late proteins (matrix (Z) and glycoprotein (GPC)) initiates budding of infectious virions.

(Franze-Fernandez et al., 1987; Meyer and Southern, 1993; Qi et al., 2010). To produce full-length RNA, the LP must read across the IGR by a currently unknown mechanism, and proceeds to the 5' end of the RNA before terminating. It has been suggested that an excess of NP prevents the secondary structure from forming by binding to the complimentary regions within the IGR, allowing the shift from mRNA transcription to anti-genomic RNA production to occur (Tortorici et al., 2001).

Arenavirus mRNA is capped through a cap-snatching mechanism that utilizes both the cap-binding properties of the NP and the endonuclease activity of LP. The endonuclease activity of the arenavirus LP has been mapped to domain I of the protein for both LASV and LCMV (Lelke et al., 2010; Morin et al., 2010). This allows for the translation of the mRNA through the use of the host cell machinery. As the trans-acting replication factors LP and NP increase in concentration, anti-genomic copies of the L and S segment begin to appear in higher concentrations. The LP incorporates a non-template G nucleotide onto the 5'-end of the RNA product during termination of replication (Raju et al., 1990). A “prime and realign” mechanism was proposed that suggests the synthesis of a $PPP\text{GpC}_{OH}$ primer by the LP from the C and G nucleotides at positions 2 and 3 of the 3'-end. The primer can then shift to align with the added G at the 5'-end of the template to begin RNA synthesis (Garcin and Kolakofsky, 1990).

The increase in anti-genomic RNA results a shift in production from the early proteins necessary for replication to the late proteins necessary for budding. The Z protein regulates transcription and replication of viral RNA through inhibition of the LP in a dose-dependent manner, and has been observed in both OW and NW arenaviruses (Cornu and de la Torre, 2001; Cornu et al., 2004; Hass et al., 2004; Lopez et al., 2001). While the mechanism of inhibition has not been elucidated for JUNV, the Z protein of TCRV locks its associated LP into a promoter-bound state to prevent elongation of the RNA strand. This mechanism was also proposed to allow for packaging of the LP into budding virions (Kranzusch and Whelan, 2011). The Z protein additionally drives budding by recruiting

the RNP to specific areas of the membrane where GPC is present in high concentrations. GPC is first translated as an inactive polyprotein precursor prior to arriving in its cleaved and fully-processed active state on the cell surface, where Z orchestrates the assembly and budding of infectious virions (Fehling et al., 2012).

VIRUS PROTEIN-PROTEIN INTERACTIONS

Z Protein Structure and Self-Interaction

The structure of Z is highly conserved among the arenavirus family, and all arenavirus Z proteins contain a highly conserved 37-amino acid central really interesting new gene (RING) domain with less conserved N- and C-terminal domains. A myristoylation site is located on the second residue (G2) of the protein, and is required for association of the protein to the plasma membrane (Urata and Yasuda, 2012). The RING domain is characterized by its conserved pattern of both histidine and cysteine residues that bind two Zinc ions in a cross-brace arrangement, which is essential in domain folding (Borden, 2000). The RING domain structure is conserved throughout eukaryotic cells with a unifying characteristic of mediating protein-protein interactions on a large scale, capable of forming large macromolecular scaffolds. Self-interaction of matrix proteins has been shown to be important in the budding of both rhabdoviruses and filoviruses (Hartlieb and Weissenhorn, 2006; Okumura and Harty, 2011). Evidence of arenavirus Z protein self-interaction has been observed in bacteria that have been transformed to express either LASV or LCMV Z protein (Kentsis et al., 2002). Further evidence has been observed in mammalian cells, where overexpressed TCRV and JUNV Z protein self-associate into oligomers, with dimers representing the major population. Additionally, neither the

integrity of the RING domain nor the specific residues required for Z-LP interaction are required for Z self-interaction. However, the myristoylation site at G2 is required for self-interaction (Loureiro et al., 2011).

Z-LP Interaction

Mutagenesis studies of the Z protein of TCRV have shown that the RING domain is essential for both binding to LP and inhibition of viral RNA synthesis. The integrity of the RING structure is essential to the inhibition of the polymerase (Jacamo et al., 2003; Loureiro et al., 2011).

The structure of the arenavirus LP has been predicted to contain 4 conserved domains, linked by 3 separate variable regions by comparing the structures of a number of different RdRps from various negative-sense RNA viruses. Domain III contains sequence motifs that are specific to the catalytic sites of these various RdRps (Ferrer-Orta et al., 2006; Loureiro et al., 2012). The structural prediction of the LP has been supported by electron micrographs of the MACV LP (Kranzusch et al., 2010), and by evidence that the LCMV LP can be expressed as two separate proteins that reconstitute into a functional polymerase (Brunotte et al., 2011).

Direct interaction of TCRV Z with the TCRV LP has been mapped to the N-terminal domain I and to domain III. The C-terminal region is not involved in Z binding (Jacamo et al., 2003; Wilda et al., 2008). Evidence of MACV Z binding directly to MACV LP in an *in vitro* system supports the findings for TCRV protein-protein interaction between LP and Z. It was reported that the Z protein locks the LP in a promoter-bound state that prevents further RNA synthesis. While Z does oligomerize, the monomeric form of Z protein appears to be responsible for inhibition of LP. *In vitro*, TCRV Z-LP complexes exist primarily as heterodimers (Kranzusch and Whelan, 2011). Additionally, Z mutants

that are unable to oligomerize are not inhibited in their ability to inhibit LP activity (Loureiro et al., 2011).

The Z protein has also been observed to interact with cellular proteins involved in replication. The RING domain of Z is capable of interacting with certain cellular proteins, such as the promyelocytic leukemia protein PML and the translation initiator eIF4E (Volpon et al., 2010). However, the biological implications for these interactions during the virus life cycle remains unknown.

Z-NP Interaction

Early evidence of Z-NP interaction within arenavirus particles was discovered after chemical crosslinking of the LCMV proteins within virions (Salvato et al., 1992). Direct interaction was later confirmed by overexpressing LASV NP and Z in vitro in mammalian cells (Eichler et al., 2004).

Using a reverse genetics-based approach to create virus-like particles (VLPs), JUNV Z protein has been shown to drive the assembly and budding of virions, and exhibits self-budding activity. The JUNV Z protein additionally recruits the TCRV NP into the budding virions, supporting the hypothesis that Z-NP interaction facilitates the incorporation of nucleocapsids into the budding particles. Additionally, both an intact RING domain and the L79 residue are required for the formation of infectious TCRV particles, and are also essential for the Z-NP interaction to occur (Casabona et al., 2009). Further investigation revealed that residues T81 and I83 (both outside of the RING domain) are also involved in JUNV Z-NP interaction, and JUNV L71 (equivalent to TCRV L79) is critical for VLP infectivity, suggesting that these residues are important for incorporation of nucleocapsid into budding particles (Capul et al., 2011). Interestingly, the ability of TCRV Z protein to initiate budding was enhanced upon co-expression of the protein with

NP (Groseth et al., 2010). However, the mechanism through which this phenomenon occurs has not been elucidated.

A highly conserved YLCL motif within the RING domain has been shown to be involved in the incorporation of NP into Z-driven TCRV VLPs (Groseth et al., 2010), and the results were replicated using the MOPV Z protein (Shtanko et al., 2011). It is noteworthy that this motif is also essential in Z-LP interaction, suggesting that Z-NP and Z-LP interaction may be mutually exclusive (Loureiro et al., 2011).

The C-terminal region of TCRV NP has been identified as the Z-binding region within the protein, and the integrity of a zinc-binding motif within this region is crucial for the ability of NP to bind Z and be recruited into budding particles (Levingston Macleod et al., 2011). The same region of MOPV and LCMV NPs was also demonstrated to be responsible for Z interaction. Interestingly, LCMV NP and LASV Z were capable of cross-interaction, whereas LCMV Z and LASV NP fail to interact with one another (Ortiz-Riano et al., 2011).

Z-GPC Interaction

Several enveloped viruses utilize glycoprotein-matrix protein interaction to incorporate the glycoprotein into budding particles (Checkley et al., 2011; Mittler et al., 2007). Experimental data indicates that the LCMV and LASV GPCs each interact with their respective Z proteins, and myristoylation of the Z protein is required for each interaction (Capul et al., 2007). The JUNV GPC has been observed to be incorporated into Z-induced VLPs (Groseth et al., 2010). This suggests the importance of Z-GPC interaction in incorporating the GPC into arenavirus particles. Interestingly, incorporation of TCRV NP into VLPs that contain JUNV Z-GPC show an increase in the GPC density on the surface of the VLP when compared to VLPs that include JUNV NP (Casabona et al., 2009).

The specific mechanisms involved in the packaging of GPC into virions during the Z-mediated budding stage remains unknown.

GLYCOPROTEIN PROCESSING AND ENDOPLASMIC RETICULUM STRESS

Protein Processing and Glycosylation Pathways

Protein synthesis in the ER involves a series of co-translational and post-translational modifications involving a number of chaperones. The vast majority of proteins located within the ER are devoted to the folding process. Targeting of a protein to the ER occurs early in the translation process, and ER signal sequences are typically located within the first ~25 amino acids of a protein (Braakman and Hebert, 2013).

Most proteins that are targeted to the ER and navigate the secretory pathway undergo N-linked glycosylation on Asn residues within the Asn-X-Ser/Thr motif. These modifications are typically added once the motif reaches 13 amino acids deep into the lumen of the ER, where the motif is aligned with the oligosaccharyltransferase (OST) (Nilsson and von Heijne, 1993). A pre-assembled branched carbohydrate that consists of three glucose, nine mannose, and two N-acetylglucosamine molecules is attached to the Asn residue (Ruiz-Canada et al., 2009). The addition of these carbohydrates have both intrinsic and extrinsic effects on the conformation of the protein, involving the recruitment of carbohydrate-binding factors involved in the maturation and sorting of the protein (Braakman and Hebert, 2013).

The intrinsic effects of glycosylation on a protein include improving the stability of the protein by masking the hydrophobic regions, cleavage sites, or immune recognition (Kundra and Kornfeld, 1999; Skehel et al., 1984). Additionally, the addition of the

hydrophilic glycan can destabilize the unfolded state of the protein, assisting the folding of the protein into the correctly folded state (Hanson et al., 2009). The necessity of a glycan to the correct folding and function of the protein is highly variable. While some glycans are absolutely necessary for the maturation of the protein, others are completely expendable (Hebert et al., 1997; Wang et al., 2008). While the locations of glycans are sometimes unimportant, the number of glycans can be critical (Braakman and Hebert, 2013).

There are two classes of ER chaperones that assist in the folding and maturation of proteins: the classical and carbohydrate-binding classes. While the classical chaperones can be found throughout the cell, the carbohydrate-binding chaperones are found only in the ER. The classical chaperones consist primarily of the heat-shock protein (Hsp) 70 and 90 families (Braakman and Hebert, 2013). Chaperones of the Hsp70 and Hsp90 families identify misfolded proteins by the presence of hydrophobic chains present on the surface of the protein. The Hsp70 protein BiP is referred to as the master regulator of the ER due to its large role in ER processes. The chaperone is responsible for maintaining the permeability barrier of the ER during the process of protein translocation, directing the correct folding of proteins, targeting misfolded proteins for retrograde translocation to the proteasome, maintaining calcium stores, and monitoring ER stress to activate the unfolded protein response (UPR) when necessary (Hendershot, 2004). Chaperones of the carbohydrate-binding family are involved in quality control and trimming of the glycan within the ER. Glucosidase I is responsible for the trimming of a terminal glucose residue from the glycan and reduces the affinity of the protein for the OST (Hubbard and Robbins, 1979). Subsequent trimming occurs with glucosidase II, which interacts with the chaperones chaperonin and calreticulin to stabilize and slow the folding process to prevent aggregation and turnover of proteins (Hebert et al., 1996; Hebert et al., 1997; Vassilakos et al., 1996). The chaperones can also retain incorrectly folded substrates for additional attempts at correctly folding and facilitate the formation of disulfide bonds (Oliver et al., 1997; Rajagopalan et al., 1994). An additional glucose is added to the glycan in order to

flag the protein for refolding (Braakman and Hebert, 2013). The protein is exported from the ER only after the protein completely passes the quality control system within the organelle.

GPC Processing within the ER and Trafficking to the Cell Surface

GPC FOLDING IN THE ENDOPLASMIC RETICULUM

The GPC of arenaviruses is translated into the ER, where it is heavily glycosylated at a number of N-linked glycosylation motifs present on both G1 and G2. The SSP is located at the N-terminal end of the GPC polyprotein and provides the signal to target the protein to the ER. Upon cleavage the SSP does not undergo immediate degradation, but is instead incorporated into the ER membrane. The SSP contains two hydrophobic transmembrane domains separated by a hydrophilic loop that contains a single positively-charged amino acid at position 33 (K33), which is located in the lumen/extracellular space (Agnihothram et al., 2007; Froeschke et al., 2003). The SSP is co-translationally cleaved by signal peptidases (SPases) within the ER and incorporated into the membrane. The SSP is myristoylated at the amino acid G2, which is important for fusion with the host membrane but has no effect on the formation of the G1/G2/SSP complex (York et al., 2004). While trans-complementation and interchange of SSPs from different arenavirus species are tolerated for proper function and trafficking of the GPC, the substitution of a generic ER signal peptide in place of the SSP is not tolerated (Messina et al., 2012). The JUNV G2 contains an ER retention motif that is masked by the SSP, allowing the GPC to escape the ER and undergo maturation in the Golgi (Agnihothram et al., 2006).

The presence of N-linked glycans on GPC are essential to assist in the folding and transport of the protein (Braakman and van Anken, 2000). While the four N-linked glycosylation motifs located in G2 are highly conserved among arenaviruses (with the exception of the OW arenaviruses LCMV, DANV, and LUJV), the motifs present in G1 vary in number and location between arenavirus species (Bonhomme et al., 2011; Eichler et al., 2006). These glycans are applied co-translationally, and in the case of LASV, all nine motifs are glycosylated. While some motifs prevent proteolytic processing, others appear to have no effect on the protein *in vitro* (Eichler et al., 2006).

While a protein is capable of reaching the correct conformation without assistance at low concentrations, the crowded environment of the ER makes assistance from chaperones essential to the folding process. Early in the folding process, disulfide bonds begin to form between cysteine residues. Both native and non-native bonds form, and chaperones in the protein disulfide isomerase (PDI) family are necessary to break the disulfide bonds and allow them to reform into the native state of the protein. Simultaneously, N-linked glycans are being added to Asn residues within N-linked glycosylation motifs by OST. The presence of glycans increases the binding affinity of the protein to calnexin and calreticulin. In the case of vesicular stomatitis virus (VSV), deletion of a single glycan from the glycoprotein decreases its affinity for calnexin. The wild-type VSV glycoprotein contains only two glycans, and does not associate with calreticulin *in vivo* (Cannon et al., 1996). A transfer from calnexin to BiP is required to complete the folding process (Hammond and Helenius, 1994). Alternatively, influenza A hemagglutinin (HA) is more heavily glycosylated and associates with both calnexin and calreticulin. The HA protein only binds BiP if binding to the lectin chaperones is prevented (Zhang et al., 1997). The folding of Semliki Forest virus (SFV) glycoprotein has been shown to involve a number of chaperones. The SFV p62 and E1 glycoproteins form a transient covalent complex with PDI and Erp57 upon translation. Erp57 recruits calnexin and calreticulin to form a noncovalent complex with the glycoproteins (Molinari and

Helenius, 1999). While the exact interactions between arenavirus GPCs and ER chaperones have not been elucidated, the extensive glycosylation of the proteins suggest that a large number of these enzymes are involved in the correct folding and export of the protein from the ER.

MATURATION AND CLEAVAGE OF ARENAVIRUS GPC

The maturation of most enveloped viruses share a similar process of priming their glycoprotein through cleavage of the protein by host proteases (Hallenberger et al., 1992; Kido et al., 2008; Ozden et al., 2008; Watanabe et al., 1995). Cleavage releases the fusion peptide of the glycoprotein, which typically consists of a hydrophobic chain of ~20-30 amino acids. This polypeptide is responsible for anchoring the glycoprotein to the target membrane and allow fusion of the virus and host membranes (White et al., 2008). The late cleavage allows the virus to fold and assume a metastable conformation that is capable of undergoing a significant conformational change upon the receptor binding and shift in pH during infection. The process also helps to ensure the formation of infectious particles since cleaved glycoproteins have been shown to be more readily incorporated into budding particles than unprocessed glycoproteins (Damonte et al., 1994; Kunz et al., 2003).

The arenavirus GPC is cleaved in the Golgi apparatus by SKI-1/S1P at the highly conserved motif RX(hydrophobic)X (Pasquato et al., 2011). This enzyme is the protease utilized by both OW and NW arenavirus GPCs, and belongs to the proprotein convertase (PC) family of proteases. A unique quality of SKI-1/S1P within the PC family is its affinity for cleavage motifs within hydrophobic regions (Pasquato et al., 2006). The motif within most arenavirus GPCs closely resembles the auto-cleavage motif of SKI-1/S1P. Both OW and NW clade B arenavirus GPCs mimic the auto-processing site RRLL (Pasquato et al., 2011). Specific amino acids around this cleavage site have shown importance in the cleavage efficiency of the GPC by SKI-1/S1P. An F259A mutation in LCMV GPC impairs

processing, and analysis of peptides that mimic the LASV cleavage motif reveal that the presence of an aromatic residue at the same position (259) negatively affects the cleavage efficiency (Beyer et al., 2003; Pasquato et al., 2006). However, cleavage of the GPC is not required for transport of the GPC to the plasma membrane (Eichler et al., 2006).

ER Stress and the Unfolded Protein Response

The inability of proteins to fold correctly, through either an increase in total protein concentration in the ER or through expression of folding-incompetent proteins, creates ER stress and triggers the UPR. Whenever the capacity of the chaperones in the ER to fold proteins is exhausted due to accumulation of unfolded proteins, the cell upregulates the production of chaperones and downregulates protein production at the transcriptional and translational level. The cell will also decrease the protein load in the ER through the upregulation of ER-associated degradation (ERAD) (Schroder and Kaufman, 2005).

In thermodynamic terms, any protein in a conformation with a higher free-energy than its native conformation is considered to be misfolded, which is typically due to exposed hydrophobic regions on the surface of the protein. These hydrophobic regions have a high affinity for the chaperones within the ER. Affinity binding assays have demonstrated that BiP preferentially binds short hydrophobic chains in an ATP-dependent mechanism. BiP cycles between a monomeric and oligomeric state, and only monomeric BiP will associate with misfolded proteins. An increase in misfolded proteins in the ER increases the monomeric pool of BiP, suggesting that oligomeric BiP serves as a storage pool from which monomeric BiP is recruited in the presence of misfolded proteins (Freiden et al., 1992; Gething, 1999).

Three different transmembrane proteins are responsible for the transduction of the UPR across the ER membrane: the kinase/endonuclease inositol-requiring protein 1 (IRE1), the PKR-like ER kinase (PERK), and the activating transcription factor 6 (ATF6).

In normal conditions, BiP binds to each of these proteins to maintain their inactive states. The presence of misfolded proteins triggers the release of BiP from the luminal domains of the transmembrane proteins, activating the UPR pathways (Schroder, 2008). The activated PERK phosphorylates eukaryotic translation initiation factor 2 α (eIF2 α), which inhibits the assembly of ribosomes and prevents cap-dependent translation of mRNA. This prevents further accumulation of proteins in the ER lumen. The phosphorylation of eIF2 α also upregulates the expression of genes such as ATF4, which can lead to apoptosis in cases through the activity of the pro-apoptotic transcription factor CHOP when the ER stress cannot be resolved (Ohoka et al., 2005; Yamaguchi and Wang, 2004). In the case of IRE1, the release of BiP triggers the dimerization and autophosphorylation of the protein. Phosphorylation activates the endoribonuclease activity of IRE1, which allows for the removal of a 26 nucleotide intron from mRNA encoding X-box-binding protein 1 (XBP1). The spliced mRNA encodes a transcription factor that upregulates the expression of several UPR-related genes (Schroder, 2008). The release of BiP from ATF6 allows for its translocation of the protein to translocate to the Golgi apparatus where it is processed by SKI-1/S1P on the luminal side of the membrane and then cleaved again by metalloprotease site 2 protease (S2P) on the cytoplasmic side of the membrane. This process releases the N-terminal fragment of ATF6 (ATF6 p50) into the cytosol, and ATF6 p50 translocates into the nucleus to stimulate the expression of UPR-related genes, including both BiP and CHOP (Schroder, 2008; Zhang and Kaufman, 2006). It is noteworthy that in the case of LCMV, the ATF6-controlled branch of the UPR pathway remains active during acute infection, whereas all three pathways are silent during persistent infection. The ATF6 pathway is required for optimal production of LCMV particles during the acute infection (Pasqual et al., 2011).

MANIPULATION OF THE ARENAVIRUS GENOME

Segment Reassortment

The bi-segmented genome of arenaviruses allows for reassortment of the genome segments, and co-infection of cells with viruses from two separate arenavirus species can lead to the production of chimeric virions. This strategy has been utilized to create reassortant viruses between different strains of the same virus, PICV and LCMV, and two closely related viruses from different species, LASV and MOPV (Kirk et al., 1980; Lukashevich, 1992; Riviere et al., 1985). Laboratory reassortment has been utilized to determine the function of arenavirus proteins in pathogenesis (Riviere et al., 1986) and arenavirus-induced immunosuppression (Matloubian et al., 1993; Matloubian et al., 1990), as well as to generate live-attenuated vaccine candidates (Lukashevich et al., 2008; Lukashevich et al., 2005). While reassortants are useful to study certain aspects of arenavirus pathogenesis, the system is limited in that specific mutations cannot be studied within the context of infection. In addition, the procedures utilized to generate the reassortant viruses is associated with poor stability and purity (Lukashevich, 1992).

Minigenome Systems

The first arenavirus-based minigenome (MG) system was developed using the OW arenavirus LCMV genome (Lee et al., 2000). MG systems were later developed for LASV, TCRV, and JUNV (Albarino et al., 2009; Hass et al., 2004; Lopez et al., 2001). Arenavirus MG systems were developed for the purpose of studying the cis- and trans-acting factors involved in genome replication and gene transcription. The development of MG systems led to the identification of LP and NP as the minimal trans-acting factors that are required to carry out replication and transcription. These systems allow for the reverse genetics-

based study of critical amino acids in LP and NP that are involved in replication and transcription (Lee et al., 2000; Ortiz-Riano et al., 2011, 2012a, b). Additional results from MG system studies revealed that the IGR serves as a transcription termination signal (Pinschewer et al., 2005), and that the Z protein inhibits LP activity in a dose-dependent manner (Kranzusch and Whelan, 2011). Outside of reverse genetics-based studies, MG systems have been used to evaluate the efficacy of siRNAs that target viral mRNAs that encode LP or NP (Sanchez et al., 2005), as well as the evaluation of anti-arenaviral drugs that target replication and transcription (Mendenhall et al., 2011; Ortiz-Riano et al., 2014).

Recombinant Arenaviruses

Reverse genetics-based rescue systems to generate recombinant virus clones from cDNA have been developed for LCMV (Flatz et al., 2006), PICV (Lan et al., 2009), LASV (Albarino et al., 2011b), and JUNV (Albarino et al., 2009). The two systems utilized to rescue recombinant arenaviruses are the T7-based systems which contain either the T7 bacteriophage RNA polymerase (T7RP) promoter, or the pol-I/II system which utilizes the RNA polymerase I (pol-I) and the RNA polymerase II (pol-II) promoters.

The T7-based systems do not require co-expression of the trans-acting factors LP and NP since the system generates sufficient genomic RNA and mRNA for rescue (Albarino et al., 2009; Albarino et al., 2011b). However, either co-transfection of a T7RP expression plasmid or transfection into a cell line that expresses T7RP is required to generate the required genomic RNA and mRNA. In order to create the functional 19-nucleotide 3' termini of the L and S segments, the hepatitis delta virus (HDV) ribozyme is required prior to the termination sequence (Sanchez and de la Torre, 2006). Since any alterations to this 19-nucleotide promoter can have a detrimental effect to its activity, the T7 system can be problematic due to the variability of the HDV ribozyme cleavage efficiency. The replication with the T7RP system also allows for the detection of the 5'

phosphate of viral RNA by cellular RIG-I and can negatively affect the efficiency of rescue (Emonet et al., 2011; Habjan et al., 2008).

The pol-I/II rescue system utilizes the pol-I to express the arenavirus genome. Pol-I is responsible for the expression of ribosomal RNA, and carries out transcription within the nucleus before the viral RNA is exported to the cytoplasm (Pinschewer et al., 2003). Although the pol-I promoter is species specific, the HDV ribozyme is not required due to the precise termination of transcription by pol-I at the nucleotide preceding the terminator. Co-transfection with pol-II-based expression plasmids for the trans-acting factors LP and NP are required to achieve rescue (Emonet et al., 2011).

PROJECT AIMS

The development of the live-attenuated Can strain of JUNV is approved for use in AHF-endemic regions and has proven successful in limiting the incidence of JUNV-associated disease. Despite the success of the vaccine, the mechanism of protection is still largely unknown. Identification of the specific mechanisms that contribute to the attenuation and immunogenicity of the Can strain would significantly improve our knowledge of AHF pathogenesis as well as our ability to rationally design novel, safe, and effective vaccines to protect against other arenavirus-associated diseases.

Specific Aim 1 (Chapter 3): Determine the contribution of the GPC amino acid substitution T168A to its altered processing.

1a: Evaluate the ability of GPC expressing the T168A substitution to reach the cell surface in comparison to the wild-type Rom GPC.

1b: Determine the mechanism of degradation for improperly processed JUNV GPC.

The GPC of Can has previously been identified as the primary attenuating gene of the Can strain (Seregin et al., 2015). Therefore, individual substitutions between Rom and Can were evaluated for a potential impact on protein production and trafficking within the cell. The T168A substitution had the greatest impact on GPC processing and surface expression in preliminary studies and its effects on GPC's pathway through the cell were studied *in vitro*.

Specific Aim 2 (Chapter 4): Evaluate the effects of the Z protein amino acid substitutions V18A and V64G on the efficiency of infectious particle production.

2a: Determine the impact of the V64G substitution in the ability of Z to interact with other virus proteins.

2b: Determine the impact of the V18A substitution in the ability of Z to interact with other virus proteins.

A chimeric Rom virus expressing the Can Z protein generated significantly fewer infectious particles *in vitro* despite slightly higher levels of viral RNA and protein within infected cells (unpublished data). The pol-I/II-based rescue system was utilized to evaluate the effects of the V18A and V64G substitutions on the ability of the virus to produce infectious progeny.

Specific Aim 3 (Chapter 5): Evaluate the ability of Can Z protein to inhibit the replication activity of the JUNV LP, and the ability of the Can LP to be inhibited by JUNV Z.

Chimeric JUNVs containing either the Can LP or Z generate more viral RNA and protein than the wild-type Rom strain *in vitro* (unpublished data). A luciferase-based MG system was utilized to study the sensitivity of Can LP to JUNV Z protein, and the inhibitory effect of Can Z protein on JUNV LP.

Chapter 2: Materials and Methods

CELLS, VIRUSES, AND BIOSAFETY

Baby hamster kidney suspension (BHK-21S) cells, Vero cells (American Tissue Culture Collection), human embryonic kidney (HEK293) cells, and adenocarcinomic human alveolar basal epithelial (A549) cells were all maintained in Dulbecco's Modified Eagle's Medium (DMEM) supplemented with 5% fetal bovine serum and L-glutamine. All DMEM was also treated with 1% penicillin/streptomycin. The original wild-type Romero strain (GenBank accession no. AY619640 and AY 619641) was provided by Dr. Thomas G. Ksiazek (University of Texas Medical Branch [UTMB]). All wild-type and recombinant viruses were propagated by infecting Vero cells (multiplicity of infection [MOI] 0.01) and collecting the supernatants at 72 hours post-infection. Cell debris was eliminated by passing the supernatant through a 0.45 μ m filter. All work performed with infectious JUNV strains was performed in the UTMB biosafety level 4 (BSL-4) facility in accordance with institutional safety and health guidelines.

RESCUE OF RECOMBINANT JUNV CLONES

All cloning for the Pol-I/II rescue system was performed previously by Emonet et al. The Rom and Can NP open reading frame (ORF) was PCR amplified with primers flanking the 5' and 3' ends of the ORF and cloned into the pCAGGS vector to yield the Rom and Can pC-NP (pC-RomNP and pC-CanNP) plasmids. The process was repeated for the LP ORF, and the gene was PCR amplified and inserted into the pCAGGS vector piece-wise in three separate steps to generate pC-RomLP and pC-CanLP. To generate the murine pol-I-S (mPol-I-Sag) and murine pol-I-L (mPol-I-Lag) plasmids for Rom and Can, the L and S segments were amplified piece-wise in three and two pieces, respectively. The genes were inserted into the pRF42 vector in anti-genomic orientation and flanked by the

murine pol-I promoter and terminator sequences (Emonet et al., 2011). BHK-21S cells were seeded into 12-well culture plates at a volume of 6×10^4 cells/well 24 hours prior to transfection. Each well of cells was transfected with mPol-I-Lag, mPol-I-Sag, pC-NP, and pC-LP at equal copy numbers with the total DNA totaling 2 μg /well. Transfections were performed with the XtremeGENE 9 transfection reagent (Roche) following the manufacturer's protocol. At 24 hours post-transfection, the cells were trypsinized and re-seeded into T75 flasks. The supernatant was harvested 72 hours after transfer to yield passage 0 (P0). To generate a working stock (P1), P0 virus was used to infect Vero cells at MOI 0.01, and the supernatant was harvested at 96 hours post-infection.

GROWTH KINETICS AND TITRATION

Titration of all virus samples was performed by plaque assay. Vero cells were seeded into 6-well plates at 3×10^5 cells/well and used for titration 24 hours after seeding. Six 10-fold serial dilutions of the virus samples were performed and used to infect each of the six wells (200 μL diluent/well) for 1h at 37°C. The cell monolayers were then overlaid with a minimum essential medium (MEM) containing 5% fetal bovine serum, 1% penicillin/streptomycin solution, and 0.5% agarose. Plates were incubated for 5 days at 37°C and then fixed with formaldehyde for 30 minutes. The agarose layer was removed and the fixed cells were stained with crystal violet to reveal the plaques. Growth kinetics of virus clones were determined by infecting Vero cells at MOI 0.01 and collecting the supernatant at the specified times.

GENERATION OF EXPRESSION PLASMIDS FOR GPC

The Rom and Can GPC ORFs were PCR amplified from the Rom and Can mPol-I-Sag plasmids using primers designed to bind the 5' and 3' ends of the ORFs. The 3'

primer (N-terminal) was given an overhang containing a restriction site specific to RsrII, and the 5' primer (C-terminal) was given an overhang containing a restriction site specific to XmaI. The amplified ORFs were digested with RsrII and XmaI (Thermo Scientific) and inserted into the pC-NP plasmid after removing the NP ORF with RsrII and XmaI to generate pC-RomGPC and pC-CanGPC. In order to generate the plasmids to express XJ13 and XJ44, the pC-CanGPC plasmid was digested with RsrII and EcoRI and inserted into the pC-RomGPC plasmid after digestion with the same enzymes to provide Rom GPC with the M109Q and E116A substitution mutations. Site-directed mutagenesis was performed on the resulting plasmid to introduce the R484G substitution mutation into the plasmid, yielding the pC-XJ13GPC plasmid. To generate the XJ44 GPC expression plasmid, site-directed mutagenesis was performed on the pC-XJ13GPC plasmid to create the T168A mutation within G1 and create the pC-XJ44GPC plasmid.

MINIGENOME ASSAY FOR ROM AND CAN

Both Rom and Can Z ORFs were PCR amplified using the same strategy as discussed for GPC and inserted into the pC-NP backbone after digestion to remove the NP ORF, yielding pC-RomZ and pC-CanZ. The mPol-I-Sag plasmids for both Rom and Can were used to create reporter plasmids by substituting the green fluorescent protein (GFP) ORF in place of NP and the firefly luciferase (FFL) ORF in place of GPC for each plasmid. This was achieved by PCR amplifying the ORFs for GFP and FFL with primers at the 5' and 3' ends that contained overhangs specific to the noncoding regions of the Rom and Can S segment that flank the NP and GPC, respectively. The resulting halves of the S segments were inserted piece-wise into the pRF42 backbone to generate the mPol-I-S-GFP/FFL plasmids for both Rom and Can. BHK-21S cells were seeded into 12-well plates at 1×10^5 cells/well and transfected with equal copy numbers of pC-NP, pC-LP, pC-Z, and mPol-I-S-GFP/FFL at a total mass of 2 μ g of DNA per well. The transfection was

performed using the XtremeGENE 9 transfection reagent (Roche) following the manufacturer's protocol, and the transfected cells were incubated at 37°C for 48 hours. The cells were lysed and prepared using the Dual-Glo Luciferase Assay System (Promega), and luminescence was measured with a GloMax Multi luminometer (Promega). All FFL measurements were normalized to Gaussia luciferase luminescence provided in the Dual-Glo kit.

WESTERN BLOTTING

Both A549 and Vero cells were cultured in 12-well plates and seeded at a density of 1×10^5 cells/well. After 24 hours, cells were infected with rJUNV clones at MOI 5 and incubated for 1h at 37°C in 100 μ L of DMEM. Another 900 μ L of DMEM (5% fetal bovine serum) was added after the incubation, and the cells were incubated for the specified time at 37°C. To collect cell lysates, the supernatant was removed and the monolayer was rinsed with phosphate buffered saline (PBS). The monolayers were then treated with 250 μ L of 1x Laemmli buffer (Bio-Rad) and incubated at 95°C for 10 minutes. Prior to loading on a 10% acrylamide gel, each sample was treated with β -mercaptoethanol (BME) equal to 10% of the total sample volume. The gels were transferred onto a PVDF membrane using a TransBlot Turbo transfer system (Bio-Rad) and incubated at room temperature for 1h in 5% milk/PBS solution. A monoclonal rabbit anti-G2 primary antibody (ProSci) was added at 1:1000 to the 5% milk solution and incubated overnight at 4°C. The membrane was rinsed 3 times in PBS before being incubated for 1h at room temperature in 5% milk/PBS containing an HRP-conjugated goat anti-rabbit secondary antibody (Cell Signaling). The membrane was rinsed 3 times in PBS and treated with Amersham ECL detection reagent (GE) prior to exposure. Peptide-N-glycosidase F (PNGase F) was used to remove the N-linked glycans from the JUNV GPC in certain blots. The PNGase F enzyme (New England Biolabs) was added to the cell lysates after dilution in ultra-pure water. The cells were

incubated in the provided buffer and run on a polyacrylamide gel following the manufacturer's protocol.

VIRUS GENOME SEQUENCING AND QUANTITATIVE PCR

Infected cell lysates were mixed into a solution with TriZol. RNA was isolated using the Direct-Zol RNA Isolation kit (Zymo Research) and sequenced using primers complimentary to the 3' and 5' conserved 19 nucleotides of the S and L segments. One additional primer pair within the intergenic region was created. While this was sufficient to sequence the entire S segment, the L segment required another 2 primer pairs complementary to two regions within the LP ORF that split the genome into three equal-length segments. The L and S segments of each virus were amplified in 3 and 2 PCR reactions, respectively. The PCR fragments were run on an agarose gel and extracted using the Zymoclean Gel DNA Recovery kit (Zymo Research) and directly sequenced to obtain the consensus sequences for the recombinant viruses. For qPCR, the same RNA purification methods as above were used to obtain purified RNA. Primer pairs within the GPC, Z, and NP genes were designed using primer3 software, and each primer pair spanned ~250 nucleotides. Reactions were prepared using the iTaq Universal qPCR SYBR green kit (Bio-Rad), and the reactions were run on a CFX96 Touch Real-Time PCR detection system (Bio-Rad). Each reaction was normalized to a standard curve created by *in vitro* transcribed purified RNA, and a melt curve analysis was run for each sample to ensure one product. The data was analyzed using the software provided by the CFX96 Touch detection system.

CONFOCAL MICROSCOPY

HEK293 cells were seeded into 24-well plates at 1×10^4 cells/well onto poly-D-lysine treated coverslips (12mm, 1.5 thickness). After 24 hours, the cells were transfected with the pC-GPC expression plasmids at a total amount of 2 μg of DNA/well using XtremeGENE 9 transfection reagent following the manufacturer's protocol. The cells were incubated at 37°C for 36 hours, then fixed with 4% paraformaldehyde for 10 minutes at room temperature. The cells were treated with 0.1% Triton-X100 in PBS to allow membrane permeability. The cells were treated with CytoPainter Red ER stain (Abcam) and Hoescht 33342 nuclear stain following the manufacturer's protocol. The cells were then treated with mouse anti-JUNV GPC primary antibody (BE08, BEI Resources) for 1 hour at room temperature, then incubated with goat anti-mouse secondary antibody conjugated with an AlexaFluor 488 green fluorophore (Life Technologies) for 30 minutes at room temperature. The coverslips were mounted onto glass slides using MOWIOL mounting media. A Zeiss LSM 510 confocal microscope was used to capture all images.

FLOW CYTOMETRY

HEK293 cells were seeded into 12-well plates at 1×10^5 cells/well and allowed to incubate at 37°C for 24 hours. The cells were then treated with each of our pC-GPC plasmids at 2 μg of DNA/well using XtremeGENE 9 transfection reagent following the manufacturer's protocol. After 36 hours of incubation at 37°C, the cells were briefly treated with 0.25% trypsin to suspend the cells. Suspended cells were fixed with 4% paraformaldehyde for 10 minutes at room temperature and permeabilized with 0.1% Triton-X100 when specified in the results. The cells were then stained with mouse anti-JUNV GPC primary antibody (BE08, BEI Resources) for 1 hour at room temperature, then incubated with goat anti-mouse secondary antibody conjugated with APC for 30 minutes at room temperature. Cells were sorted and analyzed based on fluorescence intensity using a BD Fortessa cell analyzer.

Chapter 3: Differential Processing and Trafficking of the GPCs of Rom and Can Strains

INTRODUCTION

The NW arenavirus JUNV is the causative agent of AHF, a severe disease that is endemic to the pampas region of Argentina. Infection typically occurs through mucosal exposure to the virus or direct contact of the virus with abraded skin. The disease presents with flu-like symptoms, and can progress into a hemorrhagic-neurologic phase with a case fatality rate as high as 30% (Weissenbacher et al., 1987). Due to the high stability of the virus particle, high rates of morbidity and mortality, and its ability to be easily spread by aerosol, the virus presents a threat of potential use as a biological weapon. The development of countermeasures for AHF is a top priority for the Implementation Plan of the HHS Public Health Emergency Medical Countermeasures Enterprise. Treatment options are currently limited. While treatment of infected patients with immune plasma does decrease the mortality, 10% of the patients who receive the treatment will still develop a LNS (Enria and Barrera Oro, 2002). Immune plasma is also in short supply, and presents a risk of transmitting other blood-borne pathogens (Enria et al., 2008). The efficacy of ribavirin as a treatment option has been evaluated, and the drug has been shown to be only partially effective when administered at early time points during infection. There are also side effects associated with the drug, including anemia and congenital disorders (Enria et al., 1987; Enria et al., 2008). The limitations of the current treatment options highlights the need for further development of safe and effective anti-arenaviral drugs. However, the live attenuated Can strain of JUNV has been a safe and effective vaccine in endemic regions among agricultural workers since its development and release (Maiztegui et al., 1998). The vaccine remains classified as an investigational new drug in the United States since long-term safety and immunity studies have not been conducted. The availability of

the vaccine master seed virus is unknown, and re-importation of the vaccine into the United States would be difficult due to the potential lack of FDA-compliant documentation. A TC83 replicon-based vaccine candidate had been developed and shown to induce an immune response in guinea pigs that protects against the Rom strain of JUNV (Seregin et al., 2010), but more testing is required before the candidate would be eligible for clinical trials. In order to achieve FDA approval, the vaccine candidates would need to come from a genetically well-characterized master seed stock from a safe source, and presented with a clear understanding of the mechanisms underlying disease pathogenesis and protection.

The rescue of both the Rom and Can strains from cloned cDNA using a pol-I/II-based rescue system has recently been described (Emonet et al., 2011). The Rom strain was isolated from an AHF patient and has not been subjected to multiple passages in tissue culture or animals, and is therefore expected to be representative of a true human pathogen (Yun et al., 2008). Both the Rom and Can strains have been well-characterized in a guinea pig model of AHF that accurately mimic human disease, and both recombinant viruses exhibit the same characteristics as their wild-type counterparts in the guinea pig model. Additionally, studies performed with chimeric Rom-Can JUNV clones reveal that the primary attenuating gene in Can is the GPC gene. Replacement of the Rom GPC with the Can GPC in the rRom virus changes the phenotype from uniformly lethal to completely attenuated, with no animals developing febrile illness (Seregin et al., 2015).

Each segment of the bi-segmented arenavirus genome is organized in ambisense, allowing the virus to express different proteins at key points during the virus life cycle. These genes are separated by a noncoding region that forms a secondary structure, which provides a transcription termination signal for the RdRp (Meyer and Southern, 1993, 1994; Wilson and Clegg, 1991). Both the L (~7kb) and S (~3.4kb) segments are organized in a way that allows the transcription and translation of LP and NP to promote genome replication early during the life cycle. Each segment then expresses the Z and GPC proteins late in the life cycle to promote budding. The Z protein has multiple functions in the virus

life cycle, including suppression of replication, protein-protein interaction, and budding (Fehling et al., 2012). The GPC undergoes a series of processing steps in the ER and is trafficked to the cell surface where it is recruited into budding particles by Z (Burri et al., 2012a; Burri et al., 2012b; Capul et al., 2007). During the budding phase of the life cycle, GPC must reach the cell surface efficiently to be included into the virus particles. This process is dependent on the ability of the GPC to fold within the ER, export to the Golgi, and undergo cleavage prior to reaching the cell surface.

In this chapter, I describe the use of both GPC expression and in vitro infection to illustrate the inability of Can GPC to efficiently traffic from the ER to the cell surface. The Can GPC displayed a glycosylation profile that is notably different from the pathogenic Rom GPC and a lower percentage of cleaved GPC than Rom. Additionally, Can GPC appeared to be retained in the ER and up-regulated several genes involved in the UPR, indicating that the Can GPC is triggering ER stress. This ultimately led to evidence of aggregation and degradation of the Can GPC through autophagy.

RESULTS

Preliminary Data: The glycoprotein of the JUNV Can strain is less efficiently cleaved into G1 and G2 than the glycoprotein of the Rom strain

Using our pol-I/II reverse genetics-based rescue system, our lab has previously demonstrated that the GPC is the primary gene responsible for the attenuation of the Can strain (Seregin et al., 2015). Further examination of the in vitro characteristics of the virus

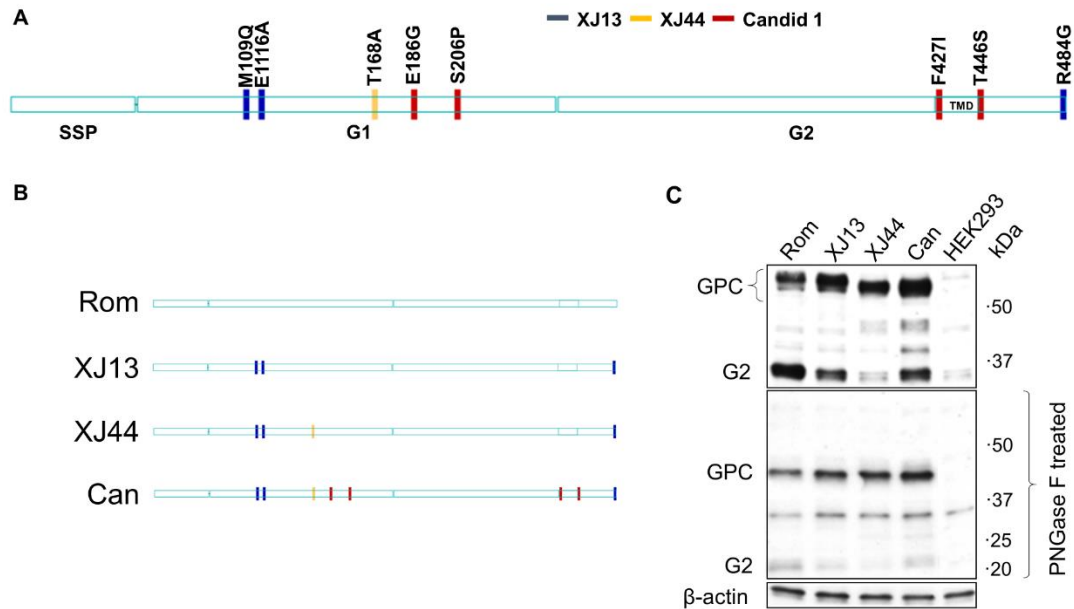


Figure 3.1: GPC Processing Phenotypes in HEK293 Cells. **A)** Schematic representation of amino acid substitutions present in Can GPC with reference to Rom GPC. Substitutions are organized based on accumulated mutations from key viruses in the passage history, with blue representing changes from Rom to XJ13, yellow representing changes from XJ13 to XJ44, and red representing changes from XJ44 to Can. **B)** Representation of GPC sequences cloned into our pC-GPC expression plasmids and subsequently transfected into HEK293 cells. **C)** HEK293 cells were transfected with expression plasmids encoding the GPC proteins from (B). The cells were incubated for 24 hours and the lysates were subjected to Western Blot analysis. In addition, samples were also treated with PNGase F and compared to untreated blots. Lysates were also probed for β -actin as a loading control.

revealed that the recombinant viruses that express Can GPC produce markedly increased levels of RNA and protein despite maintaining similar growth kinetics. Additionally, Western blot analysis of Can GPC revealed additional bands of intermediate size between the full-length GPC and G2 bands that are not present in cells expressing Rom GPC. The cells expressing Can GPC contained significantly more full-length GPC than cells expressing Rom GPC (Seregin and Manning et al., in review). We therefore decided to investigate the specific differences in Rom and Can GPC that contribute to the different Western blot phenotype between the two GPCs. Using our CMV-driven pC-GPC expression plasmid, we introduced amino acid substitutions representative of GPCs from

key passages in the history of Can creation, XJ13 and XJ44 (Fig. 3.1). We then transfected HEK293 cells with pC-RomGPC, pC-XJ13GPC, pC-XJ44GPC, and pC-CanGPC and incubated the transfected cells at 37°C for 24 hours. Western blot analysis of each GPC revealed that the amino acid substitutions between Rom and XJ13 caused a decrease in the cleavage efficiency of GPC into G1 and G2. This cleavage issue was compounded with the amino acid substitution T168A in G1 between XJ13 and XJ44, resulting in an almost undetectable level of cleaved G2 in cell lysates. Interestingly, the cleaved G2 levels were restored to a small degree with the substitutions between XJ44 and Can (Fig. 3.1).

Upon examining the migration of each full-length GPC, we observed a small shift in migration between XJ13 and XJ44, and the downward shift also occurs in Can. The T168A glycosylation motif is part of an N-linked glycosylation motif, so we hypothesized that this amino acid change would alter the glycosylation profile of the protein. We treated the lysates with PNGase F, which removes all N-linked glycans from glycoproteins. Removal of the N-linked glycans resulted in equal migration of each GPC, and the intermediate bands present in XJ44 and Can collapsed down into one band (Figure 3.1). This data supports the hypothesis that an N-linked glycan present at N166 in Rom and XJ13 G1 is absent in XJ44 and Can G1. Additionally, the presence of intermediate bands of multiple lengths in XJ44 and Can GPC-transfected cell lysates, and the resolution of these bands with PNGase F, indicates that the GPCs may be failing to pass processing checkpoints within the ER.

The T168A substitution in G1 is the primary contributor to the decrease in cleaved GPC

Deletion of N-linked glycosylation motifs in both LASV and LCMV GPC has been shown to inhibit the cleavage of the full-length protein into G1 and G2 (Bonhomme et al.,

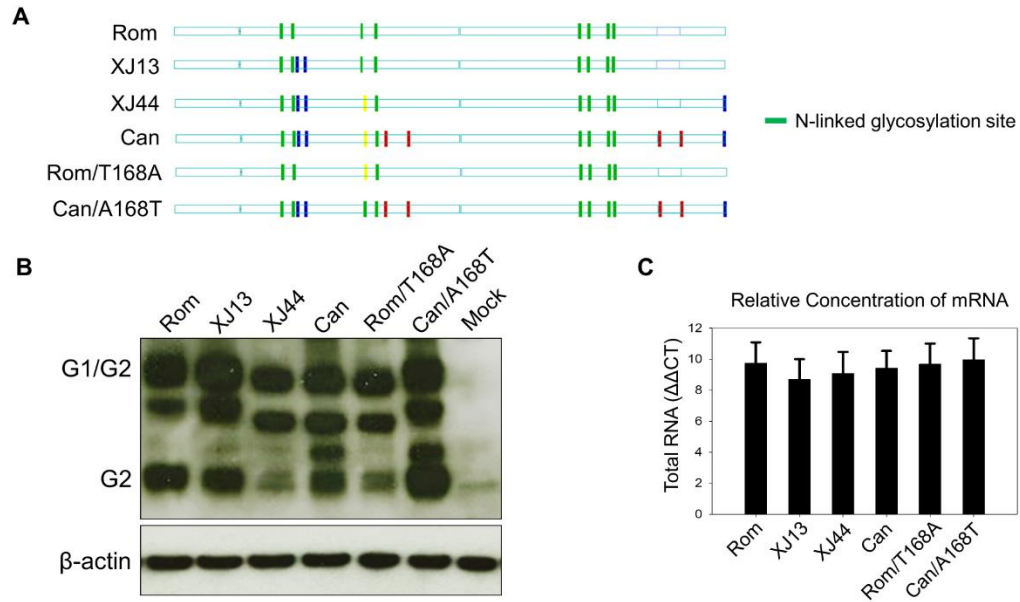


Figure 3.2: Effect of T168A Substitution on the Cleavage of GPC. **A)** Schematic representation of amino acid substitutions present in GPC expression plasmids with respect to Rom. Specific list of mutations located in Fig. 3.1A. **B)** Western blot analysis of each GPC was performed by transfecting HEK293 cells with expression plasmids pC-RomGPC, pC-XJ13GPC, pC-XJ44GPC, pC-CanGPC, pC-T168AGPC, and pC-A168TGPC for 36 hours at 37°C, and probing for G2 within cell lysates using an anti-G2 monoclonal antibody. β-actin was included as a loading control. **C)** mRNA from HEK293 cell lysates was harvested at 36 hours post-transfection. Quantitative real-time PCR was performed using primers that were normalized to *in vitro* transcribed GPC RNA, and quantified using a standard curve. Melt curve analysis was performed for each sample to insure a single amplification product.

2011; Eichler et al., 2006). Since the introduction of the T168A substitution in G1 correlates with a decrease in GPC cleavage, I decided to investigate the role of the single amino acid substitution in GPC cleavage. I introduced the single substitution into the pC-RomGPC plasmid through site-directed mutagenesis, and reverted the site to restore glycosylation in the pC-CanGPC plasmid. I repeated the transfection of HEK293 cells and Western blot analysis of cell lysates at 36 hours post-transfection. The Rom, XJ13, XJ44, and Can GPCs exhibited identical phenotypes to the preliminary data (Fig. 3.1). The T168A substitution alone in Rom GPC was sufficient to reproduce the XJ44-like phenotype in which cleaved G2 was detected only at low amounts within the cell lysates.

While reversion of the glycosylation motif to wild-type (A168T) in Can GPC did restore the amounts of cleaved G2 in cell lysates, the lowest intermediate band remained present. While the data indicates that the primary contributor to the decrease in GPC cleavage is the T168A substitution, both the Rom-XJ13 substitutions and the XJ44-Can substitutions contribute to the G1/G2 cleavage and the presence of the intermediate bands, respectively. It is noteworthy that a decrease in total protein exists among GPCs that contain the T168A substitution despite the mRNA levels remaining constant among cells transfected with each of the expression plasmids.

Absence of glycosylation at N166 results in the ER retention of GPC

During the passage history for XJ13 to XJ44, the ratio of cleaved to full-length GPC shifts, and is predominantly full-length in XJ44 due to the T168A substitution. However, the cleavage is partially rescued between XJ44 and Can (Fig. 3.2). The decrease in cleaved GPC in XJ13, XJ44, and Can GPC indicates a failure of SKI-1/S1P to recruit to the G1/G2 cleavage site, however the cause of the decrease in cleavage was unclear from the results. The SKI-1/S1P subtilase cleaves the JUNV GPC in the late Golgi, near the cell surface (Pasquato et al., 2011), suggesting that a trafficking issue could be preventing G1/G2 cleavage. Inaccessibility of the cleavage site due to misfolding could also be contributing to the reduction in cleavage. In order to test the hypothesis that XJ13, XJ44, and Can GPC are not trafficked correctly, we utilized confocal microscopy to visualize the distribution of GPC throughout the cell.

I transfected BHK-21S cells with each of our GPC expression plasmids to observe the trafficking of each GPC outside of the influence of other viral proteins. By staining the ER along with the GPC, I was able to better determine the localization of the GPCs within the cell. Additionally, ER localization can be indicative of improper processing in the event that the JUNV GPCs are co-localizing with the ER. The transfected cells were fixed

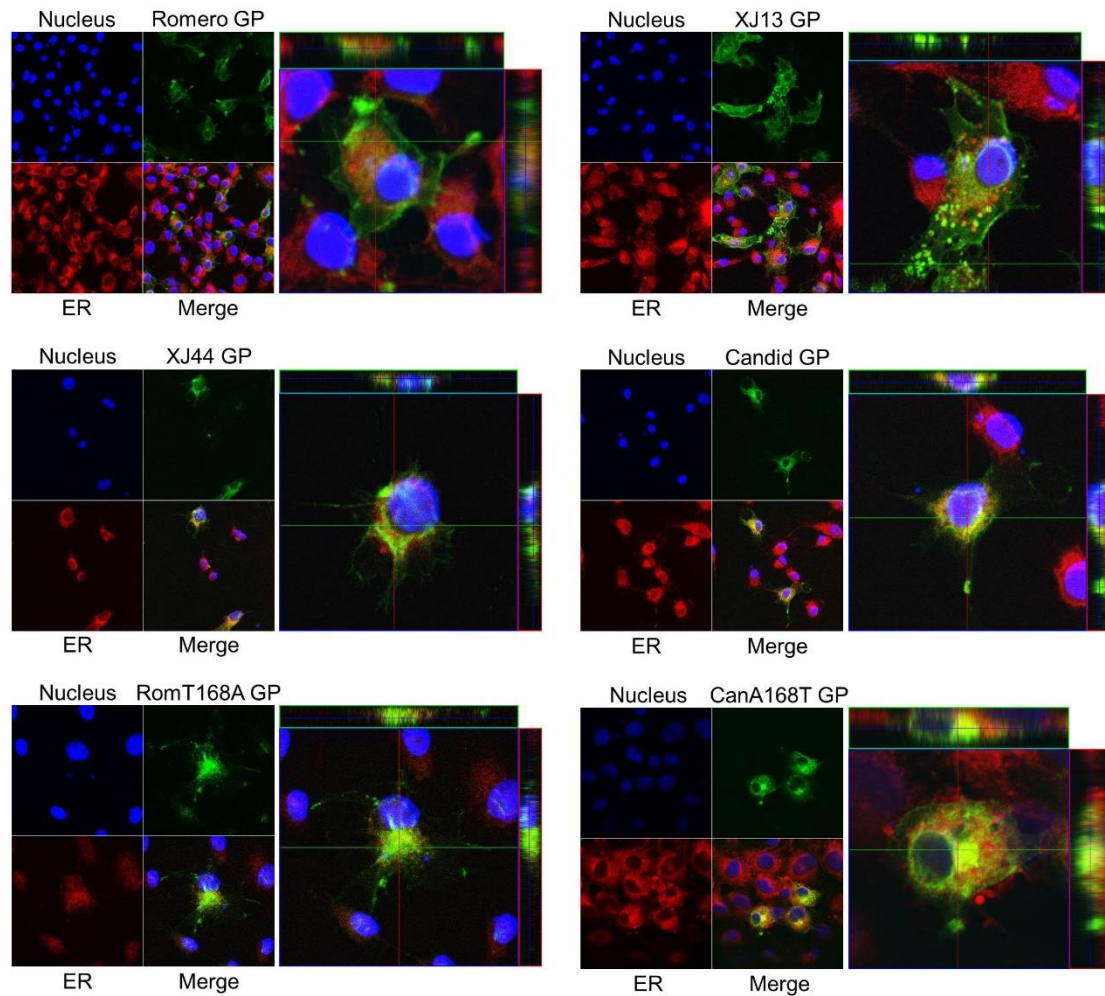


Figure 3.3: The effect of the N166 glycan on the efficiency of GPC trafficking. BHK-21S cells were seeded onto glass coverslips in 24-well plates and transfected 24 hours later with Rom, XJ13, XJ44, Can, Rom-T168A, and Can-A168T GPC expression plasmids. After incubation at 37°C for 36 hours, the cells were fixed in 4% paraformaldehyde and stained using CytoPainter ER dye (red) and anti-JUNV GPC primary antibody along with AlexaFluor 488-conjugated secondary antibody (green). Nuclei were stained with Hoescht 33342 stain (blue). Two-dimensional images (left) and three-dimensional Z-stacks (right) were generated using a Zeiss LSM 510 confocal microscope.

after incubating at 37°C for 36 hours on glass coverslips and stained using CytoPainter ER dye (Abcam) and an anti-JUNV GPC primary antibody (BEI Resources) in conjunction with a fluorophore-conjugated secondary antibody (Life Technologies). After staining and mounting the cells, I generated both cross-sectional images and 3-dimensional Z-stacks of cells transfected with each of the GPCs. Rom GPC appeared to traffic correctly to the cell

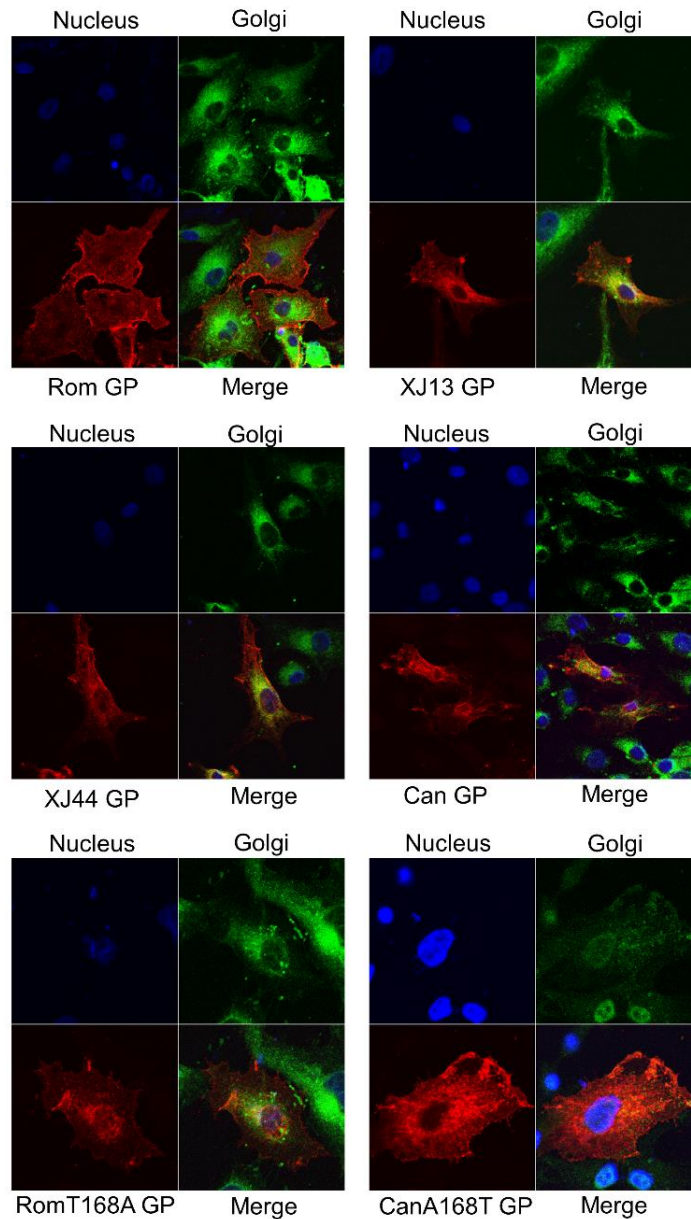


Figure 3.4: Amino acid differences between Rom and XJ13 affect trafficking of the protein through the Golgi. BHK-21S cells were seeded onto glass coverslips in 24-well plates and transfected 24 hours later with Rom, XJ13, XJ44, Can, Rom-T168A, and Can-A168T GPC expression plasmids. After incubation at 37°C for 36 hours, the cells were fixed in 4% paraformaldehyde and stained using CytoPainter Golgi dye (green) and anti-JUNV GPC primary antibody along with AlexaFluor 488-conjugated secondary antibody (red). Nuclei were stained with Hoescht 33342 stain (blue). Two-dimensional images were generated using a Zeiss LSM 510 confocal microscope.

surface with large concentrations of GPC on or near the cell membrane and very little GPC

in the ER. A fraction of XJ13 GPC co-localizes in the ER, but a significant portion reaches the cell surface. Interestingly, a fraction also co-localized with small vesicles between the ER and cell surface. The XJ44, Can, and Rom-T168A GPCs all co-localized predominantly with the ER, and were nearly undetectable at or near the cell surface. By reverting Can to T168 and restoring the N-linked glycosylation motif, a larger percentage of the GPC reached the cell surface although a portion of the GPC was still retained in the ER (Figure 3.3). These results indicate that the N-linked glycan at N166 is critical for efficient trafficking from the ER to the Golgi and cell surface. However, the amino acid substitutions that exist between Rom and XJ13 GPC also contribute to the ability of GPC to efficiently reach the cell surface to a lesser degree.

In order to investigate whether the small concentrations of XJ13 GPC between the ER and cell surface were Golgi vesicles, I again transfected BHK-21S cells with each of the GPC expression plasmids and fixed the cells on glass coverslips at 36 hours post-transfection. The cells were stained in the same manner as before, this time using the Cytopainter Golgi dye (Abcam). The distribution of each GPC was similar to the previous experiment in which the ER was stained rather than the Golgi. However, it was evident that a small fraction of the XJ13 GPC was accumulating within the Golgi, and this observation was unique to only the XJ13 and Can-A168T GPCs (Fig. 3.4). This phenomenon cannot be observed in GPCs lacking the N166 glycan, likely due to the effect that the absence of the glycan has on the inability to exit the ER. This data supports the hypothesis that the full-length GPC observed in the Western blots fails to undergo cleavage due to ER retention rather than failure due to a folding issue. However, the presence of misfolded GPC near the cell surface cannot be ruled out.

The T168A substitution in G1 limits the amount of GPC present on the cell surface

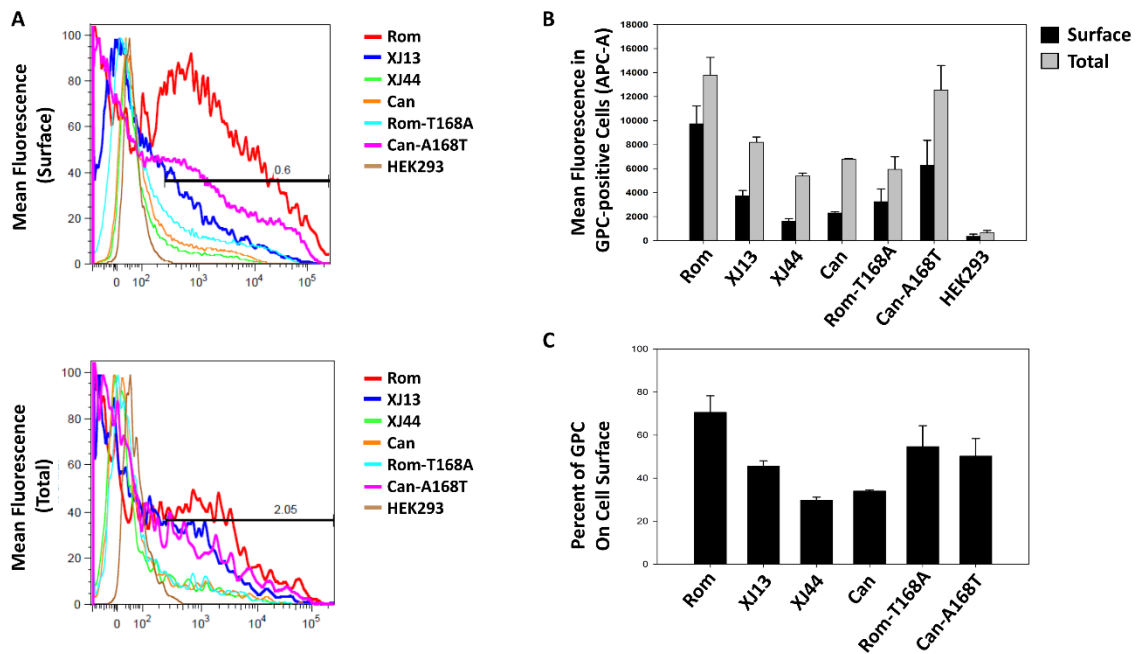


Figure 3.5: Surface expression of GPC compared to total cellular GPC. HEK293 cells were transfected with either Rom, XJ13, XJ44, Can, Rom-T168A, or Can-A168T GPC expression plasmids and incubated at 37°C for 36 hours. The cells were suspended and fixed in 4% paraformaldehyde, and then incubated in anti-JUNV GPC primary antibody and APC-conjugated secondary antibody. The cells were analyzed individually via flow cytometry for fluorescence intensity. **A)** Cells were sorted based on fluorescence intensity to analyze surface expression (top) and total protein (bottom) for each cell. **B)** Average total protein for each GPC was quantified (grey) alongside the average surface expression for each GPC (black). **C)** The ration of total to surface protein was expressed as a percentage for each GPC.

Images from confocal microscopy led me to investigate the percentage of GPC reaching the cell surface when the N-linked glycosylation motif is mutated at T168 to prevent glycosylation. I have previously shown that mRNA expression is similar among all six GPC plasmids, suggesting that relatively equal amounts of protein should be produced due to identical untranslated regions among all of the plasmids. The accumulation of GPC in the ER whenever the N-linked glycan is missing led to the hypothesis that a lower percentage of GPC is reaching the cell surface in the presence of the T168A substitution. In order to test this hypothesis, I transfected HEK293 cells with each of the six GPC expression plasmids due to the high transfection efficiency of HEK293

cells. The cells were incubated at 37°C for 24 hours prior to transfection and incubated for another 36 hours in the same conditions. After 36 hours, the cells were suspended and fixed in 4% paraformaldehyde. The membranes were made permeable using 0.1% Triton-X100 where indicated. The cells were incubated with anti-JUNV GPC primary antibody (BEI Resources) followed by APC-conjugated secondary antibody. The cells were then subjected to flow cytometry to quantify fluorescence intensity for each cell.

The mean fluorescence intensity for impermeable cells that express Rom GPC was only 25 percent less than the total protein, indicating that around 75 percent of the Rom GPC is expressed on the cell surface. This percentage decreased to only 50 percent surface expression for XJ13, while XJ44 and Can GPC only expressed 30-35 percent of the total GPC on the cell surface. By reverting the A168 residue back to the Rom genotype in Can to restore the N-linked glycosylation motif, the surface expression increased back to 55-60 percent. By mutating Rom to remove the same motif, the surface expression was reduced from 75 percent to around 50-55 percent surface expression relative to the total amount of protein in the cell (Fig. 3.5C). Interestingly, the total protein is also reduced in the XJ13, XJ44, Can, and Rom-T168A samples (Fig 3.5B). This is in agreement with my observations in Western blots, where these same plasmids appear to express less overall protein in cells (Fig. 3.2). Together, the data indicates that the glycan at position N166 is critical for the GPC to reach the cell surface efficiently. Also, the amino acid changes between Rom and XJ13 GPC appear to play a minor role in the trafficking as well.

The T168A substitution causes lysosomal degradation of GPC

The notable decrease in total GPC in samples expressing the T168A substitution exists despite equal mRNA expression in all samples. When the data is taken along with the observed ER retention in the same conditions, I hypothesized that the GPC was being degraded through either the proteasome or through autophagy in lysosomes. To determine

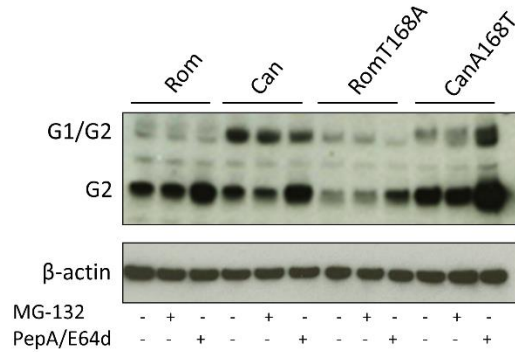
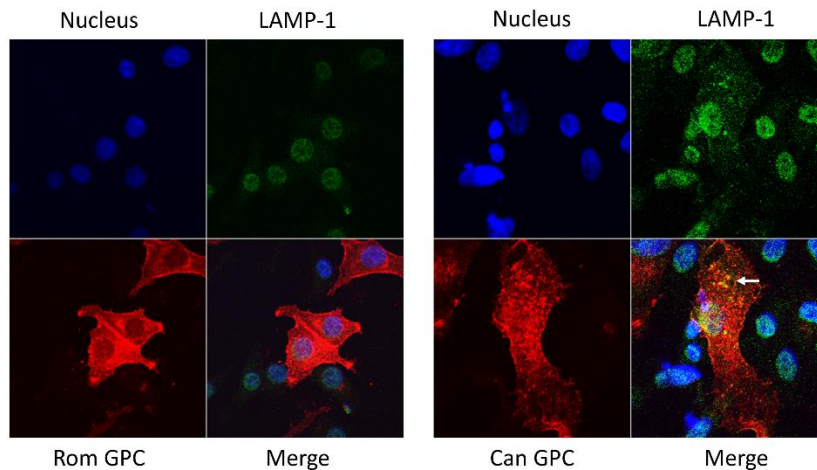
A**B**

Figure 3.6: The T168A substitution causes lysosomal degradation of GPC. **A)** HEK293 cells were transfected with Rom, Can, Rom-T168A, or Can-A168T GPC expression plasmids in equal concentrations and incubated at 37°C. At 12 hours post-transfection, the cells were treated with either MG-132 at a final concentration of 10μM, or Pepstatin-A/E64d at a final concentration of 10μg/mL at 12 hours post-transfection. The cells were lysed in Laemmli buffer at 36 hours post-transfection, and then treated with BME prior to Western blot analysis. **B)** HEK293 cells were seeded onto glass coverslips in 24-well plates and incubated for 24 hours at 37°C, and then transfected with Rom or Can GPC expression plasmids in equal concentrations and incubated for 36 hours at 37°C. The cells were then fixed by treatment with 4% paraformaldehyde for 10 minutes at room temperature. The cell membranes were made permeable by treatment with 0.1% Triton-X100, and stained with anti-JUNV GPC and anti-LAMP-1 primary antibodies. The cells were then stained with AlexaFluor-conjugated secondary antibodies for GPC (red) and LAMP-1 (green) to determine co-localization of GPC with the lysosome. Prior to mounting onto slides, the cells were stained with Hoescht 33342 nuclear stain.

the pathway through which GPC was being degraded, I inhibited both the proteasomal and

lysosomal degradation pathways of HEK293 cells through treatment with either MG-132 or Pepstatin-A/E64d.

HEK293 cells were seeded into 12-well plates and incubated for 24 hours at 37°C, and then transfected with Rom, Can, Rom-T168A, and Can-A168T GPC expression plasmids. The cells were incubated for 36 hours at 37°C, and treated with MG-132 or Pepstatin-A/E64d at 12 hours post-transfection at concentrations of 10 μ M and 10 μ g/mL, respectively. The samples were lysed in 1x Laemmli buffer and treated with BME prior to Western blot analysis. The results indicate that no significant increase in relative protein quantity exists between untreated and treated Rom samples. However, a noteworthy increase in G2 occurs in Can, Rom-T168A, and Can-A168T samples when treated with Pepstatin-A/E64d to inhibit the protease activity in the lysosome. No change in total protein occurred between untreated and MG-132 treated samples for any GPC, indicating that the proteasome is not heavily involved in the degradation of JUNV GPCs expressing the T168A substitution.

To confirm that the lysosome is responsible for the degradation of GPC, I utilized confocal microscopy to confirm co-localization of GPC with lysosomal compartments within BHK-21S cells. In order to stain lysosomes, I stained the lysosome using an anti-lysosome associated membrane protein-1 (LAMP-1) antibody. Confocal micrographs displayed co-localization of concentrated GPC with patches of concentrated LAMP-1, suggesting that Can GPC is being transported from the ER to the lysosome for degradation (Fig 3.6B, white arrow). This result contrasts with Rom GPC, where the majority of the protein is detected at or near the cell surface and LAMP-1 is relatively undetectable. Taken together, the data indicates that the absence of the N166 glycan results in large quantities of GPC being targeted to the lysosome for degradation. The rapid degradation of the GPC in bulk would likely account for the decrease in protein observed in cells expressing XJ44, Can, and Rom-T168A GPC.

Growth kinetics and plaque morphology of recombinant JUNVs expressing GPCs with or without the T168A substitution are similar in cell culture

After determining the effect of the T168A substitution on intracellular trafficking of the GPC *in vitro*, I introduced each GPC into the rRom virus to determine the effect of each GPC on the virus life cycle. The kinetics of viral protein expression within the context of infection is significantly different than the plasmid-based overexpression system, and would be more representative of GPC processing *in vivo*. The expression of GPC is delayed, and tightly regulated by Rom Z expression, and could potentially create a further discrepancy between the processing of Rom GPC and the other GPCs.

The XJ13, XJ44, Can, and Rom-T168A GPCs were introduced into the rRom backbone to create chimeric rRom JUNVs expressing each of the listed GPCs. The viruses

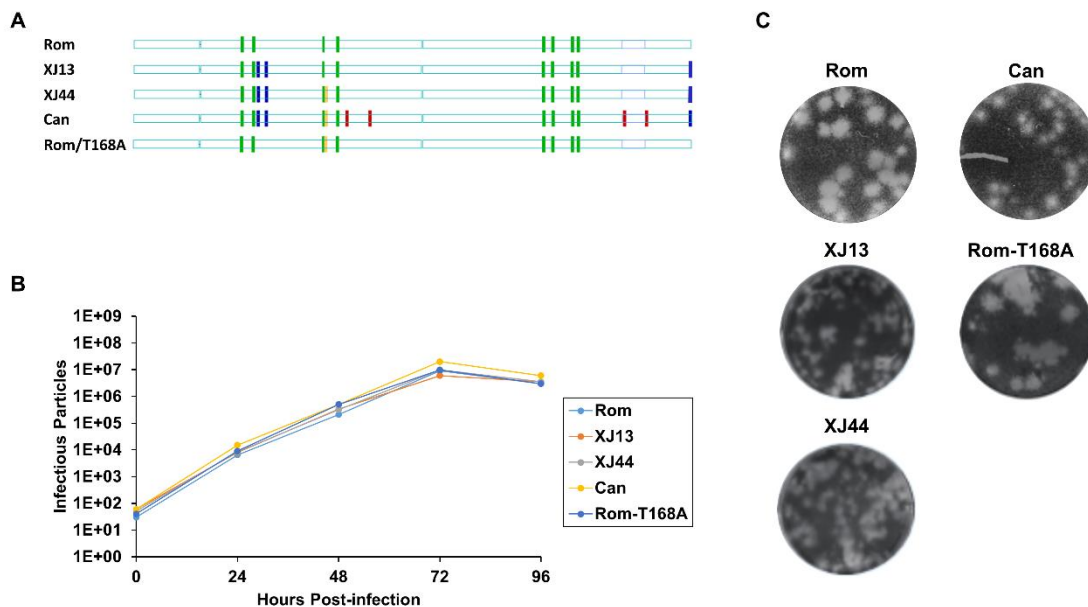


Figure 3.7: Growth kinetics and plaque phenotype of rRom viruses expressing various GPC proteins. **A)** Rom Pol-I expression plasmids were modified to express each of the GPCs schematically represented within the GPC ORF, and the plasmids were used to transfect BHK-21S cells to create rRom viruses expressing each GPC. **B)** Growth kinetics in Vero cells were determined for each virus in triplicate. Values represent the average number of infectious particles represented by plaques at each time point. **C)** Plaque phenotype in Vero cells. Viruses were allowed to incubate in Vero cells overlaid with 1% agarose in MEM. Cell cultures were formalin-fixed at 5 days post-infection and stained with crystal violet.

were rescued by transfecting and culturing BHK-21s cells for 96 hours at 37°C to create P0, and P1 was generated by infecting Vero cells with the P0 supernatant under the same conditions. The viruses all produced similar P0 titers in Vero cells, and the growth kinetics of each virus at a low MOI (MOI = 0.1) produced very similar titers across all time points through 96 hours in Vero cells (Fig. 3.7). The differences existed in the plaque morphologies of each virus. The Rom strain exhibited large plaques in Vero cells, but the plaque phenotype was transformed into small plaques upon the introduction of the two G1 substitutions and single cytoplasmic domain substitutions that are XJ13-specific. The plaque phenotype remained small for XJ44 and Can, but the plaque phenotype remained large upon the introduction of only the T168A substitution into rRom (Fig. 3.7). This data indicates that one or more of the XJ13-specific substitutions are responsible for the small plaque phenotype. However, it is interesting that none of the viruses display differences in infectious particle production. There were differences in RNA and protein levels for rRom expressing Can GPC in our previous data (unpublished data), indicating that the difference may exist in the ability of the viruses to assemble into infectious particles, making higher levels of replication necessary to maintain similar growth kinetics.

Viruses expressing the T168A substitution in G1 induce ER stress during infection

Although the growth kinetics of each virus was similar across all time points, previous data indicated that protein expression and is markedly different between rRom and rRom expressing Can GPC. The virus exhibits an increase in NP, an absence of Z, and an increase in total GPC, suggesting that the presence of Can GPC in the Rom virus has a significant effect on the protein expression of JUNV (unpublished data). Overexpression of GPCs with the T168A substitution results in ER retention, UPR activation, and ER stress. Therefore, it is likely that GPC aggregates would be detectable. If GPC is being degraded in the lysosome, autophagy of the ER would be the most likely mechanism of

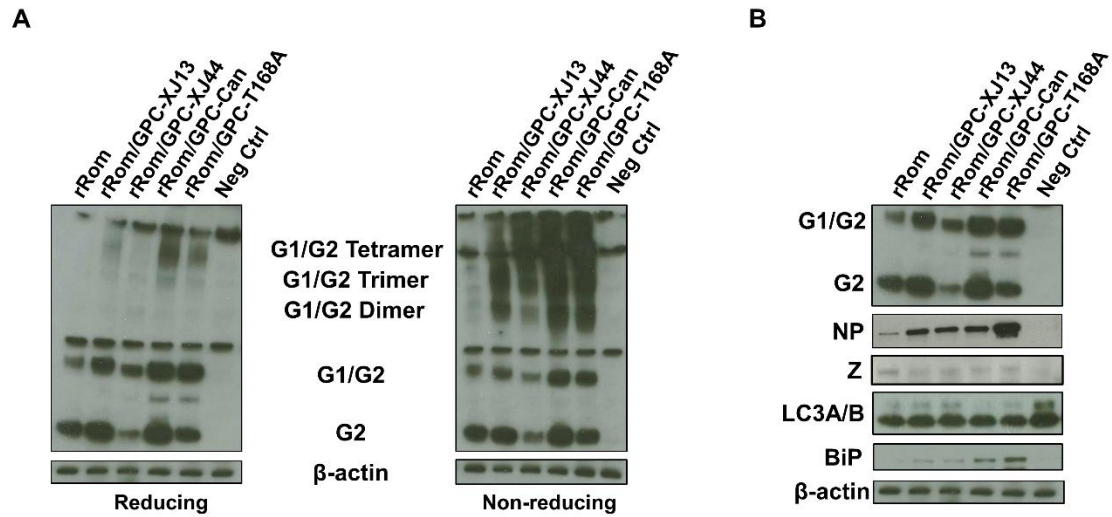


Figure 3.8: Viral protein expression profiles in Vero cells. **A)** Western blot analysis of GPC, UPR (BiP), and autophagy-related (LC3 I) proteins in reducing and non-reducing conditions. Infected Vero cells (MOI = 5) were lysed at 36 hours post-infection in 1x Laemmli buffer. The samples in reducing conditions were treated with β -mercaptoethanol prior to electrophoresis. The samples were stained with an anti-G2 primary antibody (ProSci) or anti- β -actin antibody (Cell Signaling) followed by an HRP-conjugated secondary antibody (Cell Signaling). **B)** The same samples listed in (A) were additionally stained with anti-NP and anti-Z primary antibodies (ProSci), as well as anti-BiP, anti-LC3 I primary antibodies (Cell Signaling). Detection was achieved with HRP-conjugated secondary antibodies (Cell Signaling).

degradation. During autophagy, the larger LC3A/B-I proteins are processed into slightly smaller proteins, LC3A/B-II. A decrease in LC3-I (A or B) is indicative of autophagy, and is further confirmed by a decrease in total LC3 since the protein is degraded in the lysosome along with the targeted organelle.

In order to investigate the differences in protein expression between each rRom/GPC variant, I infected Vero cells with each GPC variant and allowed the cells to incubate for 48 hours at 37°C before lysing the cells in Laemmli buffer for Western blot analysis. The GPC expression was compared in both reducing and non-reducing conditions to test for differences in disulfide bond formation. The results indicate that aggregation is in fact present in all viruses other than rRom (Fig. 3.8). It is noteworthy that rRom/GPC-XJ13 contains primarily dimer and trimers, whereas rRom/GPC-XJ44 forms higher-order

multimers. Both the rRom/GPC-Can and rRom/GPC-T168A exhibit a high number of aggregates of all sizes. The data suggests that these aggregates do not typically form in the wild-type virus where the replication and protein expression is properly regulated by Z, preventing the accumulation of GPC in the ER due to efficient folding and export. However, the presence of processing issues in GPC lead to the inevitable accumulation of these GPC proteins in the ER. The rRom virus also has the highest detectable amount of Z in the lysate as well as the lowest amount of NP (Fig. 3.8), supporting the evidence that the Z protein tightly regulates the protein expression through inhibition of replication. The Z protein remained detectable for the rRom viruses expressing each of the other GPC variants, but the amount of detectable Z was markedly lower. The decrease in Z was associated with an increase in NP. The samples in which aggregates were present also showed a significant upregulation of BiP, indicative of UPR activation. Additionally, autophagy was much more active in Vero cells infected with either rRom/GPC-Can or rRom/GPC-T168A (Fig. 3.8). Remarkably, the rRom/GPC-T168A virus exhibited the highest amount of GPC aggregation and the highest amount of NP, which is also associated with the most significant BiP upregulation and most active autophagy of any of the rRom strains expressing any of the GPC variants. Together, the data suggests that the T168A substitution causes aggregation of GPC in the ER, leading to activation of the UPR and the eventual degradation of the protein through autophagy during infection. Additionally, this process contributes to a decrease in Z and a decrease in the ability of the virus to regulate its own protein expression.

DISCUSSION

The mechanisms that are responsible for the attenuation of the JUNV Can strain, which is currently approved for use as a live-attenuated vaccine in AHF-endemic regions (Ambrosio et al., 2011), remains largely unknown. Previous studies have identified regions

within genes that are involved in the attenuation of the Can strain, but the mechanisms through which these regions serve to attenuate the Can strain remain incomplete. One previous study demonstrated that a single substitution (F427I) within the transmembrane region of G2 in the Can strain attenuates the neurovirulence of JUNV in the mouse model of infection (Albarino et al., 2011a). A separate study indicated that this substitution destabilizes the metastable conformation of the GPC, resulting in a conformational change to the fusogenic state at neutral pH (Droniou-Bonzom et al., 2011). Despite these findings, intraperitoneal inoculation of a rRom virus that expresses the F427I substitution in G2 results in a self-limiting acute disease in guinea pigs (Seregin et al., 2015). This suggests that the F427I substitution is only partially responsible for the attenuation of the Can strain. It is noteworthy that this amino acid substitution was introduced during cell culture passages in FRhL-2 cells, which took place after the virus had already achieved attenuation in both guinea pigs and nonhuman primates (Ambrosio et al., 2011). A more recent study has demonstrated that the GPC is the primary attenuating gene in the Can vaccine strain. Among the four genes of the Can strain, only a rRom virus expressing the full-length Can GPC was completely attenuated in guinea pigs (Seregin et al., 2015). Therefore, the role of the additional amino acid differences between Rom and Can GPC in the attenuation of the virus prompt further investigation. Among these differences is a single amino acid substitution (T168A) that was introduced between XJ13 and XJ44, which eliminates an N-linked glycosylation motif in G1 (Albarino et al., 2009).

As the GPC progressed through the mouse brain passages, mutations accumulated that affected the ability of the GPC to be processed by SKI-1/S1P. There is a noticeable shift in the amounts of full-length GPC and cleaved G2 in Western blot analysis of the GPC, with the amount of cleaved G2 decreasing gradually. The largest shift in cleaved G2 is observed between XJ13 and XJ44, where cleaved G2 becomes almost undetectable. This change coincides with a single amino acid substitution (T168A) which eliminates an N-linked glycosylation motif from G1. Interestingly, the full-length GPC band also

undergoes increased migration between XJ13 and XJ44 without any shift in cleaved G2. This is strongly indicative of a missing glycan at N166. By treating the Western blot samples with PNGase-F, the full-length GPC bands all migrated the same distance in the gel, demonstrating that the difference in migration observed for XJ44 and Can was due to a difference in N-linked glycosylation. The modification of the glycosylation profile of LASV has previously been shown to alter the ability of the protein to be successfully cleaved (Eichler et al., 2006). The data suggests that mutation of the N-linked glycosylation motif from N166-T168 in the G1 protein of Rom has a similar effect. Interestingly, mice with genetically decreased S1P activity (*Mbtps1^{wrt}*) are resistant to persistent LCMV Clone 13 infection, and are capable of clearing the virus despite their lymphocyte immunodeficiency. The growth of LCMV Clone 13 was severely reduced in *Mbtps1^{wrt}* bone marrow dendritic cells (bmDCs), and the growth was restored by mutating the RRLA cleavage motif into RRRR. This allows for cleavage by the Furin protease in the *Mbtps1^{wrt}* mice, which allowed the virus to re-establish a productive infection in bmDCs (Popkin et al., 2011). While this observation is cell type-specific, it raises the possibility that a decrease in G1/G2 cleavage efficiency and sub-optimal ER processing of the GPC affects the ability of JUNV to establish a productive infection in dendritic cells, a primary target cell of JUNV *in vivo*. Providing support to this possibility is the observation that the Rom strain can productively infect THP cells that were induced into macrophages *in vitro* while the Can strain cannot establish a productive infection in the same cells (unpublished data).

Retention of Can GPC within the ER is the result of a processing issue due to the absence of the glycan at N166. However, the mechanism through which the GPC is marked for retention remains unclear. It is possible that the absence of the glycan results in the protein folding into an incorrect low-energy state, triggering recognition by resident chaperones within the ER and subsequent refolding of the protein. Removal of key N-linked glycans in the human protein tripeptidyl-peptidase I (TPP I) results in the protein

reaching the incorrect conformation. Removal of the glycan at N286 results in a fraction of the misfolded protein being retained in the ER, whereas the predominant pathway for the misfolded protein is the secretory pathway. The misfolded protein forms inter-chain disulfide bridges similar to the aggregates formed by Can GPC. Only a small amount of the protein reaches its target in the lysosome, where it is processed and becomes active (Wujek et al., 2004). The removal of the N-linked glycosylation motif between N166 and T168 results in predominantly ER retention of the protein, where it forms inter-chain disulfide bridges. Only a small fraction of the protein reaches its target and is processed into functional glycoprotein complexes, sharing a parallel to TPP I. It is likely that the absence of the glycan at N166 does not directly alter the secondary structure of the domain, but rather impacts the folding kinetics of the protein. The N-linked glycans present on the hemagglutinin (HA) protein of influenza are positioned optimally for the recruitment of the lectin chaperones calnexin and calreticulin. These chaperones serve to separate the domains from one another to slow the folding process and allow the correct disulfide bridges to form. The proximity of cysteine residues to glycans allows for calnexin and calreticulin to block improper Cys-Cys interactions and promote the correct folding of the protein (Daniels et al., 2003). The crowded environment within the ER could contribute to incorrect disulfide bridge formation in the absence of the N166 glycan in JUNV G1, which would be in agreement with the observed aggregation of JUNV GPCs expressing the T168A substitution.

The reduced surface expression of XJ44, Can, and Rom-T168A GPC would be expected to have an impact on infectious particle assembly. Interestingly, the decrease in surface expression did not impact the titers in Vero and A549 cells. While attenuation of a virus can be linked with attenuated growth *in vitro*, certain arenavirus strains such as the genetically altered LCMV Clone 13^{FURIN} strain are attenuated in mice despite similar growth properties *in vitro* (Popkin et al., 2011). It is possible that the JUNV Can strain does not require concentrated GPC on the surface of the virion to infect target cells,

whereas the virus requires highly concentrated GPC to maintain infectivity *in vivo*. It is also noteworthy that the total viral protein in cells infected with XJ44, Can, and Rom-T168A is significantly greater than the total viral protein in Rom-infected cells (Fig. 3.8). Therefore, the Can strain could have developed more active replication machinery to overcome inefficient assembly in order to maintain its titer *in vitro*.

The upregulation of BiP and decrease in LC3-I, together with ER and LAMP-1 colocalization with GPCs expressing the T168A substitution, strongly suggest the activation

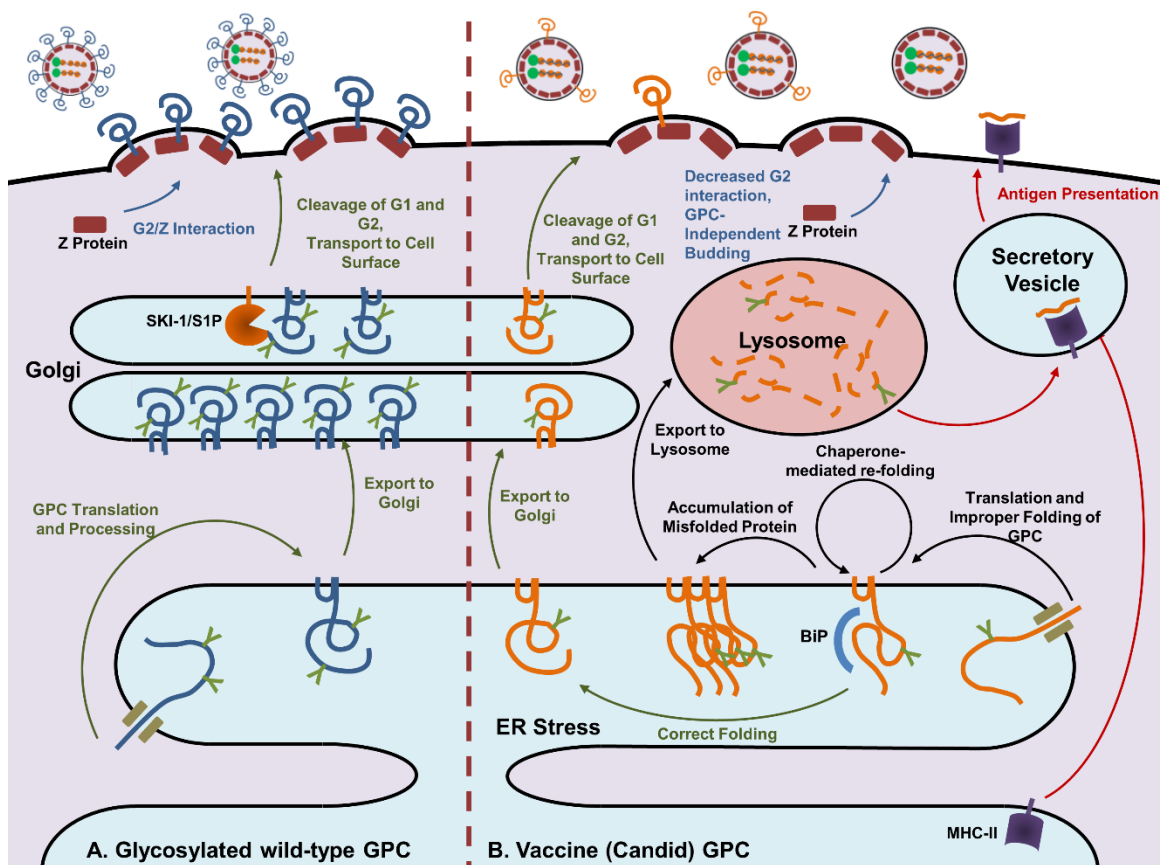


Figure 3.9: Differential intracellular processing of Rom and Can GPC. Schematic representation of my proposed model for Can GPC processing. The standard pathway for the wild type virus (green arrows) involves the efficient folding of the protein due to proper post-translational modifications in the ER. The protein is transported to the Golgi, where the predominant form that arrives in the cell surface is cleaved. GPC is included into budding particles at a high concentration. The incorrect pathway (black arrows) is the predominant pathway for the Can GPC, resulting in the aggregation and degradation of the protein in the lysosome. I hypothesize that this process will increase antigen presentation of GPC epitopes (red arrows).

of the UPR and unsuccessful resolution of the protein accumulation. The activation of the UPR and degradation of the viral GPC would potentially make viral peptides more accessible for antigen presentation through major histocompatibility complex class II (MHC-II) binding in lysosomes and autophagosomes. DCs are primary targets of JUNV during early infection, and are capable of presenting antigens from a number of sources, including autophagosomes (ten Broeke et al., 2013). The Can strain of JUNV has also been shown to activate the type I IFN response through RIG-I, and has even been described to induce apoptosis in infected cells (Huang et al., 2012; Kolokoltsova et al., 2014). These factors may all play a role in the ability of the host to elicit a strong immune response against the Can strain early in infection.

The analysis of the data from expression plasmid transfection and *in vitro* infection of cell cultures has provided a potential mechanism of differential GPC processing between the Rom and Can strains (Fig. 3.9). The Rom GPC contains the necessary primary sequence information to efficiently reach the correct conformation in the ER, and is expressed on the cell surface at a high concentration. The Can GPC is missing a key N-linked glycan that is required to reach the correct conformation in a timely manner, forcing the ER to retain the protein for refolding. The accumulation of the protein activates the UPR and eventually results in the degradation of GPC in bulk within the lysosome. Only a small percentage of the GPC passes through the Golgi successfully, where it is cleaved and expressed on the cell surface in low concentrations. Together, the data provides valuable insight into the attenuation mechanisms of the Can strain, and could provide a more universal application to vaccine design due to the somewhat conserved pathways of viral glycoprotein maturation.

Chapter 4: Effects of the N-terminal and RING Domain Substitutions in Can Z on Protein-Protein Interactions

INTRODUCTION

Arenaviruses possess a relatively small genome size, expressing only four genes during the life cycle. This strategy requires proteins to carry out multiple functions during replication and budding. The smallest gene, which encodes the Z protein, is central to the regulation of RNA replication and drives the budding of infectious virions from the cell surface. Evidence also indicates that the Z protein plays a role in interferon antagonism (Fehling et al., 2012). In the late stages of replication, the Z protein binds to the LP to inhibit replication and promote budding. During the budding stage, the Z protein binds to the GPC and is responsible for the recruitment of the RNP into the virion. The Z protein accomplishes the necessary protein-protein interactions with other viral proteins through its central RING domain and its myristoylated N-terminal domain.

The exact domains and amino acids involved in specific protein-protein interactions have not been described, but evidence in confocal microscopy and electron microscopy demonstrates that the Z protein does associate closely with GPC at the cell surface during budding (Schlie et al., 2010). The GPC-Z interaction occurs despite nonfunctional RING or C-terminal domains within the Z protein (Capul et al., 2007). However, the N-terminal myristoylation of Z is critical to its ability to interact with the GPC. Suppression of Z myristoylation affects the subcellular localization of Z, thereby preventing its association with GPC (Strecker et al., 2006). The interaction could primarily be through association with the SSP, since the Z protein has been shown to interact with SSP outside of the context of the other subunits of GPC (Capul et al., 2007). GPC-Z interaction also drives budding from the apical surface of epithelial cells. Outside of the interaction with GPC, the Z

protein buds nonspecifically from the apical and basolateral surfaces of the cell (Schlie et al., 2010).

Z interaction with LP and NP serves to inhibit replication as well as to recruit RNP into the budding virions. However, the specific mechanisms through which JUNV Z protein binds the polymerase and incorporates the RNP into budding particles has not been elucidated. Z-binding to LP has been mapped to the RING domain and the adjacent amino acids of the C-terminal region of the TCRV Z protein (Jacamo et al., 2003). Specific amino acids within domain III of the TCRV LP (H1189 and D1329) have also been described to be important in Z-LP binding (Wilda et al., 2008). The JUNV Z protein recruits NP into budding VLPs when the two proteins are co-expressed, suggesting that Z-NP interaction is likely involved in the recruitment of RNP into infectious particles. Residue L79 in the RING domain of Z has been demonstrated to be critical to this protein-protein interaction (Casabona et al., 2009). The corresponding residue, L71, has been shown to be important in Z-NP interaction in LASV. Both mutations significantly reduced the infectivity of virions (Capul et al., 2011). Direct Z-NP interaction has also been confirmed for TCRV and MOPV (Shtanko et al., 2011), and TCRV Z-NP interaction enhances the budding activity of Z (Groseth et al., 2010). Additionally, self-interaction of Z protein and self-budding independent of other viral proteins has been described for LASV and LCMV (Perez et al., 2003; Strecker et al., 2003). Although interactions between Z and LP/NP have been described, it is unclear which interactions are important for RNP incorporation into the virion.

Previously, our lab has demonstrated that the Candid GPC is the primary gene responsible for attenuation of the Can strain. However, the Can Z protein was partially attenuating when expressed in place of the Rom Z in our rRom virus (Seregin et al., 2015). This particular virus yields fewer infectious particles in cell culture despite high levels of RNA replication, suggesting that the assembly of virions is affected by the amino acid changes in the Z protein between Rom and Can.

In this chapter, I utilize our reverse genetics-based rescue system to investigate the effects of specific amino acid substitutions between Rom and Can Z on infectious particle production. The RING domain substitution V64G affected the infectious particle production significantly for the Rom strain, and this effect was rescued by providing Rom with the Candid LP. Additionally, the presence of the same RING domain substitution in Rom Z further reduced infectious particle production to almost undetectable levels when combined with the Can GPC. This effect was rescued by including the Can-like V18A substitution in the N-terminal region of Z, indicating that the Can GPC has a reduced affinity for the Rom Z N-terminal domain. The V18A substitution appeared to restore the affinity between the two proteins.

RESULTS

Preliminary data: rRom expressing the Can Z protein exhibits a decrease in infectious particle production

The slight decrease in virulence of rRom expressing Can Z in our guinea pig model of infection (Seregin et al., 2015) prompted our lab to investigate differences in the virus life cycle *in vitro*. We felt it necessary to compare the growth kinetics of this virus to our other inter- and intra-segment chimeric viruses, as well as to rRom and rCan virus. We infected Vero cells (MOI = 0.01) with each of our inter- and intra-segment chimeric viruses (rRom-CanLP/NP/GPC/Z) and compared their infectious particle production to rRom and rCan at the selected time points. All chimeric strains maintained equal infectious particle production to rRom and rCan across all time points with the exception of rRom/CanZ. The

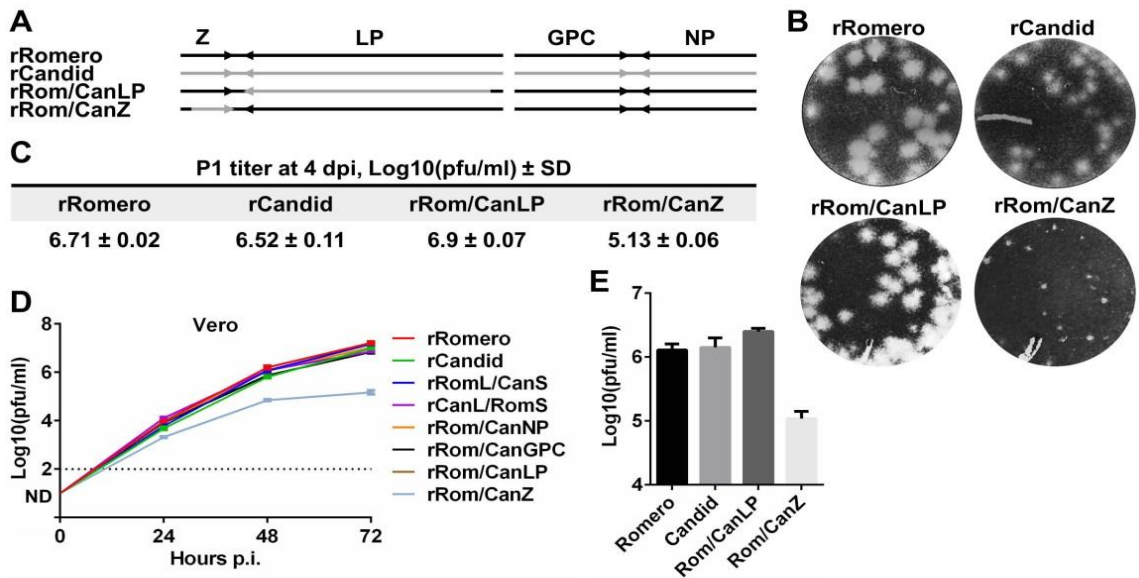


Figure 4.1: Can Z reduces infectious particle production in rRom. **A)** Schematic representation of the recombinant viruses rescued. **B)** Plaque phenotypes in Vero cells. Cells were infected and incubated with a 1% agarose overlay for 5 days. Cells were fixed with formalin and stained with crystal violet. **C)** Comparison of P1 titers in Vero cells, measured at 4 days post-infection. **D)** Growth kinetics of each recombinant virus in Vero cells (MOI = 0.01). **E)** Graphical comparison of P1 titers.

expression of Can Z decreased the infectious particle production of the Rom virus by roughly 100-fold. Interestingly, the plaque phenotype of rRom/CanZ is distinctly smaller than the plaques generated by the other viruses (Fig. 4.1). Despite the decrease in infectious particles, the virus produced more RNA and protein than the rRom virus (Seregin and Manning et al., in review), suggesting that the decrease in infectious particles is due to the efficiency of particle assembly as opposed to a decrease in replication.

The RING domain substitution in Z is responsible for the decrease in infectious particle production

The Can Z protein contains two amino acid changes with respect to the Rom GPC. One change lies within the N-terminal domain (V18A), while the other change is located within the highly conserved RING domain (V64G). These changes are both present as early as XJ13, and no GenBank sequences of wild-type JUNV strains contain either of

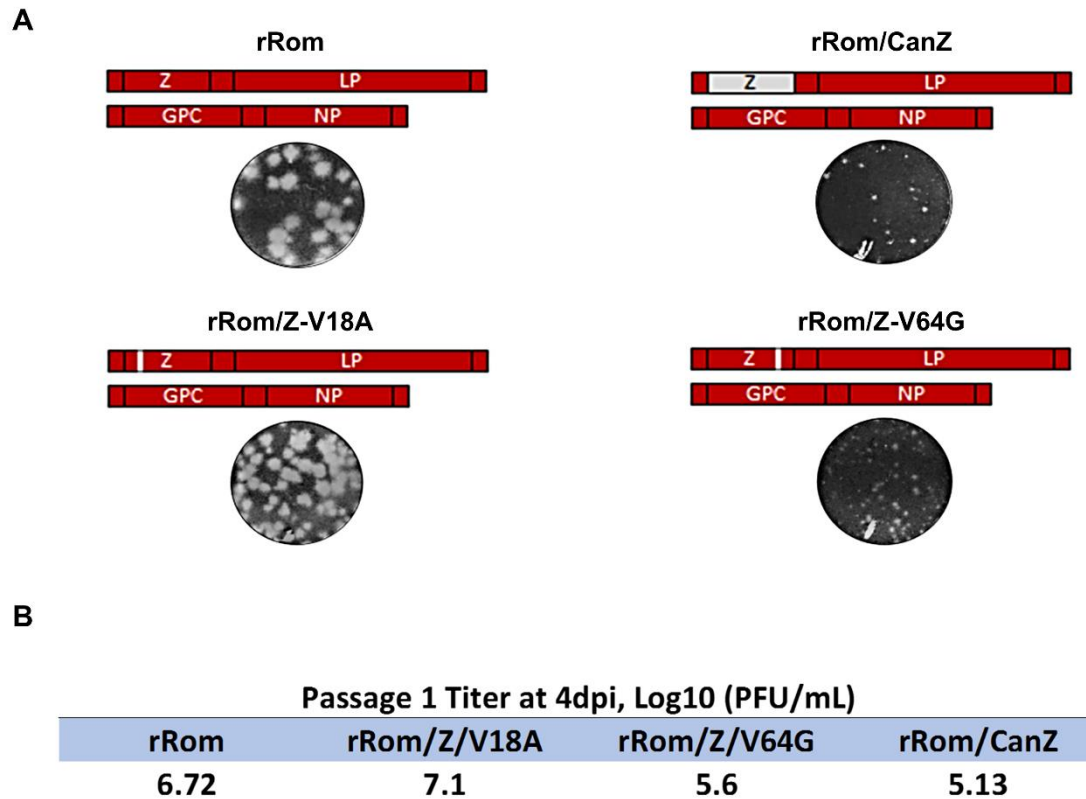


Figure 4.2: The V64G substitution decreases the titer and reduces plaque size. A) Schematic representation of the Z-mutant viruses rescued. Plaques were obtained by infecting Vero cells and incubating for 5 days with a 1% agarose overlay. The cells were fixed in formalin and stained with crystal violet. **B)** Comparison of P1 titers between each of the rescued viruses from (A).

these two Z substitutions. Although the original XJ sequence is not available on GenBank, it is likely that the XJ sequence was more similar to the Rom sequence based on this information. In order to investigate the contributions of each of these amino acid substitutions on the infectious particle production of the Rom strain, I utilized site-directed mutagenesis to introduce each of the two substitutions into the Z ORF of the Rom mPol-I-Lag plasmid independently of one another (Fig. 4.2). This allowed for the rescue of rRom viruses expressing each of the two substitutions, V18A (rRom/Z-V18A) and V64G (rRom/Z-V64G). The V18A substitution lies within the N-terminal region, which is proposed to interact with the GPC during budding. The V64G mutation is located within

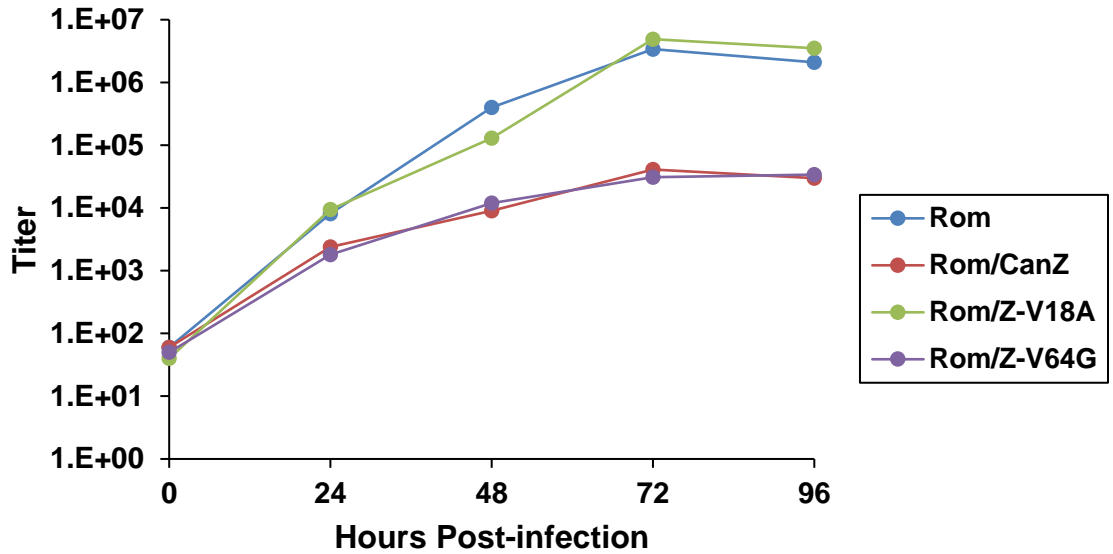


Figure 4.3: The V64G substitution decreases the infectious particle production of rRom. rRom viruses expressing either Can Z, the V18A substitution, or the V64G substitution were used to infect Vero cells (MOI = 0.01) and were incubated at 37°C for 4 days, collecting the supernatant every 24 hours. The titers of the supernatant samples were measured using plaque assay on Vero cell monolayers overlaid in 1% agarose. The cells were fixed with formalin at 5 days post-infection and stained with crystal violet.

the highly conserved RING domain of the Z protein, and has been shown to interact with both the viral NP and LP (Fehling et al., 2012). Both mutations could have an effect on particle assembly due to interruption of specific protein-protein interactions.

Both rRom/Z-V18A and rRom/Z-V64G were both rescued simultaneously with rRom and rCan in BHK-21S cells to create P0, which for which the titer was determined by plaque assay in Vero cells. I generated a P1 in Vero cells for each virus, using an equal amount of seed virus (MOI = 0.01) for each P1 stock. I then generated a titer for each P1 virus in Vero cells at day 4 post-infection and compared the plaque phenotypes for each virus to one another (Fig.4.2). The substitution directly involved in the reduction of titer, plaque size, and particle production over time is the V64G mutation that lies within the RING domain. Interestingly, the V18A substitution does not appear to have any effect on the infectious particle production in the context of rRom genes and proteins (Fig. 4.2, Fig

4.3). Based on the proposed protein-protein interacting domains between Z and the other viral proteins, it is likely that the Z protein is failing to interact with either the LP or NP.

The V64G substitution in Z decreases interaction with the LP

Previous data describing regions involved in Z interaction with other viral proteins suggests that a mutation in the RING domain would most likely affect the interaction between the Z protein and either NP or LP. However, effects on the Z-GPC interaction cannot be ruled out. The RING domain of the TCRV Z protein has been proposed to bind to both domains I and III of the TCRV LP (Jacamo et al., 2003; Wilda et al., 2008). However, the domain-specific Z-LP interactions have not been confirmed for JUNV. The specific RING domain amino acids required for interaction of Z with NP have been described in part for JUNV (Capul et al., 2011), but the specific amino acids of NP required for this interaction also remain unknown. In order to determine which protein-protein interaction is affected by the V64G substitution, I rescued rRom viruses containing either Can LP, NP, or GPC as well as the V64G mutation in Rom Z. Since the Can titer is similar to the Rom titer *in vitro*, it is likely that pairing the correct Can protein with the V64G substitution will restore the titer to normal values.

Each of the required plasmids were transfected into BHK-21S cells to rescue each of the viruses, and the P0 supernatant was collected at 4 days post-transfection. After titration in Vero cells, equal amounts of virus were used (MOI = 0.01) to infect Vero cells in order to generate P1. The P1 supernatant was collected at 4 days post-infection for each of the viruses, and the virus titer was determined by plaque assay in Vero cells. A strong correlation exists between the P1 titer and the growth kinetics over time for each of the viruses rescued in previous experiments (Fig. 3.7, Fig. 4.3). Therefore, I felt that the P1 titer of each virus would be representative of the overall growth kinetics for each of the viruses. The P1 titers reveal that the protein responsible for restoring the infectious particle

production to wild-type amounts is the LP protein, indicating that the Z-LP interaction is affected by the V64G substitution in Rom Z. The plaque phenotype is also partially restored in this virus (Fig. 4.4). The pairing of the Can NP with the V64G Z substitution did not have any effect on the P1 titer or the plaque phenotype, indicating that the substitution likely does not affect the Z-NP interaction. However, it is noteworthy that the titer was significantly decreased to almost undetectable levels when the V64G substitution was paired with the Can GPC, and the plaque phenotype remained small (Fig. 4.3). This data suggests that while the V18A substitution in Z has no effect on the infectious particle production *in vitro* when paired with other Rom proteins, it may play a role in maintaining the interaction with Can GPC. The Rom GPC appears to tolerate either V or A at amino acid position 18, however the Can GPC contains an R484G substitution in the cytoplasmic

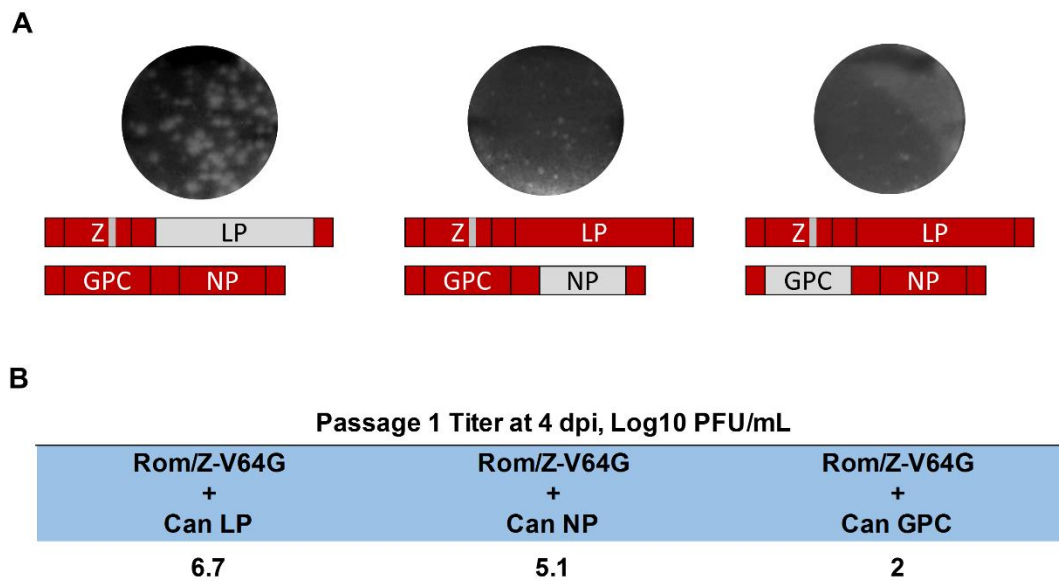


Figure 4.4: The V64G substitution reduces the affinity of Z for LP. **A)** Recombinant Rom viruses were given the V64G substitution along with either Can LP, NP, or GPC and rescued by transfecting GHK-21S cells with the required plasmids to yield infectious virus. The P0 virus was collected and used to infect Vero cells at MOI = 0.01. The Vero cells were incubated at 37°C for 4 days, then the supernatants were collected and titration was performed by plaque assay. The plaques were stained using crystal violet. **B)** The titrations for each virus are listed.

tail of G2. It is possible that this substitution in GPC requires the V18A substitution to maintain Z-GPC interaction.

The V18A substitution is required to maintain Z interaction with Can GPC

The decrease in particle production in the rRom virus containing both the V64G substitution in Z and the Can GPC is intriguing considering that the Rom GPC is tolerant of either A or V at position 18 in Z, and rRom/CanGPC maintains similar titers to rRom. Evidence suggests that the cytoplasmic tail of G2 and the SSP are both involved in interaction with the Z protein. The N-terminal domain of the Z protein also plays a significant role in this interaction due to the presence of the myristoylation at amino acid position 2 of the protein (Capul et al., 2007). However, the exact mechanism of the recruitment of GPC into budding virions and the specific amino acid interactions have not been described. In order to determine the effect that the V18A substitution has on Z-GPC interaction, I rescued a rRom virus that expresses both Can GPC and Can Z. This combination added just the V18A substitution into the rRom/Z-V64G + Can GPC virus that produces only 200 infectious particles per mL. Using the same procedure described in the previous section, the mPol-I/II rescue system was used to generate the rRom virus containing both Can Z and GPC. As expected, the titer of the P1 virus in Vero cells was restored to values similar to the observed titer for rRom/CanZ. Combining the Can GPC with the V18A substitution in Z appears to restore the interaction of the two proteins with one another.

Since the titer suggests that the V18A substitution improves Z interaction with Can GPC, I aimed to confirm the enhanced Z-GPC interaction through Western blot analysis using CMV-driven expression plasmids. I transfected HEK293 cells with plasmids expressing either Rom or Can GPC, and Rom or Can Z in combination with one-another. The cells were allowed to incubate for 48 hours at 37°C before lysing the cells in Laemmli buffer. The data supports that the Rom GPC/Rom Z combination provides the strongest

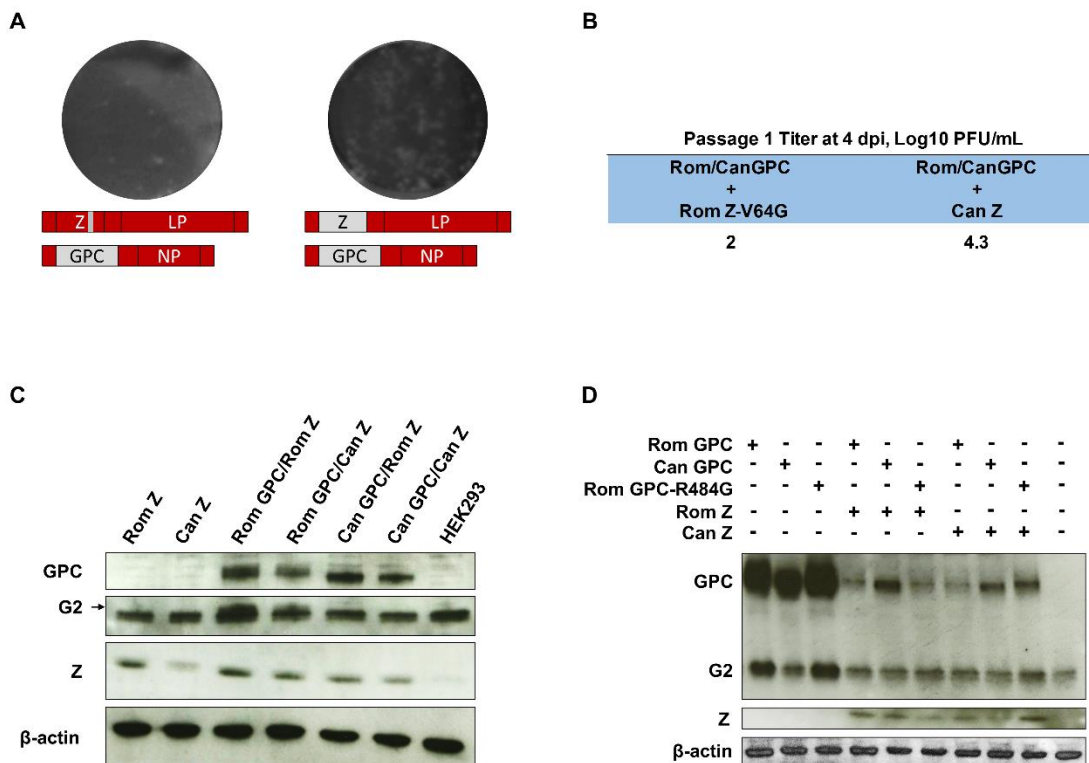


Figure 4.5: The Can GPC-Z interaction is enhanced with both the Z-V18A and GPC-R484G substitutions. **A and B)** Using our mPol-I/II rescue system, I rescued a rRom virus that substitutes the Can GPC and Can Z for the wild-type proteins. I compared this virus to the rRom/Z-V64G + Can GPC virus that was rescued in the previous experiment through both plaque phenotype (**A**) and P1 titer (**B**). The virus was rescued using the previously described conditions (Fig. 4.4) and P1 was generated in Vero cells. Titration was performed on Vero cell monolayers for each virus with a 1% agarose overlay. **C and D)** HEK293 cells were transfected with either pC-RomGPC, pC-Can GPC, or pC-RomGPC-R484G in combination with either pC-RomZ or pC-CanZ. After transfection with XtremeGENE-9 (Roche) transfection reagent, the cells were incubated for 48 hours at 37°C and lysed with Laemmli buffer. Each blot was stained with anti-JUNV GPC and Z rabbit monoclonal antibodies (ProSci) and HRP-conjugated anti-rabbit secondary antibodies (Cell Signaling).

expression and retention of both intracellular GPC and Z. Expression of Rom GPC with Can Z results in a slight loss of intracellular retention for both proteins. It is interesting to note that the expression of Can GPC decreases the intracellular levels of both Z proteins, and the least cellular retention is observed when the Can GPC and Can Z are expressed in combination (Fig. 4.5). This is more likely due to the fact that only a small percentage of GPC reaches the cell surface where the GPC-Z interaction takes place. It is also noteworthy that Rom Z remains detectable inside cells when expressed independently, but Can Z appears to leave the cell more readily (Fig. 4.5). Evidence of independent Z budding has been described (Casabona et al., 2009), so it is likely that the Can Z is more prone to bud independently than Rom Z. The data suggests that fundamental differences in both Z and GPC are contributing partially to interaction and retention. While Can Z appears to more readily bud from the cell, Can GPC affects the interaction as well. Since the Can GPC interaction with Z is enhanced with the V18A substitution present, there is most likely a contributing factor in GPC that enhances this interaction.

The only change in the cytoplasmic regions of GPC between Rom and Can is the R484G substitution in the cytoplasmic domain of G2. To investigate the importance of this substitution in Z interaction, I introduced this substitution into Rom GPC and repeated the Western blot. As observed previously, the Rom Z is retained and detectable intracellularly when expressed in combination with either Rom or Can GPC. However, the intracellular levels of Z decrease when expressed in combination with Rom GPC-R484G relative to Rom Z/Rom GPC expression levels. Intracellular Can Z levels decrease relative to Rom Z levels in the presence of either Rom or Can GPC. However, the intracellular retention of Can Z does increase substantially when paired with Rom GPC-R484G (Fig. 4.5). Collectively, the results indicate that while Can Z disappears from the cell more readily than Rom Z, the R484G substitution in G2 helps to reduce the exit of Can Z from the cell. However, the availability of GPC near the cell surface affects this interaction as well.

DISCUSSION

The mechanism of attenuation of the JUNV Can strain still remains to be confirmed. While the GPC is the primary attenuating gene and the processing of Can is affected by a missing N-linked glycan in G1, the amino acid differences in Can Z have a clear effect on the virulence of the Rom strain. The Can Z protein has two amino acid differences with respect to the Rom Z: the V18A substitution located in the N-terminal domain and a V64G substitution within the highly conserved central RING domain. The N-terminal domain is myristoylated at amino acid G2 (Urata and Yasuda, 2012), and the myristoylation site is critical for GPC-Z interaction (Casabona et al., 2009). The mechanism through which the interaction occurs between GPC and Z is currently unknown. The RING domain is a motif that is highly conserved within both arenaviruses and eukaryotic cells, and this Zinc-binding domain is responsible for orchestrating protein-protein interactions. The RING domain has been shown to be involved in interaction with NP and LP (Kranzusch et al., 2010), and self-interaction has even been observed through RING domain binding (Fehling et al., 2012; Kentsis et al., 2002). The Z protein drives arenavirus budding, and is responsible for the recruitment of the GPC and RNP into the virion.

The two substitutions in Can Z are already present in XJ13. Since no data on the sequence of the original XJ strain is readily available through GenBank, I questioned whether the can Z sequence remained unchanged from the pathogenic XJ strain. I checked each of the available JUNV sequences entered into GenBank, and found that V18 and V64 were conserved among all strains listed. It is therefore unlikely that A18 and G64 were present in XJ, and more likely that these changes occurred during early passages in mouse brain tissue. These changes partially attenuate the rRom virus in the guinea pig model, and could be a significant contributor to the partial attenuation of XJ13, which was reported to

be 70% lethal in 14 day old mice (Albarino et al., 2011a). There are a number of amino acid differences between Rom and XJ13 in each of the four proteins, which all could contribute to the complete attenuation when compared to the uniformly lethal Rom (Seregin et al., 2015). However, rRom/CanZ is only 20% lethal in the guinea pig model of disease. The decreased growth *in vitro* combined with the high levels of intracellular RNA in this virus suggested that the virion assembly is affected by the V18A and V64G substitutions. The V64G substitution was determined to be responsible for this decrease in viral titer, and pairing the G64 amino acid within the RING domain with the LP restored the titer to wild-type levels. The most reasonable assumption would be that the V64G substitution affects the ability of Z to interact with LP during budding. A decrease in Z-LP interaction could decrease the number of particles through failure to recruit either the RNP or just the polymerase into the budding particles. The Can Z more readily buds from infected cells, supported by the Western blot data from transfected cells (Fig. 4.5). This hyperactive budding would decrease the regulation of the LP, allowing replication of the genome to continue without inhibition. This is supported by the increase in intracellular RNA in infected cells.

The combination of the V64G substitution in Z and the Can GPC in rRom decreased the titer of the virus to nearly undetectable levels. Providing the V18A substitution restored the titer to levels comparable to the rRom/CanZ virus, suggesting that a Z-GPC interaction was restored. The myristoylation site at position G2 is critical to the interaction (Capul et al., 2007), but the specific amino acid residues in Z that are involved in the recognition of GPC have not been described. It is reasonable to assume that the of the N-terminal region of Z is heavily involved in GPC interaction due to both its proximity to the myristoylation site and the supporting evidence that a functional RING domain and C-terminal domain are dispensable for Z-GPC interaction (Capul et al., 2007). However, this data provides the first evidence of involvement of the N-terminal region of Z in GPC interaction outside of the myristoylation site.

The SSP has been observed to interact with Z outside of the context of the other subunits of GPC, suggesting that the peptide is involved in GPC-Z interaction (Capul et al., 2007). However, the R484G substitution within the cytoplasmic domain of G2 has a noticeable effect on GPC-Z interaction in co-transfection experiments. This particular substitution is present in G2 prior to XJ13, suggesting its co-evolution with the V18A substitution in mouse brains. This is supported by the observation that the R484G substitution is detrimental to Rom Z retention, but assists Can Z retention (Fig. 4.5). It is noteworthy that Rom Z appears partially unaffected by Can GPC since Can G2 contains the R484G substitution, and Can Z continues to bud from the cell at a high rate in the presence of Can GPC. This is likely due to the inability of Can GPC to reach the cell surface where the GPC-Z interaction takes place. The deletion of the C-terminal RRR in LCMV G2 has been shown to inhibit the cleavage and maturation of GPC while leaving the transport to the cell surface unaffected (Kunz et al., 2003). While this could affect the infectious particle production during infection, it is unlikely that G1/G2 cleavage would inhibit GPC-Z interaction of the transport to the cell surface remains unaffected. It is therefore more likely that the R484G mutation was an adaptation to the V18A mutation, or vice-versa. Additionally, the cleavage pattern of the Rom GPC appears unaffected in the presence of the R484G substitution in Western blots (Fig. 4.5).

It is intriguing that the Can Z is less detectable in cell lysates than Rom Z, even outside of the context of infection. The budding activity of the Z protein has been linked to the cellular ESCRT machinery, and budding of LASV and LCMV particles is enhanced through interaction with Tsg101 (Perez et al., 2003; Urata and Yasuda, 2012). The interaction with the ESCRT machinery is mediated through the C-terminal domain, which is identical in Rom and Can Z. The involvement of both V18A and V64G in the enhanced budding activity of Can Z must be investigated in more detail.

Chapter 5: The Can Polymerase Exhibits a Decreased Sensitivity to Z-mediated Inhibition

INTRODUCTION

After release of the RNP into the cytoplasm during the initial stages of infection, the LP begins replication of the arenavirus genome. The initial rounds of replication result in the production of both L and S anti-genomic RNA and mRNA that encodes the NP and LP ORFs. The secondary structures of the L and S IGR promote dissociation of the LP from the RNA initially due to the low concentration of NP, resulting in an excess of mRNA and accumulation of both NP and LP. As the two proteins accumulate, the production of anti-genomic RNA becomes more favored. The shift from mRNA production to anti-genomic RNA production is possibly due to the NP binding the IGR and removing the secondary structure, allowing the LP to read through the IGR and continue RNA synthesis (Tortorici et al., 2001). The entire process repeats for the accumulating anti-genomic copies, resulting in the production of mRNA encoding the GPC and Z ORFs and the eventual production of genomic RNA copies for packaging into virions (Kranzusch et al., 2010).

The Z protein plays multiple roles in the arenavirus life cycle, including the regulation of RNA synthesis. During the budding phase of the life cycle, the Z protein both inhibits the activity of the polymerase to slow RNA synthesis and recruits the polymerase and RNP into budding particles. It is currently unclear whether these events are controlled by the same mechanism or both occur as independent processes. Although initial evidence suggested that the Z protein of TCRV was required for genome replication and mRNA transcription, a growing body of evidence suggests that the effect of Z on RNA synthesis is inhibitory. The Z protein has been shown in several more recent studies to inhibit the polymerase in a dose-dependent manner, and is not a requirement for the

synthesis of RNA by the LP (Cornu and de la Torre, 2001; Cornu et al., 2004). The TCRV Z protein has been observed to lock the LP in its promoter-bound state, preventing the elongation step of RNA synthesis (Kranzusch and Whelan, 2011), but this mechanism of inhibition has not been described for other arenaviruses. Although the Z protein has been observed in oligomeric form, the Z protein appears to exert its inhibitory effect in monomeric form. Z-LP exists primarily as a heterodimer in vitro, and Z proteins that are unable to oligomerize show no decrease in their ability to inhibit LP (Kranzusch and Whelan, 2011). The inhibitory effect of Z on LCMV replication is significant enough that cells expressing the LCMV Z protein prior to infection are resistant to LCMV infection (Cornu et al., 2004). While the exact mechanism of inhibition remains unknown, data has provided insight into the process. Of the four proposed domains of the arenavirus LP, two domains have been observed to bind the Z protein. One of these sites has been mapped to domain I, at the N-terminus of the protein. The binding site lies between amino acid residues 156 and 192. A second binding site was mapped to domain II of the LP, which conducts RNA synthesis (Wilda et al., 2008). The Z protein requires a functional RING domain in order to inhibit the LP, particularly the Zinc-binding residues (Cornu and de la Torre, 2002). Since the LP retains its ability to bind to RNA in its Z-bound state, it is possible that RNP packaging involves Z-LP interaction. Furthermore, the experiments in Chapter 4 provide evidence that the Z-LP interaction is involved in packaging.

In this chapter, I investigate the inhibitory effect of Rom and Can Z on Rom and Can LP in a minigenome system. The Rom LP was only slightly more active in RNA synthesis than the Can LP in cell culture in the absence of Z. Providing either Rom or Can Z in Rom LP-expressing cells had a strong inhibitory effect on viral RNA synthesis in the cells. However, the Can LP was significantly less sensitive to both Rom and Can Z. The data indicates that the increase in viral replication observed in Can LP-expressing chimeric viruses is partially due to the decreased sensitivity of the LP to Z inhibition.

RESULTS

Preliminary Data: rRom that expresses CanLP more actively synthesizes RNA than the wild-type virus

After evaluating our chimeric rRom viruses that substituted individual Can genes for attenuation in our guinea pig model of AHF, we examined both the RNA and protein expression for each of the viruses in vitro. Since the Can GPC was determined to be the primary attenuating gene and the Can Z was determined to be partially attenuating (Seregin et al., 2015), we aimed to determine whether the viruses exhibited differences in either RNA synthesis or protein expression despite similar growth kinetics. Both rRom and rCan,

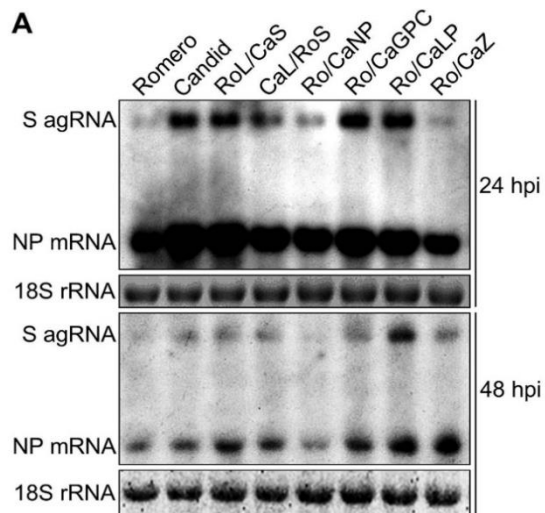


Figure 5.1: rRom viruses expressing the Can LP synthesize more RNA than viruses expressing Rom LP. Each virus was used to infect Vero cells at an MOI of 1. The cells were lysed in a Trizol solution at the specified time point and the RNA was purified using an RNeasy extraction kit (Zymo Research). The samples were analyzed by Northern blot and hybridized to RNA probes complementary to a region in the NP gene. The loading control (18SrRNA) was visualized using EtBr stain.

as well as rRom/CanNP, rRom/CanLP, rRom/CanGPC, rRom/CanZ, rRomL/CanS, and rCanL/RomS were used to infect Vero cells and collect cell lysates in Laemmli buffer and Trizol to compare protein expression and RNA synthesis, respectively.

While comparing RNA levels through Northern blot analysis at 24 and 48 hours-post infection, we noticed that the RNA synthesis varied among specific strains. Viruses that express either the Can LP or the Can GPC synthesize significantly more anti-genomic RNA than viruses expressing Rom LP and GPC at 24 hours post-infection. Interestingly, the

rRom/CanLP virus synthesizes significantly more anti-genomic RNA than all other chimeric viruses tested at 48 hours post-infection. Although the Can GPC has an effect on the RNA levels at 24 hours post infection, the difference is not as significant compared to rRom by 48 hours post-transfection. rRom/CanLP maintains significantly more anti-genomic RNA through 48 hours post-infection compared to rRom. This suggests that the Can LP is more active than the Rom LP during infection. The increased activity was due to either a more active enzymatic site in domain III or a desensitization to inhibition by the Z protein, and prompted further investigation.

The Rom polymerase synthesizes RNA at a more rapid rate than the Can polymerase

The relative activity of the Can LP is significantly higher than that of the Rom LP in a rRom virus in which all other genes are of Rom origin. The cause could be either increased activity of the catalytic site within domain III of the polymerase or decreased sensitivity to the inhibitory effect of the Z protein. In order to determine the cause, I began by investigating the relative activity of each polymerase within a minigenome system. The minigenome system utilizes CMV-driven expression plasmids to express the LP, Z, and NP (pC-LP, pC-NP, pC-Z) as well as a mPol-I-Sg expression plasmid that substitutes GFP for NP and firefly luciferase (FFL) for GPC. Transfection of each of the plasmids into a murine cell line allows for the production of FFL through transcription of mRNA generated from the S segment by the LP (Fig. 5.1).

I began by expressing only the necessary elements required for viral RNA synthesis and excluded the Z protein to provide BHK-21S cells with a basic JUNV minigenome. This strategy allows for a direct comparison of Rom and Can LP activity without inhibition. There are several nucleotide differences within the noncoding regions of the Rom S and Can S genome segments, so it was necessary to rule out any contributions that noncoding

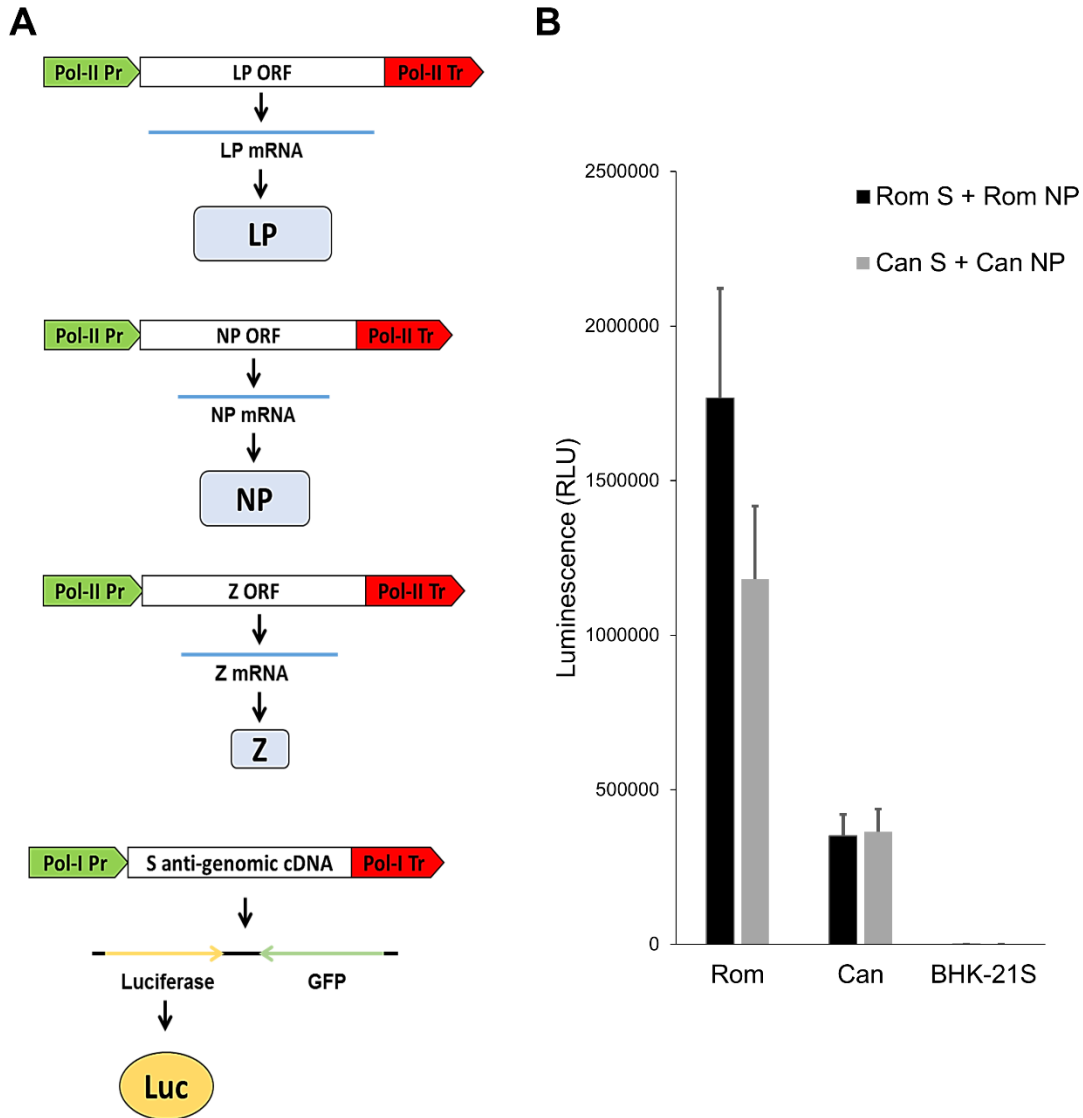


Figure 5.2: The Rom LP is more active than the Can LP in a minigenome system.

A) Schematic representation of the minigenome system utilized to study relative LP activity and inhibition by Z. CMV-driven expression plasmids provide the necessary trans-acting elements for viral RNA synthesis, while a modified mPol-I-Sg plasmid expressing both GFP and FFL is expressed to provide a means to quantify the activity of the LP. **B)** BHK-21S cells were transfected with each of the plasmids with the exception of the pC-Z plasmid. Both the Rom LP and Can LP were provided with either the Rom S + Rom NP plasmids or the Can S + Can NP plasmids and the BHK cells were allowed to incubate at 37°C for 36 hours post-transfection. The cells were then lysed and treated with FFL substrate using the DualGlo luciferase assay kit (Promega) and the relative luminescence was quantified for each sample and normalized to a Gaussia luciferase control.

regions of the genome segment may have on the efficiency of RNA synthesis and protein

expression. To accomplish this, I utilized a second mPol-I-Sg plasmid that expresses the Can S segment with GFP and FFL replacing both NP and GPC, respectively. I transfected BHK-21S cells with either Rom or Can LP (pC-LP), and provided either the Rom S + Rom NP or the Can S + Can NP (mPol-I-Sg and pC-NP) plasmids together with the pC-LP plasmids. The BHK-21S cells were transfected with equal copy numbers of each plasmid using X-tremeGENE 9 transfection reagent following the manufacturer's protocol. The cells were allowed to incubate for 36 hours post-transfection before the relative FFL luminescence was measured. The samples were lysed and treated with FFL substrate using the DualGlo luciferase assay kit (Promega) following the manufacturer's protocol. The relative luminescence was measured using a Glomax luminometer (Promega), and the relative luminescence was normalized to Gaussia luciferase. Control samples were subjected to fluorescence microscopy rather than lysed and treated with FFL substrate. The samples were compared for each control sample to ensure similar transfection efficiency by comparing the number of GFP-positive cells.

The nucleotide differences that exist between the Rom and Can noncoding regions of the S segment do not appear to play any role in the efficiency of RNA synthesis *in vitro*. Additionally, the amino acid differences in the Rom and Can NP do not appear to affect the rate of RNA synthesis for either protein. It is interesting that the Rom LP exhibited a marginally higher activity than the Can LP *in vitro*. While the difference was small, the result was unexpected considering that the Can LP produces more RNA during infection. Collectively, the results indicate that the increase in Can LP activity during infection is not due to a more active domain III or differences in the noncoding region of Can S. This difference is likely due to a decreased sensitivity to inhibition by the Z protein.

The Can LP is less sensitive to inhibition by either Rom or Can Z

When the LP of Can is inserted into rRom in place of the Rom LP, the virus produces significantly more RNA during infection at both 24 and 48 hours post-infection. After testing both polymerases in a minigenome system, the Rom polymerase was marginally more active than the Can polymerase. This effect was similar regardless of the template used for transcription. The luciferase expression by each polymerase was similar whether the Rom or Can S template was used. Since the increase in viral RNA in rRom/CanLP is not due to differences in the LPs themselves, I decided to investigate whether differences exist in the sensitivity to Z inhibition. Using a similar strategy as before with the minigenome system, I transfected BHK-21S cells with pC-NP, pC-LP, pC-Z, and a mPol-I-Sag plasmid expressing GFP and FFL. I paired the Rom LP with the Rom NP and Rom S for both Z proteins, and paired the Can LP with both Can NP and Can S for

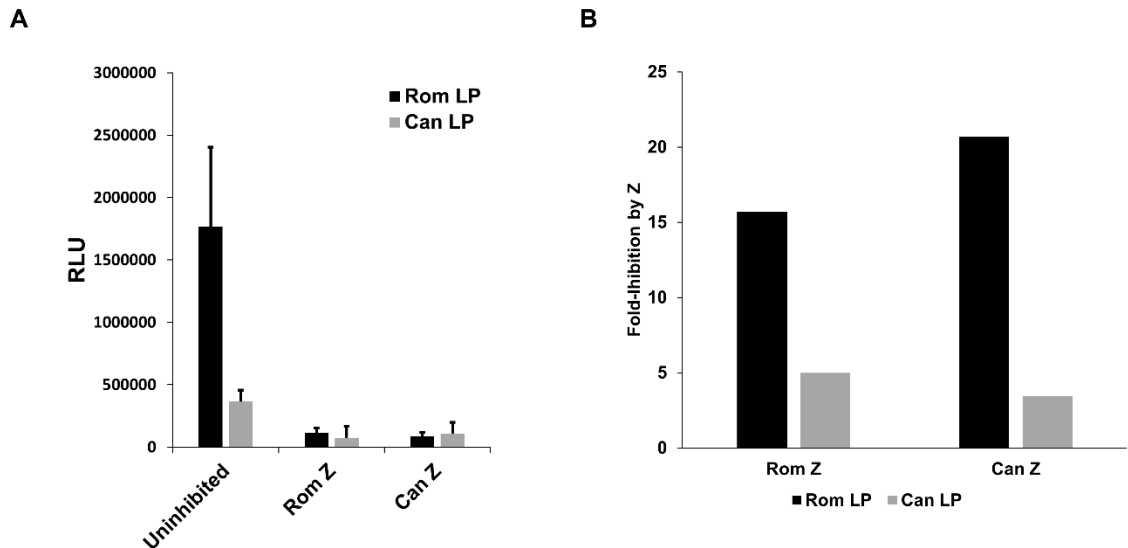


Figure 5.3: Rom LP is more sensitive to inhibition by Z than Can LP. **A)** BHK-21S cells were seeded into 12-well plates and incubated for 24 hours at 37°C. The cells were then transfected with pC-LP, pC-NP, pC-Z, and mPol-I-Sg (GFP/FFL) of either Rom or Can origin. The Rom LP was paired with both the Rom NP and Rom S (black) while the Can LP was paired with the Can NP and Can S (grey). After transfection with X-tremeGENE 9, the transfected cells were incubated for 36 hours at 37°C. The cells were lysed and treated with FFL luciferase using the DualGlo luciferase assay kit (Promega) and analyzed using a Glomax luminometer. **B)** Graph representing the fold-inhibition of each Z for each polymerase, obtained by dividing the average luminescence of uninhibited samples by the average luminescence of Z-inhibited samples.

both Z proteins. The cells were transfected using XtremeGENE-9 following the manufacturer's protocol using equal copy numbers of each plasmid. After incubation for 36 hours at 37°C, I lysed the BHK-21S cells and treated the lysates with FFL substrate using the Dual-Glo luciferase assay. The samples were each normalized to the Gaussia luciferase. Control samples were fixed in formalin and visualized using fluorescence microscopy. The percentages of GFP-positive cells were compared between control samples to ensure similar transfection efficiencies among samples.

Again, the Rom LP exhibited marginally more activity than the Can LP in terms of FFL expression. However, inhibition of the Rom LP by either Z was potent, while the

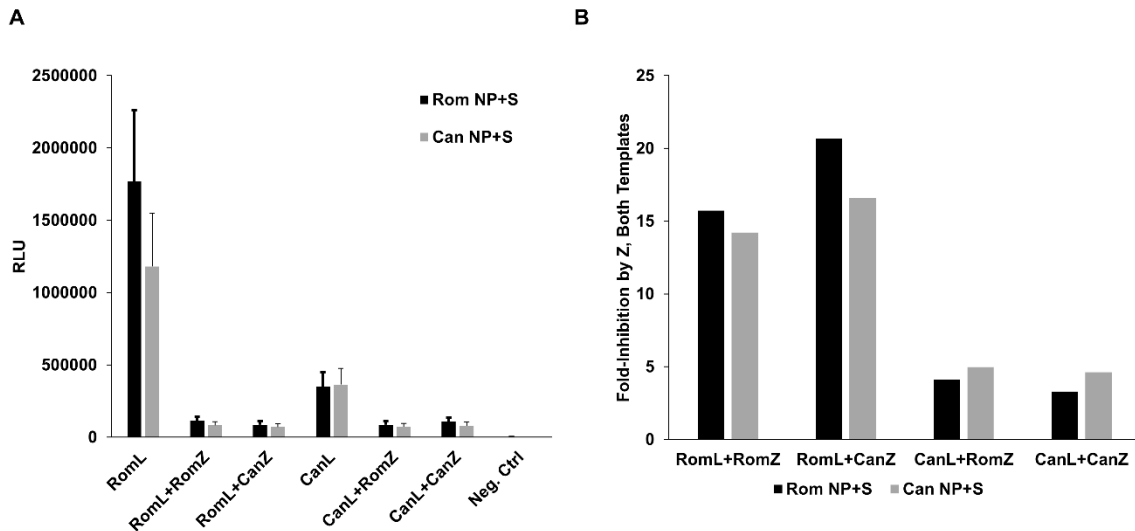


Figure 5.4: Can LP is less sensitive to Z inhibition regardless of the NP or RNA template. **A)** BHK-12S cells were prepared and transfected in the same manner as described previously (Fig. 5.3). The cells were transfected with pC-LP, pC-NP, pC-Z, and mPol-I-Sg (GFP/FFL) of either Rom or Can origin, and the Rom and Can LPs were provided with both Rom and Can NP paired with Rom and Can S in order to investigate whether the Z protein exerted any additional inhibitory effect due to the source of NP. At 36 hours post-transfection, the cells were lysed and treated with FFL substrate. The cells were analyzed with a Glomax luminometer and the results were normalized to Gaussia luciferase. **B)** Fold-inhibition was calculated by dividing the average uninhibited activity of each polymerase with each template (measured by luminescence) by the luminescence of the Z-inhibited samples.

inhibition of Can LP by Z was significantly less so. Additionally, Rom LP was similarly inhibited by both Rom and Can Z. The slight increase in inhibition by Can Z could possibly be due to the hyperactive budding of Can Z, which could package and remove components of the minigenome segment from cells. The switch from Rom LP to Can LP in the minigenome system resulted in a change in fold-inhibition from 15-20 to less than 5. Again, the fold-inhibition of Can LP transcription and protein expression was similar for both Rom and Can Z (Fig. 5.3). Therefore, the Can LP is less sensitive to inhibition by Z than Rom LP despite the base activity being slightly lower. Over time, this would likely lead to the accumulation of RNA and protein. The data from virus infection reflects this, with the most significant increase in RNA synthesis over Rom levels occurring at later time points between 24 and 48 hours post-infection.

The evidence that the Can LP is less inhibited by Z protein in the minigenome system is clear based on the data. However, there is a significant body of data that describes Z-NP interaction and inclusion of NP into VLPs, and the source of the NP could have an effect on the inhibition of RNA synthesis. In order to investigate whether the source of NP causes any difference in the fold-inhibition of the polymerase, I repeated the previous experiment using both the Rom and Can NP + S segment to test each Z-LP combination. The results provide strong evidence that neither the source of the template nor the source of the NP plays a significant role in affecting the fold-inhibition of LP by the Z protein. The results for each Z-LP combination remained similar despite the change in the source of NP and the S segment. The results further support the data that the Can LP has lost its sensitivity to the Z protein.

DISCUSSION

In the previous chapter, I described a loss of affinity for LP by the Z protein due to a V64G amino acid substitution within the RING domain. This substitution decreased the

production of infectious particles, likely through the inability to incorporate the LP into the budding particle. Upon noticing that the Can strain produced more RNA than the wild-type virus, I suspected that the interaction with Z and the LP was involved. However, the rRom/CanLP also produced significantly more RNA than rRom. I therefore suspected that the Can LP was simply more active than the Rom LP. It is interesting that the Can LP was slightly less active in the minigenome system than the Rom LP. The early appearance of the V64G substitution in the Z protein during XJ passaging affected the infectious particle production. The majority of the amino acid substitutions between Rom and Can LP were also present prior to XJ13 (Stephan et al., 2013). This raises the question as to which changes drove the others. Based on the decreased activity of the Can LP in the minigenome system, it is possible that the amino acid changes driving the decrease in activity occurred first. This would create a need to evade Z inhibition and create a more active Z protein in terms of budding.

There are 10 amino acid substitutions that exist between Rom and Can within the proposed domain III, which lies between amino acids 1000-1800 based on comparison of the JUNV LP to the predicted structure of LASV LP. The predicted structure for LASV LP suggests that the domain III lies between amino acids 1000-1500, and this domain shares homology with other polymerase active sites (Brunotte et al., 2011; Vieth et al., 2004). The changes between Rom and Can LP within this region include K1059R, R1156K, C1344F, K1506R, R1542Q, K1582R, E1652G, K1656R, Q168K, and V1700I. The decrease in overall activity of Can LP is likely attributed to one or more of these substitutions. However, the specific amino acids contributing to this change in activity remain unknown. Further analysis using site-directed mutagenesis could provide further insight into the phenotypic differences between Rom and Can LP.

The differences in the noncoding regions of the S segment had no contribution to the differences in polymerase activity. The Rom and Can S 5' UTR contains 7 nucleotide substitutions and one deletion between the two sequences, and all of the changes lie outside

of the 19-nucleotide promoter. The 3' UTR contains three substitutions, and the IGR contains three substitutions. The change in 5' UTR length was particularly intriguing considering the evidence that differences in the variable region of the Tick-borne encephalitis virus UTR affect the virulence (Sakai et al., 2015). However, in this specific instance, the UTR length had no effect on the activity of the polymerase. The differences in virulence observed by the deletions in the UTR could be attributed to a number of factors other than polymerase activity, so the result is not surprising in the case of our minigenome system.

It is interesting that the source of the Z protein had no effect on the inhibition of either polymerase, especially considering the effect of the V64G substitution on the intracellular retention of the Z protein. The data suggests that the effect is due completely to changes in the Can polymerase itself. However, it cannot be ruled out that the decrease in Rom Z/Can LP affinity created by the V64G substitution in Z may play a role in the process of inhibition. While the Rom Z could carry out a more direct role of LP inhibition through direct binding and locking of the polymerase onto the promoter similar to the mechanism described for TCRV (Kranzusch and Whelan, 2011), the Can Z could simply bud from the cell and recruit the LP into the budding particles, providing indirect inhibition of replication by removing the replication machinery from the cell. This is supported by the fact that the compatibility of the LP and Z of Rom and Can are strain-specific, with neither RING domain of Z maintaining compatibility with the opposite LP. However, the Can Z is unable to inhibit Can LP in an overexpression system whereas the Rom Z is still capable of strongly inhibiting the Rom LP (Fig. 5.3).

While the lack of inhibition of Can LP appears directly linked to changes within the LP, I felt it necessary to rule out any LP-NP interactions that may contribute to decreases activity due to differences in the Rom and Can NP. The LP-NP interaction has been recently shown to be important in RNA synthesis, and is dependent on virus-specific RNA sequences in the UTR (Iwasaki et al., 2015). There are a number of amino acid

changes in both functional domains of Rom and Can NP, and it is possible that these changes could have affected the required LP and NP interaction to carry out RNA synthesis. The levels of RNA synthesis and relative inhibition by Z remained unchanged regardless of the NP, ruling out any possible contributions by NP to the decreased activity or decreased sensitivity to Z.

The apparent differences in the Rom and Can LP could significantly alter the kinetics of RNA synthesis and protein expression in the virus life cycle. The high activity and sensitivity to Rom Z would make the Rom strain highly adaptable to the conditions in the cell. The virus would be able to establish a quick infection, and then regulate protein expression over time to prevent excessive activation of the cellular immune response. The slower initial replication in Can would ramp up over time as copies of LP accumulated,

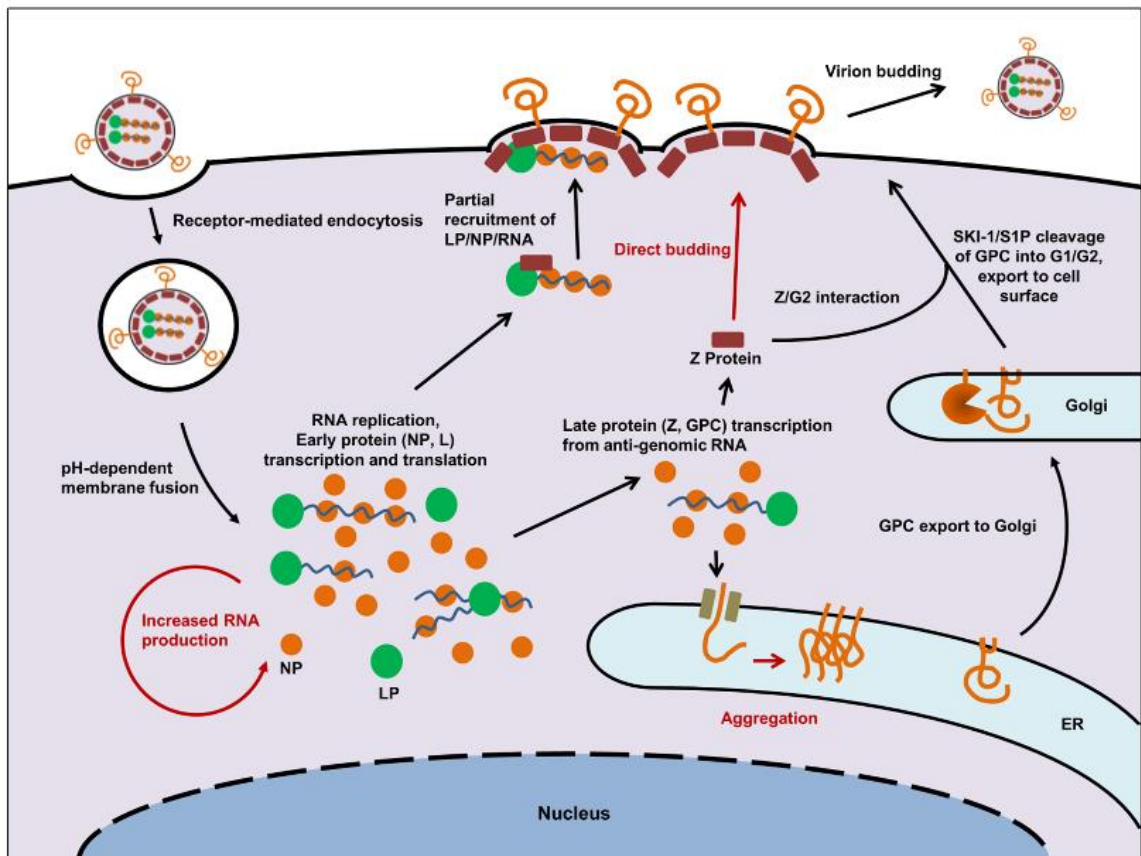


Figure 5.5: Can life cycle. Decreases in Z-LP interaction lead to an increase in RNA and protein synthesis, further compounding ER stress from inefficient GPC processing.

and the lack of sensitivity to the Z protein would prevent the virus from properly regulating its protein production. This would lead to greater accumulation of protein within the cell at later time points, which is observable in Western blots (Fig. 3.8).

When combined with the information from the previous chapters, the mechanisms of attenuation are becoming clearer. The LP of Can would in theory ramp up protein production over time, and the polymerase continues this protein production due to a decreased sensitivity to the inhibitory effect provided by a functional Z. Regardless, the Z protein appears to readily bud from the cell independently (Fig. 3.8), creating non-infectious particles. The primary attenuating factor is the GPC, which accumulates in the ER due to a missing N-linked glycan, triggering the UPR and activating cell stress-related genes. This process is likely more detrimental to the cell during Can infection, where the polymerase does not slow its production of GPC as the late proteins (GPC and Z) accumulate within the cell (Fig. 5.5). This would further increase the ER stress, providing more epitopes for the cell to present to the immune system and eventually leading to apoptosis of the infected cell. The observation of apoptosis in Can-infected cells supports this model of the Can life cycle (Kolokoltsova et al., 2014). Although the mechanism of Can attenuation is not completely understood at this point, the results presented here provide clear evidence of mechanisms that likely play a crucial role in the attenuation of the virus.

The data presented in this dissertation provides a mechanistic understanding of the genetic factors that contribute to the attenuation of the JUNV Can strain. The life cycle of the virus is affected at multiple stages by non-wild-type amino acids within the GPC, Z, and LP proteins to create de-optimized regulation of RNA and protein synthesis, inefficient GPC processing and surface expression, and inefficient assembly of infectious particles. In the future, it is necessary to confirm that the T168A substitution in GPC is sufficient to attenuate the Rom strain in Hartley guinea pigs. This substitution is central to the processing issues in Can GPC and has the greatest impact on GPC trafficking *in vitro*.

Additionally, it would be useful to investigate whether the Can GPC is more immunogenic *in vivo* due to the degradation of the protein. The virus targets monocytes during infection (Gonzalez et al., 1980), which actively sample and present epitopes via MHC. The degradation of Can GPC could lead to rapid detection of the virus and a robust adaptive immune response. The Can virus has already been shown to induce more robust RIG-I signaling in infected cells, although this is likely due to the increased LP activity (Huang et al., 2012). Gaining a more complete understanding of the mechanisms underlying the attenuation of the Can strain will provide valuable insight into the strategies for the rational design of recombinant attenuated vaccine candidates for other pathogenic arenaviruses. Both the N-linked glycosylation patterns of GPC and the RING domain structure of Z are highly conserved among arenaviruses, making strategies to target these proteins feasible for attenuation.

Bibliography

Agnihothram, S.S., York, J., Nunberg, J.H., 2006. Role of the stable signal peptide and cytoplasmic domain of G2 in regulating intracellular transport of the Junin virus envelope glycoprotein complex. *Journal of virology* 80, 5189-5198.

Agnihothram, S.S., York, J., Trahey, M., Nunberg, J.H., 2007. Bitopic membrane topology of the stable signal peptide in the tripartite Junin virus GP-C envelope glycoprotein complex. *Journal of virology* 81, 4331-4337.

Albarino, C.G., Bergeron, E., Erickson, B.R., Khristova, M.L., Rollin, P.E., Nichol, S.T., 2009. Efficient reverse genetics generation of infectious junin viruses differing in glycoprotein processing. *Journal of virology* 83, 5606-5614.

Albarino, C.G., Bird, B.H., Chakrabarti, A.K., Dodd, K.A., Flint, M., Bergeron, E., White, D.M., Nichol, S.T., 2011a. The major determinant of attenuation in mice of the Candid1 vaccine for Argentine hemorrhagic fever is located in the G2 glycoprotein transmembrane domain. *Journal of virology* 85, 10404-10408.

Albarino, C.G., Bird, B.H., Chakrabarti, A.K., Dodd, K.A., White, D.M., Bergeron, E., Shrivastava-Ranjan, P., Nichol, S.T., 2011b. Reverse genetics generation of chimeric infectious Junin/Lassa virus is dependent on interaction of homologous glycoprotein stable signal peptide and G2 cytoplasmic domains. *Journal of virology* 85, 112-122.

Ambrosio, A., Saavedra, M., Mariani, M., Gamboa, G., Maiza, A., 2011. Argentine hemorrhagic fever vaccines. *Human Vaccines* 7, 694-700.

Ambrosio, A.M., Gamboa, G.S., Feuillade, M.R., Briggiler, A.M., Rimoldi, M.T., 1992. Peripheral blood leukocytes of patients with Argentine hemorrhagic fever as effectors of antibody-dependent cell-cytotoxicity. *Journal of medical virology* 37, 232-236.

Archer, A.M., Rico-Hesse, R., 2002. High genetic divergence and recombination in Arenaviruses from the Americas. *Virology* 304, 274-281.

Avila, M.M., Samoilovich, S.R., Laguens, R.P., Merani, M.S., Weissenbacher, M.C., 1987. Protection of Junin virus-infected marmosets by passive administration of immune serum: association with late neurologic signs. *Journal of medical virology* 21, 67-74.

Avila, M.M., Samoilovich, S.R., Weissenbacher, M.C., 1979. [Infection of guinea pigs with an attenuated strain of Junin virus XJCL3]. *Medicina* 39, 597-603.

Baize, S., Kaplon, J., Faure, C., Pannetier, D., Georges-Courbot, M.C., Deubel, V., 2004. Lassa virus infection of human dendritic cells and macrophages is productive but fails to activate cells. *J Immunol* 172, 2861-2869.

Beyer, W.R., Popplau, D., Garten, W., von Laer, D., Lenz, O., 2003. Endoproteolytic processing of the lymphocytic choriomeningitis virus glycoprotein by the subtilase SKI-1/S1P. *Journal of virology* 77, 2866-2872.

Blattman, J.N., Sourdive, D.J., Murali-Krishna, K., Ahmed, R., Altman, J.D., 2000. Evolution of the T cell repertoire during primary, memory, and recall responses to viral infection. *J Immunol* 165, 6081-6090.

Bonhomme, C.J., Capul, A.A., Lauron, E.J., Bederka, L.H., Knopp, K.A., Buchmeier, M.J., 2011. Glycosylation modulates arenavirus glycoprotein expression and function. *Virology* 409, 223-233.

Borden, K.L., 2000. RING domains: master builders of molecular scaffolds? *Journal of molecular biology* 295, 1103-1112.

Borremans, B., Leirs, H., Gryseels, S., Gunther, S., Makundi, R., de Bellocq, J.G., 2011. Presence of Mopeia virus, an African arenavirus, related to biotope and individual rodent host characteristics: implications for virus transmission. *Vector Borne Zoonotic Dis* 11, 1125-1131.

Bowen, M.D., Peters, C.J., Nichol, S.T., 1997. Phylogenetic analysis of the Arenaviridae: patterns of virus evolution and evidence for cospeciation between arenaviruses and their rodent hosts. *Molecular phylogenetics and evolution* 8, 301-316.

Boxaca, M., de Guerrero, L.B., Savy, V.L., 1973. The occurrence of virus, interferon, and circulating antibodies in mice after experimental infection with Junin virus. *Archiv fur die gesamte Virusforschung* 40, 10-20.

Braakman, I., Hebert, D.N., 2013. Protein folding in the endoplasmic reticulum. *Cold Spring Harbor perspectives in biology* 5, a013201.

Braakman, I., van Anken, E., 2000. Folding of viral envelope glycoproteins in the endoplasmic reticulum. *Traffic* 1, 533-539.

Brunotte, L., Lelke, M., Hass, M., Kleinstaub, K., Becker-Ziaja, B., Gunther, S., 2011. Domain structure of Lassa virus L protein. *Journal of virology* 85, 324-333.

Buchmeier, M.J., Charrel, R., Clegg, C.S., Emonet, S., Gonzalez, J.P., Lukashevich, I.S., Peters, C.J., Radoshitzky, S.R., Romanowski, V., Salvato, M., DeRisi, J.L., Stenglein, M.D., de la Torre, J.C., 2014. *Familly Arenaviridae*. Academic Press, 1-6.

Buchmeier, M.J., De la Torre, J.C., Peters, C.J., 2013. *Arenaviridae*, in: Knipe, D.M., Holey, P.M. (Eds.), *Fields Virology*, Sixth Edition, pp. 1283-1303.

Buchmeier, M.J., Welsh, R.M., Dutko, F.J., Oldstone, M.B., 1980. The virology and immunobiology of lymphocytic choriomeningitis virus infection. *Advances in immunology* 30, 275-331.

Burri, D.J., da Palma, J.R., Kunz, S., Pasquato, A., 2012a. Envelope glycoprotein of arenaviruses. *Viruses* 4, 2162-2181.

Burri, D.J., Pasqual, G., Rochat, C., Seidah, N.G., Pasquato, A., Kunz, S., 2012b. Molecular characterization of the processing of arenavirus envelope glycoprotein precursors by subtilisin kexin isozyme-1/site-1 protease. *Journal of virology* 86, 4935-4946.

Butz, E.A., Bevan, M.J., 1998. Massive expansion of antigen-specific CD8⁺ T cells during an acute virus infection. *Immunity* 8, 167-175.

Cajimat, M.N., Milazzo, M.L., Borchert, J.N., Abbott, K.D., Bradley, R.D., Fulhorst, C.F., 2008. Diversity among Tacaribe serocomplex viruses (family Arenaviridae) naturally associated with the Mexican woodrat (*Neotoma mexicana*). *Virus research* 133, 211-217.

Cajimat, M.N., Milazzo, M.L., Bradley, R.D., Fulhorst, C.F., 2007. Catarina virus, an arenaviral species principally associated with *Neotoma micropus* (southern plains woodrat) in Texas. *The American journal of tropical medicine and hygiene* 77, 732-736.

Campetella, O.E., Barrios, H.A., Galassi, N.V., 1988. Junin virus-induced delayed-type hypersensitivity suppression in adult mice. *Journal of medical virology* 25, 227-235.

Candurra, N.A., Damonte, E.B., Coto, C.E., 1989. Antigenic relationships between attenuated and pathogenic strains of Junin virus. *Journal of medical virology* 27, 145-150.

- Cannon, K.S., Hebert, D.N., Helenius, A., 1996. Glycan-dependent and -independent association of vesicular stomatitis virus G protein with calnexin. *The Journal of biological chemistry* 271, 14280-14284.
- Capul, A.A., de la Torre, J.C., Buchmeier, M.J., 2011. Conserved residues in Lassa fever virus Z protein modulate viral infectivity at the level of the ribonucleoprotein. *Journal of virology* 85, 3172-3178.
- Capul, A.A., Perez, M., Burke, E., Kunz, S., Buchmeier, M.J., de la Torre, J.C., 2007. Arenavirus Z-glycoprotein association requires Z myristoylation but not functional RING or late domains. *Journal of virology* 81, 9451-9460.
- Casabona, J.C., Levingston Macleod, J.M., Loureiro, M.E., Gomez, G.A., Lopez, N., 2009. The RING domain and the L79 residue of Z protein are involved in both the rescue of nucleocapsids and the incorporation of glycoproteins into infectious chimeric arenavirus-like particles. *Journal of virology* 83, 7029-7039.
- Charrel, R.N., de Lamballerie, X., Fulhorst, C.F., 2001. The Whitewater Arroyo virus: natural evidence for genetic recombination among Tacaribe serocomplex viruses (family Arenaviridae). *Virology* 283, 161-166.
- Charrel, R.N., Feldmann, H., Fulhorst, C.F., Khelifa, R., de Chesse, R., de Lamballerie, X., 2002. Phylogeny of New World arenaviruses based on the complete coding sequences of the small genomic segment identified an evolutionary lineage produced by intrasegmental recombination. *Biochemical and biophysical research communications* 296, 1118-1124.
- Charrel, R.N., Lemasson, J.J., Garbutt, M., Khelifa, R., De Micco, P., Feldmann, H., de Lamballerie, X., 2003. New insights into the evolutionary relationships between arenaviruses provided by comparative analysis of small and large segment sequences. *Virology* 317, 191-196.
- Checkley, M.A., Luttge, B.G., Freed, E.O., 2011. HIV-1 envelope glycoprotein biosynthesis, trafficking, and incorporation. *Journal of molecular biology* 410, 582-608.
- Cornu, T.I., de la Torre, J.C., 2001. RING finger Z protein of lymphocytic choriomeningitis virus (LCMV) inhibits transcription and RNA replication of an LCMV S-segment minigenome. *Journal of virology* 75, 9415-9426.

Cornu, T.I., de la Torre, J.C., 2002. Characterization of the arenavirus RING finger Z protein regions required for Z-mediated inhibition of viral RNA synthesis. *Journal of virology* 76, 6678-6688.

Cornu, T.I., Feldmann, H., de la Torre, J.C., 2004. Cells expressing the RING finger Z protein are resistant to arenavirus infection. *Journal of virology* 78, 2979-2983.

Cossio, P., Laguens, R., Arana, R., Segal, A., Maiztegui, J., 1975. Ultrastructural and immunohistochemical study of the human kidney in Argentine haemorrhagic fever. *Virchows Archiv. A, Pathological anatomy and histology* 368, 1-9.

Cresta, B., Padula, P., de Martinez Segovia, M., 1980. Biological properties of Junin virus proteins. I. Identification of the immunogenic glycoprotein. *Intervirology* 13, 284-288.

Cuevas, C.D., Lavanya, M., Wang, E., Ross, S.R., 2011. Junin virus infects mouse cells and induces innate immune responses. *Journal of virology* 85, 11058-11068.

Cuevas, C.D., Ross, S.R., 2014. Toll-like receptor 2-mediated innate immune responses against Junin virus in mice lead to antiviral adaptive immune responses during systemic infection and do not affect viral replication in the brain. *Journal of virology* 88, 7703-7714.

Damonte, E.B., Mersich, S.E., Candurra, N.A., 1994. Intracellular processing and transport of Junin virus glycoproteins influences virion infectivity. *Virus research* 34, 317-326.

Daniels, R., Kurowski, B., Johnson, A.E., Hebert, D.N., 2003. N-linked glycans direct the cotranslational folding pathway of influenza hemagglutinin. *Molecular cell* 11, 79-90.

de Bracco, M.M., Rimoldi, M.T., Cossio, P.M., Rabinovich, A., Maiztegui, J.I., Carballal, G., Arana, R.M., 1978. Argentine hemorrhagic fever. Alterations of the complement system and anti-Junin-virus humoral response. *The New England journal of medicine* 299, 216-221.

de Guerrero, L.B., Boxaca, M.C., Malumbres, E., de las Mercedes Gomez, M., 1985. Pathogenesis of attenuated Junin virus in the guinea pig model. *Journal of medical virology* 15, 197-202.

Dejean, C.B., Ayerra, B.L., Teyssie, A.R., 1987. Interferon response in the guinea pig infected with Junin virus. *Journal of medical virology* 23, 83-91.

Dejean, C.B., Oubina, J.R., Carballal, G., Teyssie, A.R., 1988. Circulating interferon in the guinea pig infected with the XJ, prototype Junin virus strain. *Journal of medical virology* 24, 97-99.

Delgado, M.F., Coviello, S., Monsalvo, A.C., Melendi, G.A., Hernandez, J.Z., Batalle, J.P., Diaz, L., Trento, A., Chang, H.Y., Mitzner, W., Ravetch, J., Melero, J.A., Irusta, P.M., Polack, F.P., 2009. Lack of antibody affinity maturation due to poor Toll-like receptor stimulation leads to enhanced respiratory syncytial virus disease. *Nature medicine* 15, 34-41.

Delgado, S., Erickson, B.R., Agudo, R., Blair, P.J., Vallejo, E., Albarino, C.G., Vargas, J., Comer, J.A., Rollin, P.E., Ksiazek, T.G., Olson, J.G., Nichol, S.T., 2008. Chapare virus, a newly discovered arenavirus isolated from a fatal hemorrhagic fever case in Bolivia. *PLoS pathogens* 4, e1000047.

Droniou-Bonzom, M.E., Reignier, T., Oldenburg, J.E., Cox, A.U., Exline, C.M., Rathbun, J.Y., Cannon, P.M., 2011. Substitutions in the glycoprotein (GP) of the Candid#1 vaccine strain of Junin virus increase dependence on human transferrin receptor 1 for entry and destabilize the metastable conformation of GP. *Journal of virology* 85, 13457-13462.

Eichler, R., Lenz, O., Garten, W., Strecker, T., 2006. The role of single N-glycans in proteolytic processing and cell surface transport of the Lassa virus glycoprotein GP-C. *Virology journal* 3, 41.

Eichler, R., Strecker, T., Kolesnikova, L., ter Meulen, J., Weissenhorn, W., Becker, S., Klenk, H.D., Garten, W., Lenz, O., 2004. Characterization of the Lassa virus matrix protein Z: electron microscopic study of virus-like particles and interaction with the nucleoprotein (NP). *Virus research* 100, 249-255.

Elsner, B., Schwarz, E., Mando, O.G., Maiztegui, J., Vilches, A., 1973. Pathology of 12 fatal cases of Argentine hemorrhagic fever. *The American journal of tropical medicine and hygiene* 22, 229-236.

Emonet, S.F., de la Torre, J.C., Domingo, E., Sevilla, N., 2009. Arenavirus genetic diversity and its biological implications. *Infection, genetics and evolution : journal of molecular epidemiology and evolutionary genetics in infectious diseases* 9, 417-429.

Emonet, S.F., Seregin, A.V., Yun, N.E., Poussard, A.L., Walker, A.G., de la Torre, J.C., Paessler, S., 2011. Rescue from cloned cDNAs and in vivo characterization of recombinant pathogenic Romero and live-attenuated Candid #1 strains of Junin virus, the causative agent of Argentine hemorrhagic fever disease. *Journal of virology* 85, 1473-1483.

Enria, D., Bowen, M.D., Mills, J.N., Shieh, W.J., Bausch, D., Peters, C.J., 2004. Arenavirus infections, in: Guerrant, R.L., Walker, D.H., Weller, P.F., Saunders, W.B. (Eds.), *Tropical Infectious Diseases: Principles, Pathogens, and Practice*. Saunders, pp. 1191-1212.

Enria, D.A., Barrera Oro, J.G., 2002. Junin virus vaccines. *Current topics in microbiology and immunology* 263, 239-261.

Enria, D.A., Briggiler, A.M., Levis, S., Vallejos, D., Maiztegui, J.I., Canonico, P.G., 1987. Tolerance and antiviral effect of ribavirin in patients with Argentine hemorrhagic fever. *Antiviral research* 7, 353-359.

Enria, D.A., Briggiler, A.M., Sanchez, Z., 2008. Treatment of Argentine hemorrhagic fever. *Antiviral research* 78, 132-139.

Enria, D.A., de Damilano, A.J., Briggiler, A.M., Ambrosio, A.M., Fernandez, N.J., Feuillade, M.R., Maiztegui, J.I., 1985. [Late neurologic syndrome in patients with Argentinian hemorrhagic fever treated with immune plasma]. *Medicina* 45, 615-620.

Fehling, S.K., Lennartz, F., Strecker, T., 2012. Multifunctional nature of the arenavirus RING finger protein Z. *Viruses* 4, 2973-3011.

Fennewald, S.M., Aronson, J.F., Zhang, L., Herzog, N.K., 2002. Alterations in NF-kappaB and RBP-Jkappa by arenavirus infection of macrophages in vitro and in vivo. *Journal of virology* 76, 1154-1162.

Ferrer-Orta, C., Arias, A., Escarmis, C., Verdaguer, N., 2006. A comparison of viral RNA-dependent RNA polymerases. *Current opinion in structural biology* 16, 27-34.

Flatz, L., Bergthaler, A., de la Torre, J.C., Pinschewer, D.D., 2006. Recovery of an arenavirus entirely from RNA polymerase I/II-driven cDNA. *Proceedings of the National Academy of Sciences of the United States of America* 103, 4663-4668.

Franze-Fernandez, M.T., Zetina, C., Iapalucci, S., Lucero, M.A., Bouissou, C., Lopez, R., Rey, O., Daheli, M., Cohen, G.N., Zakin, M.M., 1987. Molecular structure and early events in the replication of Tacaribe arenavirus S RNA. *Virus research* 7, 309-324.

Freiden, P.J., Gaut, J.R., Hendershot, L.M., 1992. Interconversion of three differentially modified and assembled forms of BiP. *The EMBO journal* 11, 63-70.

Froeschke, M., Basler, M., Groettrup, M., Dobberstein, B., 2003. Long-lived signal peptide of lymphocytic choriomeningitis virus glycoprotein pGP-C. *The Journal of biological chemistry* 278, 41914-41920.

Fulginiti, V.A., Eller, J.J., Downie, A.W., Kempe, C.H., 1967. Altered reactivity to measles virus. Atypical measles in children previously immunized with inactivated measles virus vaccines. *Jama* 202, 1075-1080.

Fulhorst, C.F., Charrel, R.N., Weaver, S.C., Ksiazek, T.G., Bradley, R.D., Milazzo, M.L., Tesh, R.B., Bowen, M.D., 2001. Geographic distribution and genetic diversity of Whitewater Arroyo virus in the southwestern United States. *Emerging infectious diseases* 7, 403-407.

Garcin, D., Kolakofsky, D., 1990. A novel mechanism for the initiation of Tacaribe arenavirus genome replication. *Journal of virology* 64, 6196-6203.

Gething, M.J., 1999. Role and regulation of the ER chaperone BiP. *Seminars in cell & developmental biology* 10, 465-472.

Gomez, R.M., Pozner, R.G., Lazzari, M.A., D'Atri, L.P., Negrotto, S., Chudzinski-Tavassi, A.M., Berria, M.I., Schattner, M., 2003. Endothelial cell function alteration after Junin virus infection. *Thrombosis and haemostasis* 90, 326-333.

Goni, S.E., Iserte, J.A., Stephan, B.I., Borio, C.S., Ghiringhelli, P.D., Lozano, M.E., 2010. Molecular analysis of the virulence attenuation process in Junin virus vaccine genealogy. *Virus genes* 40, 320-328.

Gonzalez, P.H., Cossio, P.M., Arana, R., Maiztegui, J.I., Laguens, R.P., 1980. Lymphatic tissue in Argentine hemorrhagic fever. Pathologic features. *Archives of pathology & laboratory medicine* 104, 250-254.

- Gonzalez, P.H., Lampuri, J.S., Coto, C.E., Laguens, R.P., 1982. In vitro infection of murine macrophages with Junin virus. *Infection and immunity* 35, 356-358.
- Grant, A., Seregin, A., Huang, C., Kolokoltsova, O., Brasier, A., Peters, C., Paessler, S., 2012. Junin virus pathogenesis and virus replication. *Viruses* 4, 2317-2339.
- Groseth, A., Hoenen, T., Weber, M., Wolff, S., Herwig, A., Kaufmann, A., Becker, S., 2011. Tacaribe virus but not junin virus infection induces cytokine release from primary human monocytes and macrophages. *PLoS neglected tropical diseases* 5, e1137.
- Groseth, A., Wolff, S., Strecker, T., Hoenen, T., Becker, S., 2010. Efficient budding of the tacaribe virus matrix protein z requires the nucleoprotein. *Journal of virology* 84, 3603-3611.
- Habjan, M., Penski, N., Spiegel, M., Weber, F., 2008. T7 RNA polymerase-dependent and -independent systems for cDNA-based rescue of Rift Valley fever virus. *The Journal of general virology* 89, 2157-2166.
- Hallenberger, S., Bosch, V., Angliker, H., Shaw, E., Klenk, H.D., Garten, W., 1992. Inhibition of furin-mediated cleavage activation of HIV-1 glycoprotein gp160. *Nature* 360, 358-361.
- Hammond, C., Helenius, A., 1994. Folding of VSV G protein: sequential interaction with BiP and calnexin. *Science* 266, 456-458.
- Hanson, S.R., Culyba, E.K., Hsu, T.L., Wong, C.H., Kelly, J.W., Powers, E.T., 2009. The core trisaccharide of an N-linked glycoprotein intrinsically accelerates folding and enhances stability. *Proceedings of the National Academy of Sciences of the United States of America* 106, 3131-3136.
- Hartlieb, B., Weissenhorn, W., 2006. Filovirus assembly and budding. *Virology* 344, 64-70.
- Hass, M., Golnitz, U., Muller, S., Becker-Ziaja, B., Gunther, S., 2004. Replicon system for Lassa virus. *Journal of virology* 78, 13793-13803.
- Hebert, D.N., Foellmer, B., Helenius, A., 1996. Calnexin and calreticulin promote folding, delay oligomerization and suppress degradation of influenza hemagglutinin in microsomes. *The EMBO journal* 15, 2961-2968.

Hebert, D.N., Zhang, J.X., Chen, W., Foellmer, B., Helenius, A., 1997. The number and location of glycans on influenza hemagglutinin determine folding and association with calnexin and calreticulin. *The Journal of cell biology* 139, 613-623.

Heller, M.V., Marta, R.F., Sturk, A., Maiztegui, J.I., Hack, C.E., Cate, J.W., Molinas, F.C., 1995. Early markers of blood coagulation and fibrinolysis activation in Argentine hemorrhagic fever. *Thrombosis and haemostasis* 73, 368-373.

Hendershot, L.M., 2004. The ER function BiP is a master regulator of ER function. *The Mount Sinai journal of medicine, New York* 71, 289-297.

Huang, C., Kolokoltsova, O.A., Yun, N.E., Seregin, A.V., Poussard, A.L., Walker, A.G., Brasier, A.R., Zhao, Y., Tian, B., de la Torre, J.C., Paessler, S., 2012. Junin virus infection activates the type I interferon pathway in a RIG-I-dependent manner. *PLoS neglected tropical diseases* 6, e1659.

Huang, C., Walker, A.G., Grant, A.M., Kolokoltsova, O.A., Yun, N.E., Seregin, A.V., Paessler, S., 2014. Potent inhibition of Junin virus infection by interferon in murine cells. *PLoS neglected tropical diseases* 8, e2933.

Hubbard, S.C., Robbins, P.W., 1979. Synthesis and processing of protein-linked oligosaccharides in vivo. *The Journal of biological chemistry* 254, 4568-4576.

Iwasaki, M., Ngo, N., Cubitt, B., de la Torre, J.C., 2015. Efficient Interaction between Arenavirus Nucleoprotein (NP) and RNA-Dependent RNA Polymerase (L) Is Mediated by the Virus Nucleocapsid (NP-RNA) Template. *Journal of virology* 89, 5734-5738.

Jacamo, R., Lopez, N., Wilda, M., Franze-Fernandez, M.T., 2003. Tacaribe virus Z protein interacts with the L polymerase protein to inhibit viral RNA synthesis. *Journal of virology* 77, 10383-10393.

Jahrling, P.B., Hesse, R.A., Eddy, G.A., Johnson, K.M., Callis, R.T., Stephen, E.L., 1980. Lassa virus infection of rhesus monkeys: pathogenesis and treatment with ribavirin. *The Journal of infectious diseases* 141, 580-589.

Justines, G., Johnson, K.M., 1968. Use of oral swabs for detection of Machupo-virus infection in rodents. *The American journal of tropical medicine and hygiene* 17, 788-790.

Kentsis, A., Gordon, R.E., Borden, K.L., 2002. Self-assembly properties of a model RING domain. *Proceedings of the National Academy of Sciences of the United States of America* 99, 667-672.

Kenyon, R.H., Canonico, P.G., Green, D.E., Peters, C.J., 1986. Effect of ribavirin and tributylribavirin on argentine hemorrhagic fever (Junin virus) in guinea pigs. *Antimicrobial agents and chemotherapy* 29, 521-523.

Kenyon, R.H., Condie, R.M., Jahrling, P.B., Peters, C.J., 1990. Protection of guinea pigs against experimental Argentine hemorrhagic fever by purified human IgG: importance of elimination of infected cells. *Microbial pathogenesis* 9, 219-226.

Kenyon, R.H., Green, D.E., Maiztegui, J.I., Peters, C.J., 1988. Viral strain dependent differences in experimental Argentine hemorrhagic fever (Junin virus) infection of guinea pigs. *Intervirology* 29, 133-143.

Kenyon, R.H., Green, D.E., Peters, C.J., 1985. Effect of immunosuppression on experimental Argentine hemorrhagic fever in guinea pigs. *Journal of virology* 53, 75-80.

Kenyon, R.H., McKee, K.T., Jr., Zack, P.M., Rippey, M.K., Vogel, A.P., York, C., Meegan, J., Crabbs, C., Peters, C.J., 1992. Aerosol infection of rhesus macaques with Junin virus. *Intervirology* 33, 23-31.

Kido, H., Okumura, Y., Takahashi, E., Pan, H.Y., Wang, S., Chida, J., Le, T.Q., Yano, M., 2008. Host envelope glycoprotein processing proteases are indispensable for entry into human cells by seasonal and highly pathogenic avian influenza viruses. *Journal of molecular and genetic medicine : an international journal of biomedical research* 3, 167-175.

Kirk, W.E., Cash, P., Peters, C.J., Bishop, D.H.L., 1980. Formation and Characterization of an Intertypic Lymphocytic Choriomeningitis Recombinant Virus. *Journal of General Virology* 51, 213-218.

Klewitz, C., Klenk, H.D., ter Meulen, J., 2007. Amino acids from both N-terminal hydrophobic regions of the Lassa virus envelope glycoprotein GP-2 are critical for pH-dependent membrane fusion and infectivity. *The Journal of general virology* 88, 2320-2328.

Kolokoltsova, O.A., Grant, A.M., Huang, C., Smith, J.K., Poussard, A.L., Tian, B., Brasier, A.R., Peters, C.J., Tseng, C.T., de la Torre, J.C., Paessler, S., 2014. RIG-I

enhanced interferon independent apoptosis upon Junin virus infection. PloS one 9, e99610.

Kranzusch, P.J., Schenk, A.D., Rahmeh, A.A., Radoshitzky, S.R., Bavari, S., Walz, T., Whelan, S.P., 2010. Assembly of a functional Machupo virus polymerase complex. Proceedings of the National Academy of Sciences of the United States of America 107, 20069-20074.

Kranzusch, P.J., Whelan, S.P., 2011. Arenavirus Z protein controls viral RNA synthesis by locking a polymerase-promoter complex. Proceedings of the National Academy of Sciences of the United States of America 108, 19743-19748.

Kundra, R., Kornfeld, S., 1999. Asparagine-linked oligosaccharides protect Lamp-1 and Lamp-2 from intracellular proteolysis. The Journal of biological chemistry 274, 31039-31046.

Kunz, S., Edelmann, K.H., de la Torre, J.C., Gorney, R., Oldstone, M.B., 2003. Mechanisms for lymphocytic choriomeningitis virus glycoprotein cleavage, transport, and incorporation into virions. Virology 314, 168-178.

Lampuri, J.S., Vidal, M.D., Coto, C.E., 1982. [Response of calomys musculinus to experimental infection with Junin virus]. Medicina 42, 61-66.

Lan, S., McLay Schelde, L., Wang, J., Kumar, N., Ly, H., Liang, Y., 2009. Development of infectious clones for virulent and avirulent pichinde viruses: a model virus to study arenavirus-induced hemorrhagic fevers. Journal of virology 83, 6357-6362.

Lascano, E.F., Berria, M.I., 1974. Ultrastructure of Junin virus in mouse whole brain and mouse brain tissue cultures. Journal of virology 14, 965-974.

Lecompte, E., ter Meulen, J., Emonet, S., Daffis, S., Charrel, R.N., 2007. Genetic identification of Kodoko virus, a novel arenavirus of the African pigmy mouse (*Mus Nannomys minutoides*) in West Africa. Virology 364, 178-183.

Lee, K.J., Novella, I.S., Teng, M.N., Oldstone, M.B., de La Torre, J.C., 2000. NP and L proteins of lymphocytic choriomeningitis virus (LCMV) are sufficient for efficient transcription and replication of LCMV genomic RNA analogs. Journal of virology 74, 3470-3477.

- Lelke, M., Brunotte, L., Busch, C., Gunther, S., 2010. An N-terminal region of Lassa virus L protein plays a critical role in transcription but not replication of the virus genome. *Journal of virology* 84, 1934-1944.
- Lerer, G.D., Saavedra, M.C., Falcoff, R., Maiztegui, J.I., Molinas, F.C., 1991. Activity of a platelet protein kinase that phosphorylates fibrinogen and histone in Argentine hemorrhagic fever. *Acta physiologica, pharmacologica et therapeutica latinoamericana : organo de la Asociacion Latinoamericana de Ciencias Fisiologicas y [de] la Asociacion Latinoamericana de Farmacologia* 41, 377-386.
- Levingston Macleod, J.M., D'Antuono, A., Loureiro, M.E., Casabona, J.C., Gomez, G.A., Lopez, N., 2011. Identification of two functional domains within the arenavirus nucleoprotein. *Journal of virology* 85, 2012-2023.
- Levis, S.C., Saavedra, M.C., Ceccoli, C., Falcoff, E., Feuillade, M.R., Enria, D.A., Maiztegui, J.I., Falcoff, R., 1984. Endogenous interferon in Argentine hemorrhagic fever. *The Journal of infectious diseases* 149, 428-433.
- Levis, S.C., Saavedra, M.C., Ceccoli, C., Feuillade, M.R., Enria, D.A., Maiztegui, J.I., Falcoff, R., 1985. Correlation between endogenous interferon and the clinical evolution of patients with Argentine hemorrhagic fever. *Journal of interferon research* 5, 383-389.
- Lopez, N., Jacamo, R., Franze-Fernandez, M.T., 2001. Transcription and RNA replication of tacaribe virus genome and antigenome analogs require N and L proteins: Z protein is an inhibitor of these processes. *Journal of virology* 75, 12241-12251.
- Loureiro, M.E., D'Antuono, A., Levingston Macleod, J.M., Lopez, N., 2012. Uncovering viral protein-protein interactions and their role in arenavirus life cycle. *Viruses* 4, 1651-1667.
- Loureiro, M.E., Wilda, M., Levingston Macleod, J.M., D'Antuono, A., Foscaldi, S., Marino Buslje, C., Lopez, N., 2011. Molecular determinants of arenavirus Z protein homo-oligomerization and L polymerase binding. *Journal of virology* 85, 12304-12314.
- Lukashevich, I.S., 1992. Generation of reassortants between African arenaviruses. *Virology* 188, 600-605.
- Lukashevich, I.S., Carrion, R., Jr., Salvato, M.S., Mansfield, K., Brasky, K., Zapata, J., Cairo, C., Goicochea, M., Hoosien, G.E., Ticer, A., Bryant, J., Davis, H., Hammamieh, R., Mayda, M., Jett, M., Patterson, J., 2008. Safety, immunogenicity, and efficacy of the

ML29 reassortant vaccine for Lassa fever in small non-human primates. *Vaccine* 26, 5246-5254.

Lukashevich, I.S., Maryankova, R., Vladyko, A.S., Nashkevich, N., Koleda, S., Djavani, M., Horejsh, D., Voitenok, N.N., Salvato, M.S., 1999. Lassa and Mopeia virus replication in human monocytes/macrophages and in endothelial cells: different effects on IL-8 and TNF-alpha gene expression. *Journal of medical virology* 59, 552-560.

Lukashevich, I.S., Patterson, J., Carrion, R., Moshkoff, D., Ticer, A., Zapata, J., Brasky, K., Geiger, R., Hubbard, G.B., Bryant, J., Salvato, M.S., 2005. A live attenuated vaccine for Lassa fever made by reassortment of Lassa and Mopeia viruses. *Journal of virology* 79, 13934-13942.

Mahanty, S., Bausch, D.G., Thomas, R.L., Goba, A., Bah, A., Peters, C.J., Rollin, P.E., 2001. Low levels of interleukin-8 and interferon-inducible protein-10 in serum are associated with fatal infections in acute Lassa fever. *The Journal of infectious diseases* 183, 1713-1721.

Maiztegui, J., Feuillade, M., Briggiler, A., 1986. Progressive extension of the endemic area and changing incidence of Argentine Hemorrhagic Fever. *Medical microbiology and immunology* 175, 149-152.

Maiztegui, J.I., 1975. Clinical and epidemiological patterns of Argentine haemorrhagic fever. *Bulletin of the World Health Organization* 52, 567-575.

Maiztegui, J.I., Fernandez, N.J., de Damilano, A.J., 1979. Efficacy of immune plasma in treatment of Argentine haemorrhagic fever and association between treatment and a late neurological syndrome. *Lancet* 2, 1216-1217.

Maiztegui, J.I., McKee, K.T., Jr., Barrera Oro, J.G., Harrison, L.H., Gibbs, P.H., Feuillade, M.R., Enria, D.A., Briggiler, A.M., Levis, S.C., Ambrosio, A.M., Halsey, N.A., Peters, C.J., 1998. Protective efficacy of a live attenuated vaccine against Argentine hemorrhagic fever. AHF Study Group. *The Journal of infectious diseases* 177, 277-283.

Marta, R.F., Montero, V.S., Hack, C.E., Sturk, A., Maiztegui, J.I., Molinas, F.C., 1999. Proinflammatory cytokines and elastase-alpha-1-antitrypsin in Argentine hemorrhagic fever. *The American journal of tropical medicine and hygiene* 60, 85-89.

Martinez, M.G., Cordo, S.M., Candurra, N.A., 2007. Characterization of Junin arenavirus cell entry. *The Journal of general virology* 88, 1776-1784.

Matloubian, M., Kolhekar, S.R., Somasundaram, T., Ahmed, R., 1993. Molecular determinants of macrophage tropism and viral persistence: importance of single amino acid changes in the polymerase and glycoprotein of lymphocytic choriomeningitis virus. *Journal of virology* 67, 7340-7349.

Matloubian, M., Somasundaram, T., Kolhekar, S.R., Selvakumar, R., Ahmed, R., 1990. Genetic basis of viral persistence: single amino acid change in the viral glycoprotein affects ability of lymphocytic choriomeningitis virus to persist in adult mice. *The Journal of experimental medicine* 172, 1043-1048.

McKee, K.T., Jr., Oro, J.G., Kuehne, A.I., Spisso, J.A., Mahlandt, B.G., 1992. Candid No. 1 Argentine hemorrhagic fever vaccine protects against lethal Junin virus challenge in rhesus macaques. *Intervirology* 34, 154-163.

McKee, K.T., Jr., Oro, J.G., Kuehne, A.I., Spisso, J.A., Mahlandt, B.G., 1993. Safety and immunogenicity of a live-attenuated Junin (Argentine hemorrhagic fever) vaccine in rhesus macaques. *The American journal of tropical medicine and hygiene* 48, 403-411.

Medeot, S.I., Contigiani, M.S., Brandan, E.R., Sabattini, M.S., 1990. Neurovirulence of wild and laboratory Junin virus strains in animal hosts. *Journal of medical virology* 32, 171-182.

Mendenhall, M., Russell, A., Juelich, T., Messina, E.L., Smee, D.F., Freiberg, A.N., Holbrook, M.R., Furuta, Y., de la Torre, J.C., Nunberg, J.H., Gowen, B.B., 2011. T-705 (favipiravir) inhibition of arenavirus replication in cell culture. *Antimicrobial agents and chemotherapy* 55, 782-787.

Messina, E.L., York, J., Nunberg, J.H., 2012. Dissection of the role of the stable signal peptide of the arenavirus envelope glycoprotein in membrane fusion. *Journal of virology* 86, 6138-6145.

Meyer, B.J., Southern, P.J., 1993. Concurrent sequence analysis of 5' and 3' RNA termini by intramolecular circularization reveals 5' nontemplated bases and 3' terminal heterogeneity for lymphocytic choriomeningitis virus mRNAs. *Journal of virology* 67, 2621-2627.

Meyer, B.J., Southern, P.J., 1994. Sequence heterogeneity in the termini of lymphocytic choriomeningitis virus genomic and antigenomic RNAs. *Journal of virology* 68, 7659-7664.

- Milazzo, M.L., Cajimat, M.N., Haynie, M.L., Abbott, K.D., Bradley, R.D., Fulhorst, C.F., 2008. Diversity among tacaribe serocomplex viruses (family Arenaviridae) naturally associated with the white-throated woodrat (*Neotoma albigula*) in the southwestern United States. *Vector Borne Zoonotic Dis* 8, 523-540.
- Mills, J.N., Ellis, B.A., Childs, J.E., McKee, K.T., Jr., Maiztegui, J.I., Peters, C.J., Ksiazek, T.G., Jahrling, P.B., 1994. Prevalence of infection with Junin virus in rodent populations in the epidemic area of Argentine hemorrhagic fever. *The American journal of tropical medicine and hygiene* 51, 554-562.
- Mittler, E., Kolesnikova, L., Strecker, T., Garten, W., Becker, S., 2007. Role of the transmembrane domain of marburg virus surface protein GP in assembly of the viral envelope. *Journal of virology* 81, 3942-3948.
- Molinari, M., Helenius, A., 1999. Glycoproteins form mixed disulphides with oxidoreductases during folding in living cells. *Nature* 402, 90-93.
- Molinas, F.C., de Bracco, M.M., Maiztegui, J.I., 1989. Hemostasis and the complement system in Argentine hemorrhagic fever. *Reviews of infectious diseases* 11 Suppl 4, S762-770.
- Morin, B., Coutard, B., Lelke, M., Ferron, F., Kerber, R., Jamal, S., Frangeul, A., Baronti, C., Charrel, R., de Lamballerie, X., Vonnrhein, C., Lescar, J., Bricogne, G., Gunther, S., Canard, B., 2010. The N-terminal domain of the arenavirus L protein is an RNA endonuclease essential in mRNA transcription. *PLoS pathogens* 6, e1001038.
- Murali-Krishna, K., Altman, J.D., Suresh, M., Sourdive, D.J., Zajac, A.J., Miller, J.D., Slansky, J., Ahmed, R., 1998. Counting antigen-specific CD8 T cells: a reevaluation of bystander activation during viral infection. *Immunity* 8, 177-187.
- Murphy, F.A., Whitfield, S.G., 1975. Morphology and morphogenesis of arenaviruses. *Bulletin of the World Health Organization* 52, 409-419.
- Nilsson, I.M., von Heijne, G., 1993. Determination of the distance between the oligosaccharyltransferase active site and the endoplasmic reticulum membrane. *The Journal of biological chemistry* 268, 5798-5801.
- Ohoka, N., Yoshii, S., Hattori, T., Onozaki, K., Hayashi, H., 2005. TRB3, a novel ER stress-inducible gene, is induced via ATF4-CHOP pathway and is involved in cell death. *The EMBO journal* 24, 1243-1255.

Okumura, A., Harty, R.N., 2011. Rabies virus assembly and budding. *Advances in virus research* 79, 23-32.

Oliver, J.D., van der Wal, F.J., Bulleid, N.J., High, S., 1997. Interaction of the thiol-dependent reductase ERp57 with nascent glycoproteins. *Science* 275, 86-88.

Ortiz-Riano, E., Cheng, B.Y., de la Torre, J.C., Martinez-Sobrido, L., 2011. The C-terminal region of lymphocytic choriomeningitis virus nucleoprotein contains distinct and segregable functional domains involved in NP-Z interaction and counteraction of the type I interferon response. *Journal of virology* 85, 13038-13048.

Ortiz-Riano, E., Cheng, B.Y., de la Torre, J.C., Martinez-Sobrido, L., 2012a. D471G mutation in LCMV-NP affects its ability to self-associate and results in a dominant negative effect in viral RNA synthesis. *Viruses* 4, 2137-2161.

Ortiz-Riano, E., Cheng, B.Y., de la Torre, J.C., Martinez-Sobrido, L., 2012b. Self-association of lymphocytic choriomeningitis virus nucleoprotein is mediated by its N-terminal region and is not required for its anti-interferon function. *Journal of virology* 86, 3307-3317.

Ortiz-Riano, E., Ngo, N., Devito, S., Eggink, D., Munger, J., Shaw, M.L., de la Torre, J.C., Martinez-Sobrido, L., 2014. Inhibition of arenavirus by A3, a pyrimidine biosynthesis inhibitor. *Journal of virology* 88, 878-889.

Ozden, S., Lucas-Hourani, M., Ceccaldi, P.E., Basak, A., Valentine, M., Benjannet, S., Hamelin, J., Jacob, Y., Mamchaoui, K., Mouly, V., Despres, P., Gessain, A., Butler-Browne, G., Chretien, M., Tangy, F., Vidalain, P.O., Seidah, N.G., 2008. Inhibition of Chikungunya virus infection in cultured human muscle cells by furin inhibitors: impairment of the maturation of the E2 surface glycoprotein. *The Journal of biological chemistry* 283, 21899-21908.

Palacios, G., Druce, J., Du, L., Tran, T., Birch, C., Briese, T., Conlan, S., Quan, P.L., Hui, J., Marshall, J., Simons, J.F., Egholm, M., Paddock, C.D., Shieh, W.J., Goldsmith, C.S., Zaki, S.R., Catton, M., Lipkin, W.I., 2008. A new arenavirus in a cluster of fatal transplant-associated diseases. *The New England journal of medicine* 358, 991-998.

Parker, W.B., 2005. Metabolism and antiviral activity of ribavirin. *Virus research* 107, 165-171.

Parodi, A.S., Greenway, D.J., Rugiero, H.R., Frigerio, M., De La Barrera, J.M., Mettler, N., Garzon, F., Boxaca, M., Guerrero, L., Nota, N., 1958. [Concerning the epidemic outbreak in Junin]. *El Dia medico* 30, 2300-2301.

Pasqual, G., Burri, D.J., Pasquato, A., de la Torre, J.C., Kunz, S., 2011. Role of the host cell's unfolded protein response in arenavirus infection. *Journal of virology* 85, 1662-1670.

Pasquato, A., Burri, D.J., Traba, E.G., Hanna-El-Daher, L., Seidah, N.G., Kunz, S., 2011. Arenavirus envelope glycoproteins mimic autoprocessing sites of the cellular proprotein convertase subtilisin kexin isozyme-1/site-1 protease. *Virology* 417, 18-26.

Pasquato, A., Pullikotil, P., Asselin, M.C., Vacatello, M., Paolillo, L., Ghezzi, F., Basso, F., Di Bello, C., Dettin, M., Seidah, N.G., 2006. The proprotein convertase SKI-1/S1P. In vitro analysis of Lassa virus glycoprotein-derived substrates and ex vivo validation of irreversible peptide inhibitors. *The Journal of biological chemistry* 281, 23471-23481.

Peralta, L.A., Laguens, R.P., Cossio, P.M., Sabattini, M.S., Maiztegui, J.I., Arana, R.M., 1979. Presence of viral particles in the salivary gland of *Calomys musculinus* infected with Junin virus by a natural route. *Intervirology* 11, 111-116.

Perez, M., Craven, R.C., de la Torre, J.C., 2003. The small RING finger protein Z drives arenavirus budding: implications for antiviral strategies. *Proceedings of the National Academy of Sciences of the United States of America* 100, 12978-12983.

Peters, C.J., 2006. Emerging infections: lessons from the viral hemorrhagic fevers. *Transactions of the American Clinical and Climatological Association* 117, 189-196; discussion 196-187.

Pinschewer, D.D., Perez, M., de la Torre, J.C., 2003. Role of the virus nucleoprotein in the regulation of lymphocytic choriomeningitis virus transcription and RNA replication. *Journal of virology* 77, 3882-3887.

Pinschewer, D.D., Perez, M., de la Torre, J.C., 2005. Dual role of the lymphocytic choriomeningitis virus intergenic region in transcription termination and virus propagation. *Journal of virology* 79, 4519-4526.

Popkin, D.L., Teijaro, J.R., Sullivan, B.M., Urata, S., Rutschmann, S., de la Torre, J.C., Kunz, S., Beutler, B., Oldstone, M., 2011. Hypomorphic mutation in the site-1 protease

Mbtps1 endows resistance to persistent viral infection in a cell-specific manner. *Cell host & microbe* 9, 212-222.

Pozner, R.G., Ure, A.E., Jaquenod de Giusti, C., D'Atri, L.P., Italiano, J.E., Torres, O., Romanowski, V., Schattner, M., Gomez, R.M., 2010. Junin virus infection of human hematopoietic progenitors impairs in vitro proplatelet formation and platelet release via a bystander effect involving type I IFN signaling. *PLoS pathogens* 6, e1000847.

Qi, X., Lan, S., Wang, W., Schelde, L.M., Dong, H., Wallat, G.D., Ly, H., Liang, Y., Dong, C., 2010. Cap binding and immune evasion revealed by Lassa nucleoprotein structure. *Nature* 468, 779-783.

Radoshitzky, S.R., Abraham, J., Spiropoulou, C.F., Kuhn, J.H., Nguyen, D., Li, W., Nagel, J., Schmidt, P.J., Nunberg, J.H., Andrews, N.C., Farzan, M., Choe, H., 2007. Transferrin receptor 1 is a cellular receptor for New World haemorrhagic fever arenaviruses. *Nature* 446, 92-96.

Rajagopalan, S., Xu, Y., Brenner, M.B., 1994. Retention of unassembled components of integral membrane proteins by calnexin. *Science* 263, 387-390.

Raju, R., Raju, L., Hacker, D., Garcin, D., Compans, R., Kolakofsky, D., 1990. Nontemplated bases at the 5' ends of Tacaribe virus mRNAs. *Virology* 174, 53-59.

Riviere, Y., Ahmed, R., Oldstone, M.B., 1986. The use of lymphocytic choriomeningitis virus reassortants to map viral genes causing virulence. *Medical microbiology and immunology* 175, 191-192.

Riviere, Y., Ahmed, R., Southern, P.J., Buchmeier, M.J., Oldstone, M.B., 1985. Genetic mapping of lymphocytic choriomeningitis virus pathogenicity: virulence in guinea pigs is associated with the L RNA segment. *Journal of virology* 55, 704-709.

Ruggiero, H., Magnoni, C., de Guerrero, L.B., Milani, H.A., Izquierdo, F.P., Milani, H.L., Weber, E.L., 1981. Persistence of antibodies and clinical evaluation in volunteers 7 to 9 years following the vaccination against Argentine hemorrhagic fever. *Journal of medical virology* 7, 227-232.

Ruiz-Canada, C., Kelleher, D.J., Gilmore, R., 2009. Cotranslational and posttranslational N-glycosylation of polypeptides by distinct mammalian OST isoforms. *Cell* 136, 272-283.

Sabattini, M.S., Maiztegui, J.I., 1970. [Argentine hemorrhagic fever]. *Medicina* 30, Suppl 1:111-128.

Sakai, M., Muto, M., Hirano, M., Kariwa, H., Yoshii, K., 2015. Virulence of tick-borne encephalitis virus is associated with intact conformational viral RNA structures in the variable region of the 3'-UTR. *Virus research* 203, 36-40.

Salazar-Bravo, J., Ruedas, L.A., Yates, T.L., 2002. Mammalian reservoirs of arenaviruses. *Current topics in microbiology and immunology* 262, 25-63.

Salazar, M., Yun, N.E., Poussard, A.L., Smith, J.N., Smith, J.K., Kolokoltsova, O.A., Patterson, M.J., Linde, J., Paessler, S., 2012. Effect of ribavirin on junin virus infection in guinea pigs. *Zoonoses and public health* 59, 278-285.

Salvato, M.S., Clegg, J.C.S., Buchmeier, M.J., Charrel, R.N., Gonzales, J.P., Lukashevich, I.S., Peters, C.J., Rico-Hesse, R., R., V., 2012. Family Arenaviridae, *Virus Taxonomy: Ninth Report of the International Committee on Taxonomy of Viruses*. . Academic Press, pp. 714-723.

Salvato, M.S., Schweighofer, K.J., Burns, J., Shimomaye, E.M., 1992. Biochemical and immunological evidence that the 11 kDa zinc-binding protein of lymphocytic choriomeningitis virus is a structural component of the virus. *Virus research* 22, 185-198.

Salvato, M.S., Shimomaye, E.M., 1989. The completed sequence of lymphocytic choriomeningitis virus reveals a unique RNA structure and a gene for a zinc finger protein. *Virology* 173, 1-10.

Samoilovich, S.R., Calello, M.A., Laguens, R.P., Weissenbacher, M.C., 1988. Long-term protection against Argentine hemorrhagic fever in Tacaribe virus infected marmosets: virologic and histopathologic findings. *Journal of medical virology* 24, 229-236.

Samoilovich, S.R., Pecci Saavedra, J., Frigerio, M.J., Weissenbacher, M.C., 1984. Nasal and intrathalamic inoculations of primates with Tacaribe virus: protection against Argentine hemorrhagic fever and absence of neurovirulence. *Acta virologica* 28, 277-281.

Sanchez, A.B., de la Torre, J.C., 2006. Rescue of the prototypic Arenavirus LCMV entirely from plasmid. *Virology* 350, 370-380.

Sanchez, A.B., Perez, M., Cornu, T., de la Torre, J.C., 2005. RNA interference-mediated virus clearance from cells both acutely and chronically infected with the prototypic arenavirus lymphocytic choriomeningitis virus. *Journal of virology* 79, 11071-11081.

Schlie, K., Maisa, A., Freiberg, F., Groseth, A., Strecker, T., Garten, W., 2010. Viral protein determinants of Lassa virus entry and release from polarized epithelial cells. *Journal of virology* 84, 3178-3188.

Schroder, M., 2008. Endoplasmic reticulum stress responses. *Cellular and molecular life sciences : CMLS* 65, 862-894.

Schroder, M., Kaufman, R.J., 2005. ER stress and the unfolded protein response. *Mutation research* 569, 29-63.

Seregin, A.V., Yun, N.E., Miller, M., Aronson, J., Smith, J.K., Walker, A.G., Smith, J.N., Huang, C., Manning, J.T., de la Torre, J.C., Paessler, S., 2015. The glycoprotein precursor gene of Junin virus determines the virulence of the Romero strain and the attenuation of the Candid #1 strain in a representative animal model of Argentine hemorrhagic fever. *Journal of virology* 89, 5949-5956.

Seregin, A.V., Yun, N.E., Poussard, A.L., Peng, B.H., Smith, J.K., Smith, J.N., Salazar, M., Paessler, S., 2010. TC83 replicon vectored vaccine provides protection against Junin virus in guinea pigs. *Vaccine* 28, 4713-4718.

Shtanko, O., Watanabe, S., Jasenosky, L.D., Watanabe, T., Kawaoka, Y., 2011. ALIX/AIP1 is required for NP incorporation into Mopeia virus Z-induced virus-like particles. *Journal of virology* 85, 3631-3641.

Skehel, J.J., Stevens, D.J., Daniels, R.S., Douglas, A.R., Knossow, M., Wilson, I.A., Wiley, D.C., 1984. A carbohydrate side chain on hemagglutinins of Hong Kong influenza viruses inhibits recognition by a monoclonal antibody. *Proceedings of the National Academy of Sciences of the United States of America* 81, 1779-1783.

Skinner, H.H., Knight, E.H., Grove, R., 1977. Murine lymphocytic choriomeningitis: the history of a natural cross-infection from wild to laboratory mice. *Laboratory animals* 11, 219-222.

Stephan, B.I., Lozano, M.E., Goni, S.E., 2013. Watching every step of the way: junin virus attenuation markers in the vaccine lineage. *Current genomics* 14, 415-424.

Strecker, T., Eichler, R., Meulen, J., Weissenhorn, W., Dieter Klenk, H., Garten, W., Lenz, O., 2003. Lassa virus Z protein is a matrix protein and sufficient for the release of virus-like particles [corrected]. *Journal of virology* 77, 10700-10705.

Strecker, T., Maisa, A., Daffis, S., Eichler, R., Lenz, O., Garten, W., 2006. The role of myristoylation in the membrane association of the Lassa virus matrix protein Z. *Virology journal* 3, 93.

ten Broeke, T., Wubbolts, R., Stoorvogel, W., 2013. MHC class II antigen presentation by dendritic cells regulated through endosomal sorting. *Cold Spring Harbor perspectives in biology* 5, a016873.

Tortorici, M.A., Ghiringhelli, P.D., Lozano, M.E., Albarino, C.G., Romanowski, V., 2001. Zinc-binding properties of Junin virus nucleocapsid protein. *The Journal of general virology* 82, 121-128.

Urata, S., Yasuda, J., 2012. Molecular mechanism of arenavirus assembly and budding. *Viruses* 4, 2049-2079.

Vallejos, D.A., Ambrosio, A.M., Feuillade, M.R., Maiztegui, J.I., 1989. Lymphocyte subsets alteration in patients with argentine hemorrhagic fever. *Journal of medical virology* 27, 160-163.

Varga, S.M., 2009. Fixing a failed vaccine. *Nature medicine* 15, 21-22.

Vassilakos, A., Cohen-Doyle, M.F., Peterson, P.A., Jackson, M.R., Williams, D.B., 1996. The molecular chaperone calnexin facilitates folding and assembly of class I histocompatibility molecules. *The EMBO journal* 15, 1495-1506.

Videla, C., Carballal, G., Remorini, P., La Torre, J., 1989. Formalin inactivated Junin virus: immunogenicity and protection assays. *Journal of medical virology* 29, 215-220.

Vieth, S., Torda, A.E., Asper, M., Schmitz, H., Gunther, S., 2004. Sequence analysis of L RNA of Lassa virus. *Virology* 318, 153-168.

Vitullo, A.D., Hodara, V.L., Merani, M.S., 1987. Effect of persistent infection with Junin virus on growth and reproduction of its natural reservoir, *Calomys musculinus*. *The American journal of tropical medicine and hygiene* 37, 663-669.

- Vitullo, A.D., Merani, M.S., 1988. Is vertical transmission sufficient to maintain Junin virus in nature? *The Journal of general virology* 69 (Pt 6), 1437-1440.
- Vitullo, A.D., Merani, M.S., 1990. Vertical transmission of Junin virus in experimentally infected adult *Calomys musculinus*. *Intervirology* 31, 339-344.
- Volpon, L., Osborne, M.J., Capul, A.A., de la Torre, J.C., Borden, K.L., 2010. Structural characterization of the Z RING-eIF4E complex reveals a distinct mode of control for eIF4E. *Proceedings of the National Academy of Sciences of the United States of America* 107, 5441-5446.
- Wang, N., Glidden, E.J., Murphy, S.R., Pearse, B.R., Hebert, D.N., 2008. The cotranslational maturation program for the type II membrane glycoprotein influenza neuraminidase. *The Journal of biological chemistry* 283, 33826-33837.
- Watanabe, M., Hirano, A., Stenglein, S., Nelson, J., Thomas, G., Wong, T.C., 1995. Engineered serine protease inhibitor prevents furin-catalyzed activation of the fusion glycoprotein and production of infectious measles virus. *Journal of virology* 69, 3206-3210.
- Weissenbacher, M., De Guerrero, L.B., Frigerio, M.J., 1976. [Subclinical infection, clinical infection and vaccination with Junin virus]. *Medicina* 36, 1-8.
- Weissenbacher, M.C., Avila, M.M., Calello, M.A., Merani, M.S., McCormick, J.B., Rodriguez, M., 1986. Effect of ribavirin and immune serum on Junin virus-infected primates. *Medical microbiology and immunology* 175, 183-186.
- Weissenbacher, M.C., Calello, M.A., Colillas, O.J., Rondinone, S.N., Frigerio, M.J., 1979. Argentine hemorrhagic fever: a primate model. *Intervirology* 11, 363-365.
- Weissenbacher, M.C., Coto, C.E., Calello, M.A., 1975a. Cross-protection between Tacaribe complex viruses. Presence of neutralizing antibodies against Junin virus (Argentine hemorrhagic fever) in guinea pigs infected with Tacaribe virus. *Intervirology* 6, 42-49.
- Weissenbacher, M.C., Coto, C.E., Calello, M.A., Rondinone, S.N., Damonte, E.B., Frigerio, M.J., 1982. Cross-protection in nonhuman primates against Argentine hemorrhagic fever. *Infection and immunity* 35, 425-430.

Weissenbacher, M.C., de Guerrero, L.B., Boxaca, M.C., 1975b. Experimental biology and pathogenesis of Junin virus infection in animals and man. *Bulletin of the World Health Organization* 52, 507-515.

Weissenbacher, M.C., Laguens, R.P., Coto, C.E., 1987. Argentine hemorrhagic fever. *Current topics in microbiology and immunology* 134, 79-116.

Weissenbacher, M.C., Schmunis, G.A., Parodi, A.S., 1969. Junin virus multiplication in thymectomized mice. Effect of thymus and immunocompetent cells grafting. *Archiv fur die gesamte Virusforschung* 26, 63-73.

White, J.M., Delos, S.E., Brecher, M., Schornberg, K., 2008. Structures and mechanisms of viral membrane fusion proteins: multiple variations on a common theme. *Critical reviews in biochemistry and molecular biology* 43, 189-219.

Wilda, M., Lopez, N., Casabona, J.C., Franze-Fernandez, M.T., 2008. Mapping of the tacaribe arenavirus Z-protein binding sites on the L protein identified both amino acids within the putative polymerase domain and a region at the N terminus of L that are critically involved in binding. *Journal of virology* 82, 11454-11460.

Wilson, S.M., Clegg, J.C., 1991. Sequence analysis of the S RNA of the African arenavirus Mopeia: an unusual secondary structure feature in the intergenic region. *Virology* 180, 543-552.

Wujek, P., Kida, E., Walus, M., Wisniewski, K.E., Golabek, A.A., 2004. N-glycosylation is crucial for folding, trafficking, and stability of human tripeptidyl-peptidase I. *The Journal of biological chemistry* 279, 12827-12839.

Wulff, H., Lange, J.V., Webb, P.A., 1978. Interrelationships Among Arenaviruses Measured by Indirect Immunofluorescence. *Intervirology* 9, 344-350.

Yamaguchi, H., Wang, H.G., 2004. CHOP is involved in endoplasmic reticulum stress-induced apoptosis by enhancing DR5 expression in human carcinoma cells. *The Journal of biological chemistry* 279, 45495-45502.

York, J., Romanowski, V., Lu, M., Nunberg, J.H., 2004. The signal peptide of the Junin arenavirus envelope glycoprotein is myristoylated and forms an essential subunit of the mature G1-G2 complex. *Journal of virology* 78, 10783-10792.

Yun, N.E., Linde, N.S., Dziuba, N., Zacks, M.A., Smith, J.N., Smith, J.K., Aronson, J.F., Chumakova, O.V., Lander, H.M., Peters, C.J., Paessler, S., 2008. Pathogenesis of XJ and Romero strains of Junin virus in two strains of guinea pigs. *The American journal of tropical medicine and hygiene* 79, 275-282.

Zapata, J.C., Salvato, M.S., 2013. Arenavirus variations due to host-specific adaptation. *Viruses* 5, 241-278.

Zeitlin, L., Geisbert, J.B., Deer, D.J., Fenton, K.A., Bohorov, O., Bohorova, N., Goodman, C., Kim, D., Hiatt, A., Pauly, M.H., Velasco, J., Whaley, K.J., Altmann, F., Gruber, C., Steinkellner, H., Honko, A.N., Kuehne, A.I., Aman, M.J., Sahandi, S., Enterlein, S., Zhan, X., Enria, D., Geisbert, T.W., 2016. Monoclonal antibody therapy for Junin virus infection. *Proceedings of the National Academy of Sciences of the United States of America* 113, 4458-4463.

Zhang, J.X., Braakman, I., Matlack, K.E., Helenius, A., 1997. Quality control in the secretory pathway: the role of calreticulin, calnexin and BiP in the retention of glycoproteins with C-terminal truncations. *Molecular biology of the cell* 8, 1943-1954.

Zhang, K., Kaufman, R.J., 2006. The unfolded protein response: a stress signaling pathway critical for health and disease. *Neurology* 66, S102-109.

Vita

NAME: John Tyler Manning

PRESENT POSITION AND ADDRESS: 09/2011 – present: Graduate Student, UTMB

BIOGRAPHICAL: Birthdate: 2/10/1986
Birthplace: Brownwood, TX; United States Citizen
Parents: John and Diane Manning
Business Address and Phone Number:

301 University Boulevard
Galveston, Texas 77555
Phone: (409)747-2489

EDUCATION: 09/2010: B.S. in Biology at Hardin-Simmons University; Abilene, Texas

MEMBERSHIP IN SCIENTIFIC SOCIETIES/PROFESSIONAL ORGANIZATIONS:

Texas Academy of Science Student Member

HONORS:

Holland School of Sciences Scholarship, Hardin-Simmons University 2009-2010

Sealy Center for Vaccine Development Predoctoral Fellowship, University of Texas Medical Branch 2013-present

Edward S. Reynolds Award, University of Texas Medical Branch 2014

James W. McLaughlin Travel Award, University of Texas Medical Branch 2014

PUBLISHED:

A. PUBLICATIONS

Manning JT, Seregin AV, Yun NE, Koma T, Huang C, Barral J, de la Torre JC, Paessler S. (2016) Absence of an N-linked glycosylation motif in the glycoprotein of the live-attenuated Argentine hemorrhagic fever vaccine, Candid #1, results in its improper processing and reduced surface expression. *Frontiers in Cellular and Infection Microbiology* (in review)

Manning JT, Forrester N, Paessler S. (2015) Lassa virus isolates from Mali and the Ivory Coast represent an emerging fifth lineage. *Frontiers in Microbiology*. 6(1037). Doi:10.3389/fmicb.2015.01037.

Manning JT, Yun NE, Paessler S. (2016) Lassa virus genetic diversity. *Antiviral Research*. (in review)

Seregin AV, Yun NE, Miller M, Aronson J, Smith JK, Walker AG, Smith JN, Huang C, Manning JT de la Torre JC, Paessler S. (2015) The glycoprotein precursor gene of Junin virus determines the virulence of the Romero strain and the attenuation of the Candid strain in a representative animal model of Argentine Hemorrhagic Fever. *J Virol*. 89(11):5949-5956.

B. ABSTRACTS:

Activation of Mammalian/Mechanistic Target of Rapamycin (mTOR) in Human Endothelial Cells Infected with Pathogenic Rickettsia. ED Thomasson, A Sahni, **JT Manning**, PM Colonne, SK Sahni.

C. POSTERS:

MECHANISMS OF JUNIN VIRUS ATTENUATION. JT Manning, AV Seregin, NE Yun, T Koma, S Paessler. McLaughlin Symposium; Galveston, Texas, USA

DIFFERENCES IN VIRULENCE BETWEEN LASV ISOLATES. **JT Manning**, NE Yun, SL Paessler. McLaughlin Symposium; Galveston, Texas, USA

SEQUENCING AND COMPARISON OF RECENT LASSA VIRUS HUMAN ISOLATES FROM SIERRA LEONE. **John T. Manning**, Nadezda E. Yun, Alexey Seregin, and Slobodan Paessler. McLaughlin Symposium; Galveston, Texas, USA

Assembly of Rift Valley fever virus and the role of N-linked glycosylations. A.N. Freiberg, M. Rusu, T.E. Hill, M. Huante, M. Hermance, J.T. Manning, T. Ikegami, W. Wriggers. Emerging Viruses: Disease Models and Strategies for Vaccine Development Symposium; Galveston, Texas, USA

Chimeric Monoclonal Antibodies Specific to HER2/neu Function as T-Cell Mimic Receptors. Johnson BG, Gupta P, **Manning JT**, Weidanz J. Texas Academy of Science Annual Symposium; Stephenville, Texas, USA